completed in February 2008

PERFORMANCE ESTIMATION AT 90GHz (3.3mm) OF THE MEDICINA AND NOTO SITES

A. Orfei

Rapporto Interno IRA 418/08

D:/Didattica/Teoria/Atmosfera/IRA418_08sefd90.doc

INDEX

1. INTRODUCTION

In a previous report [1] an evaluation of the Medicina and Noto sites was done with the aim to investigate the possibility to use the antennas also at higher frequencies than they were designed for. In the same report data taken in many years of VLBI and GPS measurements showed a similar behaviour of the two sites in term of water column values. For this reason general conclusions for Medicina coming from the investigation described in this report can be assumed also for the Noto site.
In [1] it was assessed that a PWV (Precipitable Water Vapour) value less than 10mm should give an acceptable absorption coefficient up to 90 GHz in an interesting amount of days during winter. In the following chart a summary is shown,

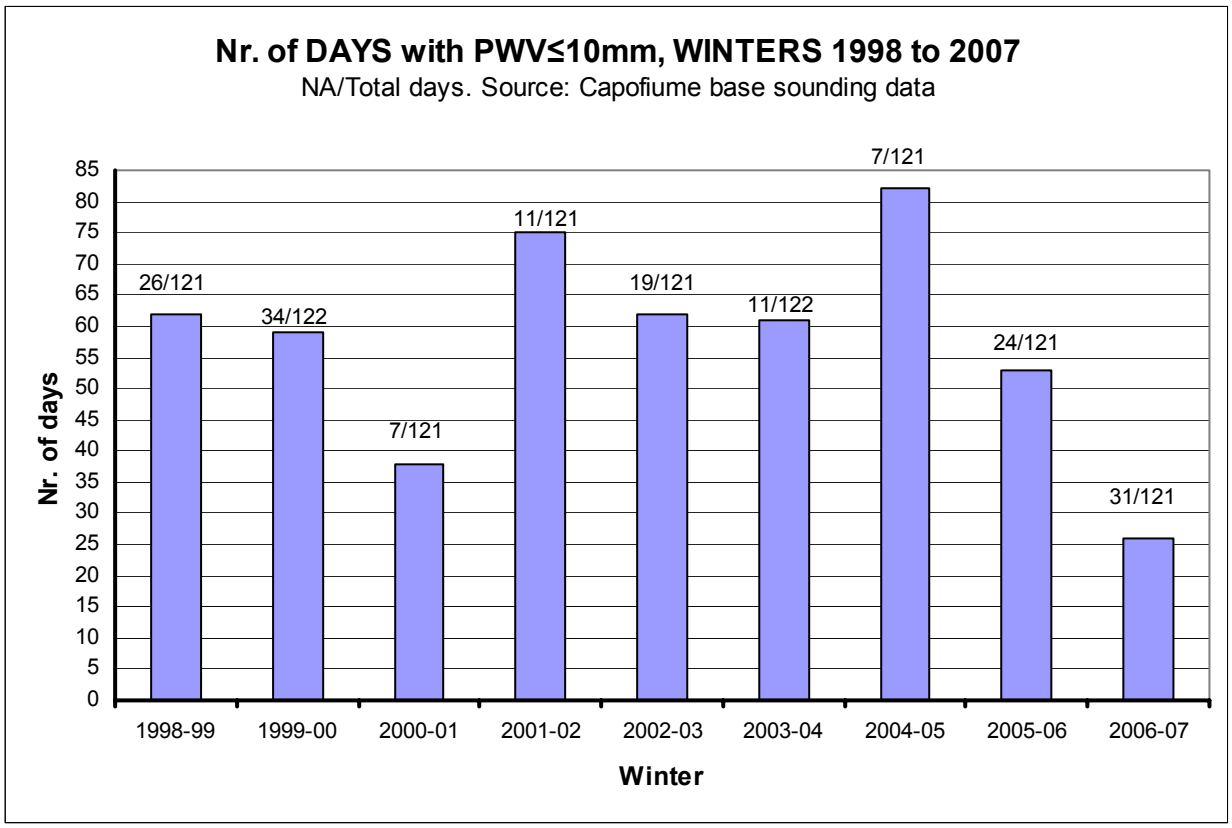

Fig. 1.1 Number of days suitable for observing at 90GHz in nine winters at Medicina site

Numbers attached to each histogram show the total number of days available (on the right of the backlash) and the number of days where PWV measures are not available (on the left of the backlash). 2000 and 2004 are leap years.
The data come from measurements by soundings of the atmosphere made at specific sites across Europe (Fig. 1.2, http://weather.uwyo.edu/upperair/sounding.html).

Fig. 1.2 European map of the sounding bases

Medicina observatory uses the base 16144 at S. Pietro Capofiume location. They are only 15 Km apart (Fig. 1.3), suggesting the idea that the base could supply values of PWV also valid for the observatory site.

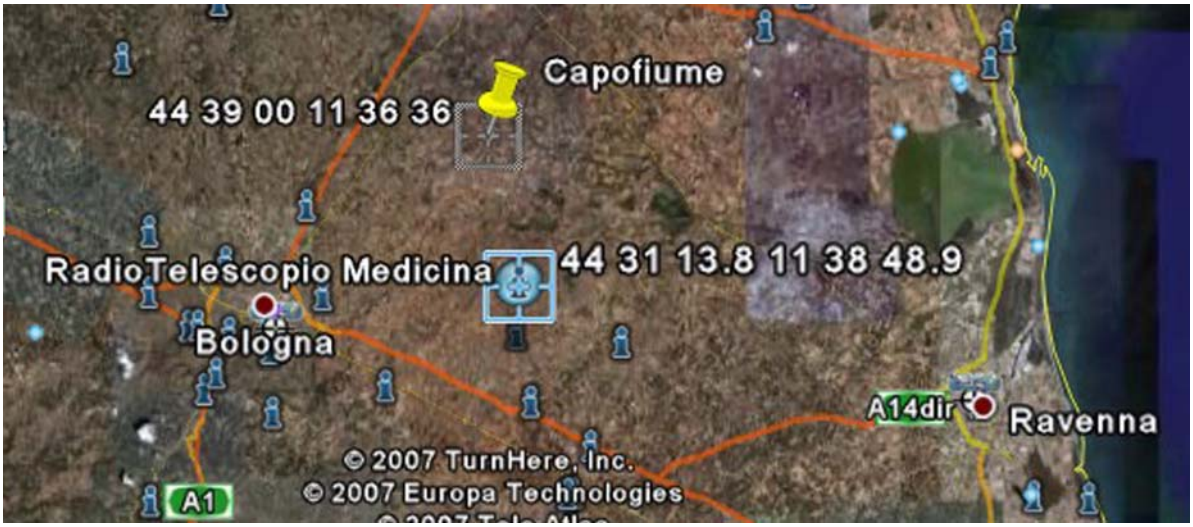

Fig. 1.3 Medicina observatory and Capofiume base coordinates

The aim of this second report is to provide a deeper investigation on the performance at 3mm exploiting one year data acquired at Medicina of the zenith attenuation coefficient (τ_o) at 22 GHz together with local weather and PWV data coming from Capofiume.
These allow a comparison between calculated and measured PWV and their correlation with measured $\tau_o(22)$. Measured $\tau_o(22)$ could be compared with simulations using the program ATM (Atmospheric Transmission at Microwave, developed by Pardo in 2001 and routinely used at IRAM mm/submm antennas) which provides $\tau_o(90)$ as well. As a result, a prediction of τ_o at 90 GHz becomes available permitting a closer evaluation of the SEFD (System Equivalent Flux Density) at the sites for each elevation at that frequency.
It must be stressed that an accurate determination of the parameters PWV and $\tau_o(90)$, hopefully obtainable only by a radiometer and after a few years of acquisition campaign, is not necessary. The aim of this report is to assess realistic values of $\tau_o(90)$ in order to get a feeling about SEFD performance at the sites. A rough accuracy in the estimation of $\tau_o(90)$ for PWV$\leq$ 10mm within 30-

40% is sufficient and, for this reason, calculations will be made both with estimated mean and worst case values, where PWV and $\tau_o(90)$ are thought to assume extreme values.
In the diagram of Fig. 1.4 a sketch of the quantities affecting the SEFD is shown. Arrows pointing to a block mean this is affected by the quantity from which the arrow departs. For a brief description of the quantities see [2].
The meaning of the symbols in Fig. 1.4 is,

SEFD = System Equivalent Flux Density (Jansky)
Tsys = Total Noise Temperature of the receiving system (Kelvin)
G = antenna gain (K/Jy)
λ = wavelength (m)
Ag = projected area of the primary mirror surface on the wavefront plane (m)
τ_o = attenuation coefficient at zenith
$e^{-\tau o}$ = signal attenuation due to the crossing of the atmosphere at zenith
$290*(1- e^{-\tau o})$ = noise contribution due to atmosphere at zenith (Kelvin)
T_{rx} = receiver noise temperature (Kelvin)
T_{spill} = noise temperature due to antenna spillover (Kelvin)
η_{sub} = antenna spillover of the secondary mirror alone
η_{prim} = antenna spillover of the primary mirror alone
η_{spill} = antenna efficiency due to antenna spillover ($= \eta_{sub}*\eta_{prim}$)
η_{taper} = antenna efficiency due to feed illumination of the antenna
η= antenna efficiency due to all contributions except η_{surf} ($= \eta_{spill}*\eta_{taper}*$other)
η_{surf} = antenna efficiency due to total rms surface accuracy
η_{ant} = total antenna efficiency ($= \eta_{surf}*\eta$')

An overall view of the steps followed in this study to get SEFD estimation is given by the flow chart in Fig. 1.5.

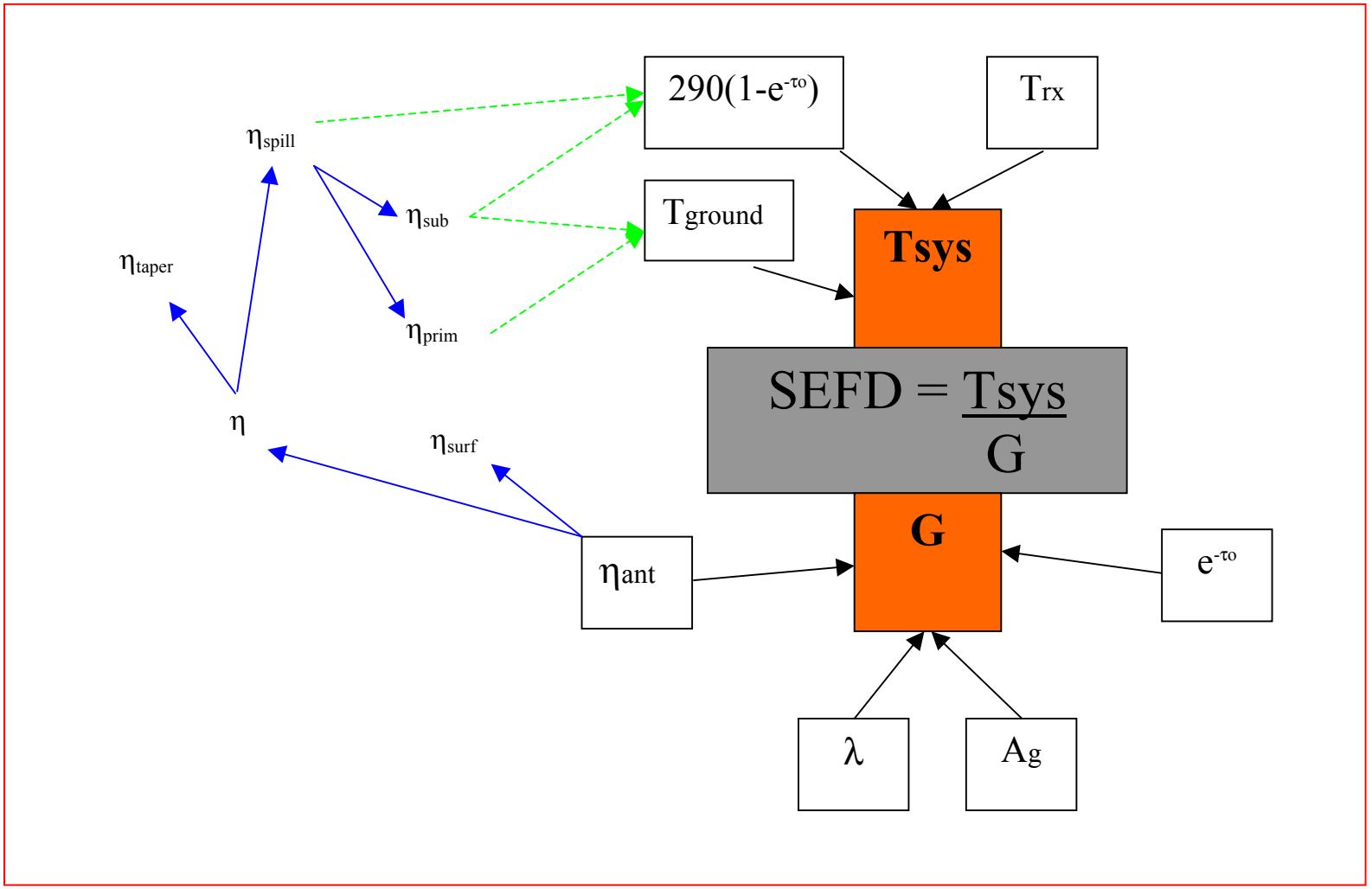

Fig. 1.4 Diagram of the relationship between SEFD and receiving system quantities

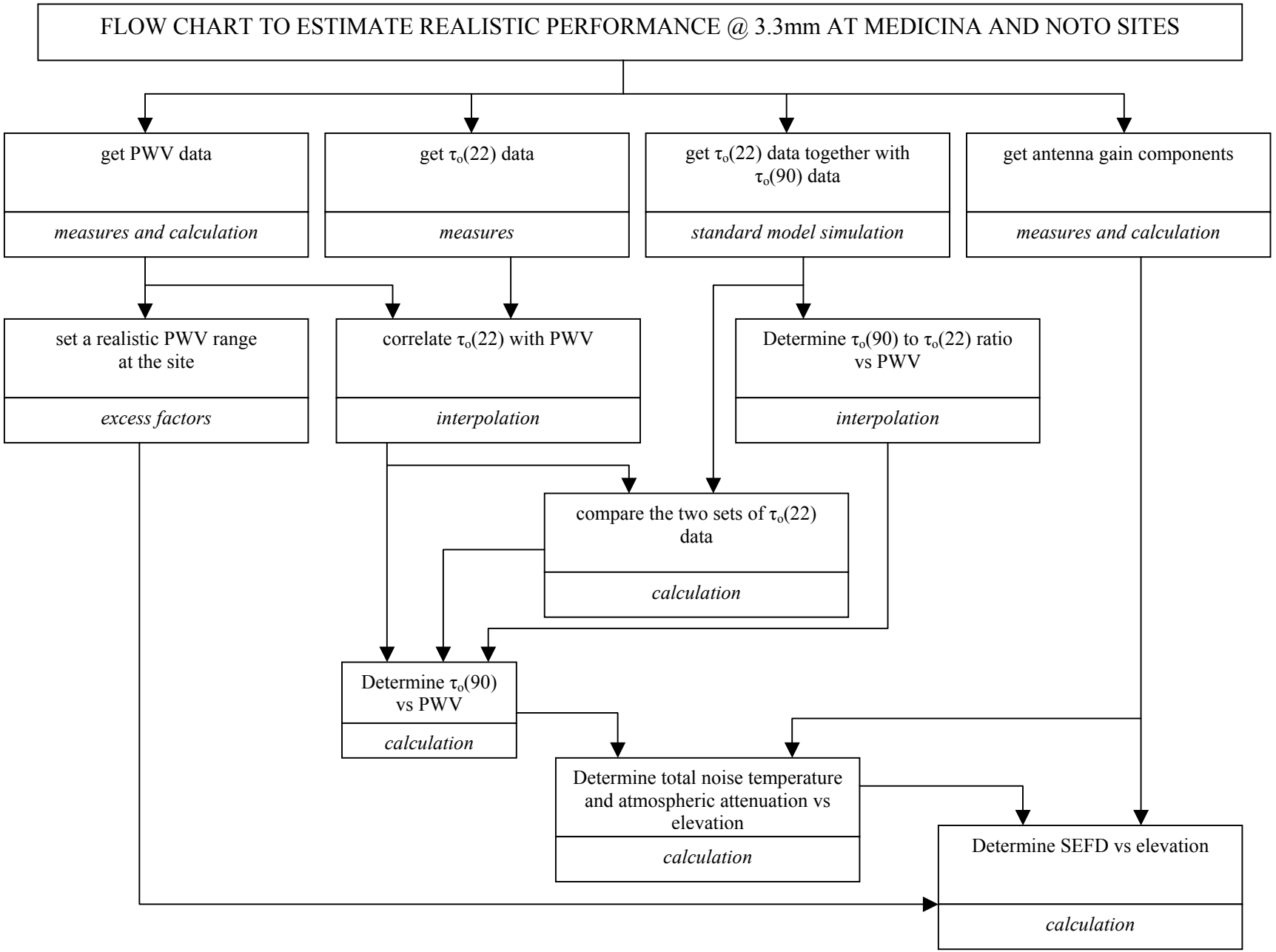

Fig. 1.5 Flow chart describing the method used in this report

2. OVERVIEW of the QUANTITIES DETERMINING SEFD

The main aim of this report is the estimation of the SEFD at 90 GHz. It is useful to recall which parameters enter in its calculation and the adopted assumptions.

2.1 Amplitude of the Received Signal

The radiation picked-up by a radiotelescope is attenuated by the atmosphere (the loss is variable with time and weather) and then converted into a temperature by the whole receiving system (antenna plus receiver). The overall conversion factor G (antenna gain) measured in Kelvin/Jansky, depends on the parameters depicted in Fig.1.4.

2.1.1 Antenna Efficiency due to surface accuracy (η_{surf})

This is an important contribution, related to the structural deformation of the antenna (first of all due to gravity), to the manufacturing accuracy of the antenna mirrors and to the alignment of primary mirror panels. Gain loss is strongly dependent on the ratio between the total surface rms accuracy (σ) and the wavelength of the radiation. The decrease factor with respect to the maximum antenna efficiency is calculated by,

$$\eta_{surf} = e^{-(4\pi\sigma/\lambda)^2}$$

2.1.2 Antenna Efficiency due to other causes (η)

There are many causes affecting the total antenna efficiency over η_{surf} and they are described in [2]. For the purpose of this report typical values of Medicina and Noto will be used.

2.1.3 Signal attenuation due to atmosphere ($e^{-\tau o}$)

As mentioned before the attenuation depends on the τ_o parameter. The formula used for the attenuation calculation at each elevation is:

$$A = e^{-\tau_o / \cos(90-El)}$$

2.2 Noise contributions

The total amount of noise temperature of the receiving system is the sum of the receiver noise and the noise spilled over from the antenna. It is usually known as system temperature, Tsys.

2.2.1 Receiver noise temperature

A matter to deal with in order to give an estimate of the SEFD is the evaluation of the noise of a cryogenic receiver in the 90 GHz band. Of course this depends on the possibility to access state-of-the-art technology and the capability to produce a complete Low Noise Amplifier (LNA).
In order to give realistic values about Trx, it will be taken the best result to our knowledge, and this will be treated like the best performance achievable, and an estimate, with a safe margin, based on state-of-the-art MMIC chips the Istituto di Radioastronomia (IRA) has available now.

a) the best achievable.
University of Massachussets provides complete 85-115 GHz cryogenic multifeed receiver (SEQUOIA) using InP based MMIC LNAs. The MMICs were produced by a foundry process by TRW company.
In fig. 2.2.1.1 the receiver noise temperature for each pixel is reported [3]: about 60 K are achievable for most of the band.

b) IRA MMIC chips.
IRA has available InP MMIC LNAs made by TRW (now NGC) as well, working in the 70-95 GHz band. Measurements at ambient temperature of the LNAs give about 300 K noise [4]. Previous experience permits to extrapolate this value to cryogenic temperature, normally a reducing factor 4 to 7 is achieved. Therefore a worst case of 75 K coming from the chip has to be taken into account. Then it must be packaged and connected to a WR10 waveguide which adds loss. Loss will arise also from the vacuum window. All included, a worst case estimate for an IRA 90 GHz complete receiver could be 100 K.

These two limiting values, 60 and 100K, will be later used in the calculation of SEFD.

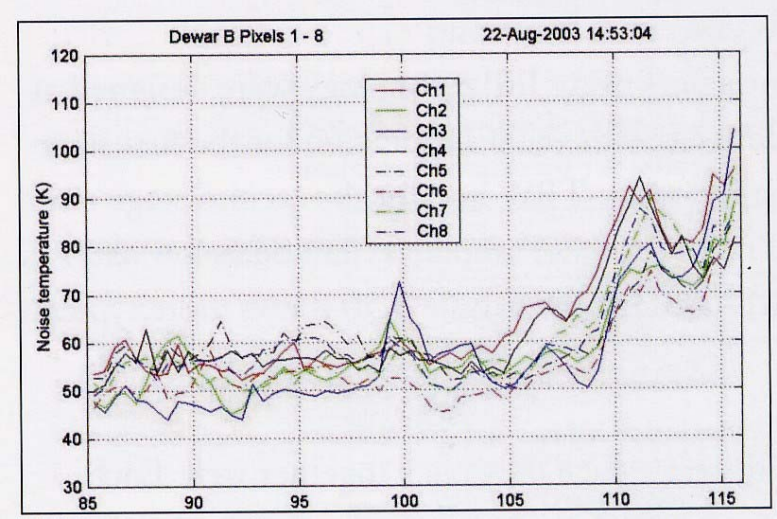

Fig. 2.2.1.1 Best known 3mm band receiver noise temperature

2.2.2 Spillover

The noise picked-up by the antenna due to its spillover depends on the contribution from ground, atmosphere and cosmic brightnesses. The amount of each of them affecting the total noise temperature depends on the illumination of the optics, involving all antenna mirrors focussing the radiation into the horn mouth. A simplified analysis of the problem permits to write down a formula giving the total noise due to spillover effects: the first and third addend are the contributions picked-up from the sky, the second one from the ground. It must also be underlined that efficiencies related to spillover (η_{spill}, η_{sub}, η_{prim}) also show a weak dependence on the elevation but for the purpose of this report it can be neglected.
The formula for calculating the noise temperature due to spillover is [5],

$$T_{spill} = \eta_{spill} * [290 * (1 - e^{-\tau o / \cos(90 - El)}) + 2.73] + 290 * \eta_{sub} * (1 - \eta_{prim}) + [290 * (1 - e^{-\tau o / \cos(90 - El)}) + 2.73] * (1 - \eta_{sub})$$

$290*(1- e^{-\tau o/\cos(90-El)})+2.73$ is the brightness temperature of the sky, essentially due to the atmosphere contribution (the CMB contribution could be neglected) and 290 is the assumed temperature over the principal layers of the water column (the true value is season and day dependent but it ranges between 260 and 300K).

3. ATMOSPHERIC EFFECTS @ 3.3 mm AT THE MEDICINA SITE

3.1 Evaluation of PWV

A correct evaluation of PWV (Precipitable Water Vapour) needs a sounding of the water column in the line of sight of the telescope, up to many kilometers in altitude. As mentioned in the introduction there are many sounding bases all over Europe. Medicina has a very close base, located at San Pietro Capofiume, issuing meteorological data every day and two values of PWV at 00:00 and 12:00. A similar base is near the Sardinia Radio Telescope (SRT) site at a distance of about 26 Km. Unfortunately this is not the case for Noto.
An approximate method is to derive from air pressure, temperature and relative humidity (P,T,RH) the amount of water as precipitated at ground. Thus the following parameters are defined,

Pvs_o = saturation pressure of water vapour

$$[\text{mbar}]Pvs_o = 6.105 * (\frac{T}{273})^{-5.31} * e^{\frac{25.22(T-273)}{T}}$$

T = temperature, Kelvin

Pv_o = partial pressure of water vapour

$$[\text{mbar}]Pv_o = \frac{Pvs_o * RH/100}{[1-(1-RH/100) * \frac{Pvs_o}{P}]}$$

RH = relative humidity, %

P = total pressure, mbar

ρ_{vo} = water vapour density at ground

$$[g/m^3]\rho_{v_o} = \frac{Pv_o * 217}{T}$$

Pv_o, mbar

T, Kelvin

It is assumed that ρ_v has an exponential law with altitude whose characteristic constant is the "scale heigth" H, and ground value equal to ρ_{vo},

$$[g/m^3]\rho_v = \rho_{v0} * e^{-h/H}$$

h and H, km

Finally the Integrated PWV, PWV from here on, is

$$[\text{mm}]IPWV = \frac{1}{\rho_w} * \int_0^\infty \rho_v(h)dh$$

ρ_w = liquid water density, 10^6 g/m^3

Due to the exponential assumption it holds

$$[\mathrm{km}]\,\mathrm{IPWV} = H * \frac{\rho_{vo}}{\rho_w} \qquad \text{or} \qquad [\mathrm{mm}]\,\mathrm{IPWV} = H * \rho_{vo}$$

ρ_{vo} and $\rho_{w,}$ g/m^3

H, km

For a standard atmosphere H=2km.

3.1.1 Medicina and Capofiume PWV data comparison

A question arises which of the two data sets, wheter from local measurement or from the sounding base, are more useful in order to have a reliable evaluation of PWV at the Medicina site. PWV values coming from meteorological data taken at the site have the advantage they come from local data but the disadvantage they are derived from ground measures and models. On the other hand, values coming from the Capofiume base have the advantage to sound the whole water column but the problem this does not come from the line of sight of the telescope.
In order to give a taste of the accuracy of the formulae reported in the previous paragraph, the PWV data by Capofiume may be compared with its calculation using P,T,RH values at ground also provided by the station. A common set of seven months data were used from May to December 2006.
In Fig. 3.1.1.1 the difference, in percentage of the value, between measured PWV and formula outcome is given,

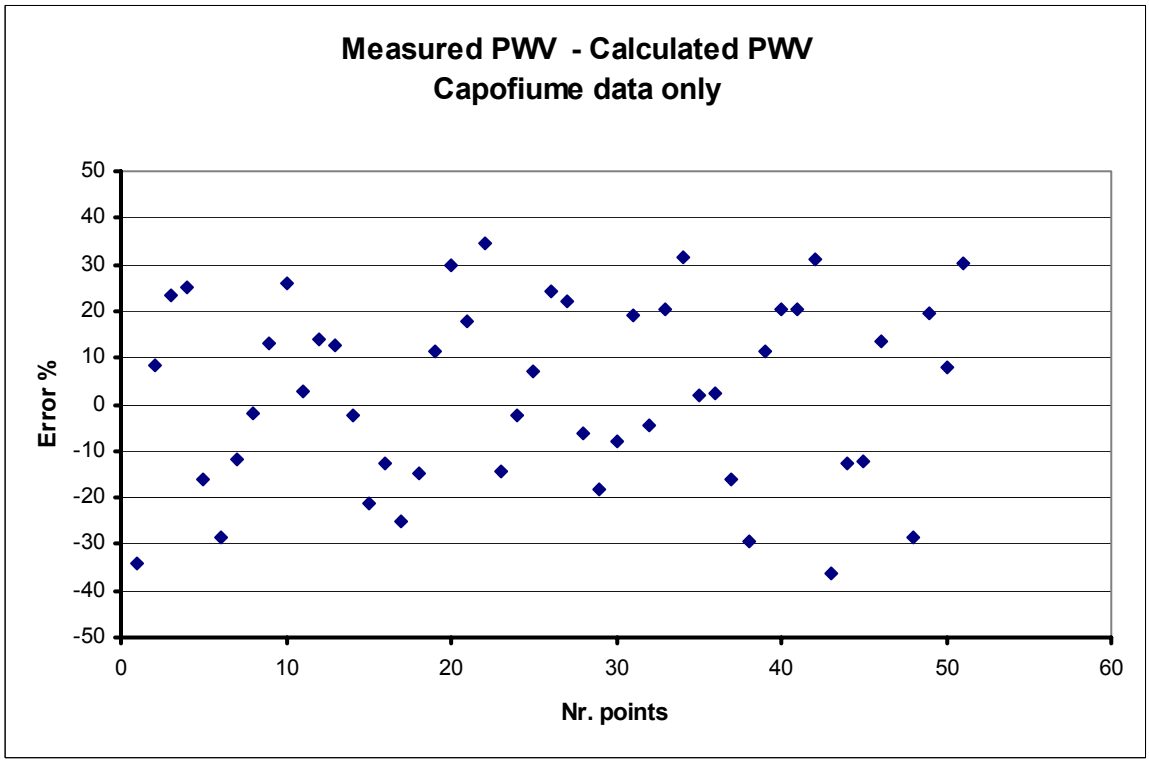

Fig. 3.1.1.1 Accuracy of PWV formula, Capofiume data only

On the other hand, if measured PWV by Capofiume and PWV calculated by using ground meteorological data at Medicina site are compared and a similar graph is produced we have Fig. 3.1.1.2,

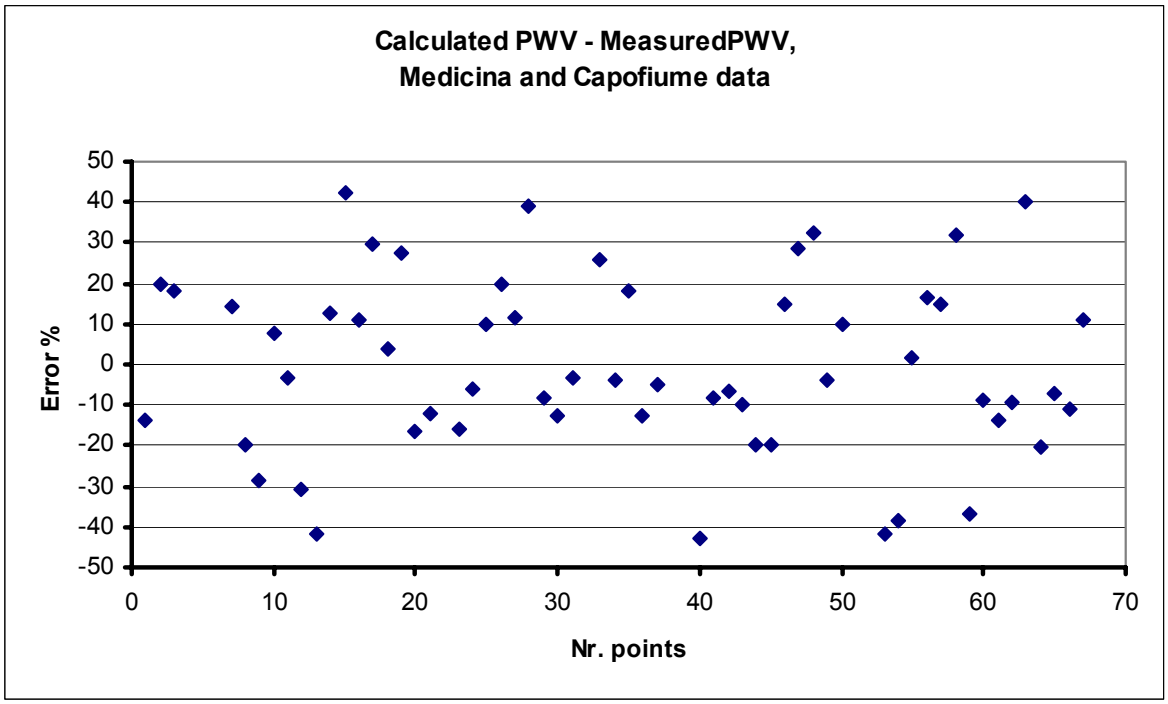

Fig. 3.1.1.2 Accuracy of PWV formula, Medicina and Capofiume data

In both cases we see that differences with respect to measured PWV range in a band ±40% wide, so setting a formula accuracy in that order of magnitude.
From another point of view, calculated PWV and measured PWV can be plotted one against other, giving Fig. 3.1.1.3,

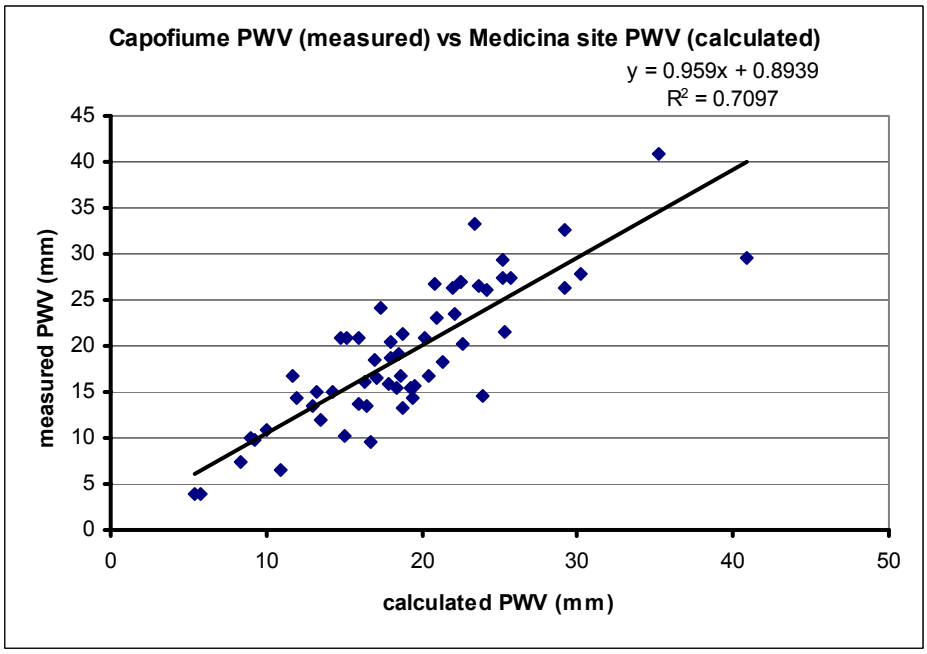

Fig. 3.1.1.3 Measured vs Calculated PWV data

In an ideal case the straight line should have zero offset and unit slope. In a real case like in these set of data, these coefficients are not so far from the ideal.

A conclusion could be that we can use any of the sets of PWV data, but taking into account that the true value may be 1.4 times, using a very conservative *excess factor*, the chosen value.

3.1.2 Daily fluctuations of PWV

One further topic to deal with is the amount of variation of PWV. As already described in paragraph 3.1, S. Pietro Capofiume base delivers only two PWV measurements per day. This prevents a precise study of the fluctuations but in the spirit to get an idea of the phenomena a data survey is anyway worth. The variations will be shown day by day and, in order to add one more datum, every day will consider three values, at 00:00, 12:00 and at 24:00, this last taken from the 00:00 data of the next day. Nine winters will be studied, from 1998-99 to 2006-07. For each winter four months, from december to march included, are considered. Thus a complete set of 121 days (122 in the leap years) are analyzed. Capofiume base sometime fails to measure PWV, so it is important to evaluate how many days are available for getting a reliable statistics. This can be derived from Fig. 1.1, from which shows that the sample is large enough (Table 3.1.2.1)

Winter	Amount of days where Capofiume delivers two PWV measures per day
1998-99	95
1999-00	88
2000-01	114
2001-02	110
2002-03	102
2003-04	111
2004-05	114
2005-06	97
2006-07	90

Table 3.1.2.1

The figures from 3.1.2.1 to 3.1.2.36 allow a visual overall view for each month of each winter period. Then statistical graphs focussed on those days having al least one PWV value less than 10mm will allow a more analytic description of the PWV fluctuations.
Of course this second set of data takes into account a subsample of the previous one and the amount of the days considered can be seen in Fig. 1.1.

The statistics calculates the usual standard deviation for each day (from three values at best, two values at worst) and the percentage deviation with respect to the mean PWV value of the day, (st.dev./mean, in %).

An overview of all these graphs confirms what already stated in [1], i.e. every winter provides quite a large number of days suitable for observations at 90 GHz and

a) there are an interesting amount of days where PWV is less than 8mm (Figures 3.1.2.1 to 3.1.2.36)

b) there are periods where PWV≤10mm persists for days
In Table 3.1.2.2 a summary of periods greater than 1 day are reported. The numbers in the table indicate how many subsequent days show “good sky”. The table can be derived taking a close look at Figures 3.1.2.1 to 3.1.2.36.

	December	January	February	March
1998-99	5;4;4	4;7;6;4	8;8;5	5
1999-00	3;3	2;2;4	6;8	3;6
2000-01	4	3	9;3	0
2001-02	22	19	0	4;9
2002-03	2	6;2;8	3;23	14
2003-04	3;4	4;5;4	2;9	5
2004-05	5;4;2	8;5;11	10;16	10
2005-06	3	14;8	6;6;3	2;3;3;3
2006-07	2;2;4	2;8	2;4	2

Tab. 3.1.2.2

c) days with PWV≤10mm show absolute daily fluctuations mostly less than 3mm (Fig. 3.1.2.37, 39,41,43,45,47,49,51,53)

d) days with PWV≤10mm show daily fluctuations of 25-30% with respect to daily mean value (Fig. 3.1.2.38, 40,42,44,46,48,50,52,54), so an *excess factor* of 1.25-1.3 could be used in order to take into account the effect of this phenomenon on the fluctuations of τ_o and consequently on SEFD.

1998-1999 WINTER

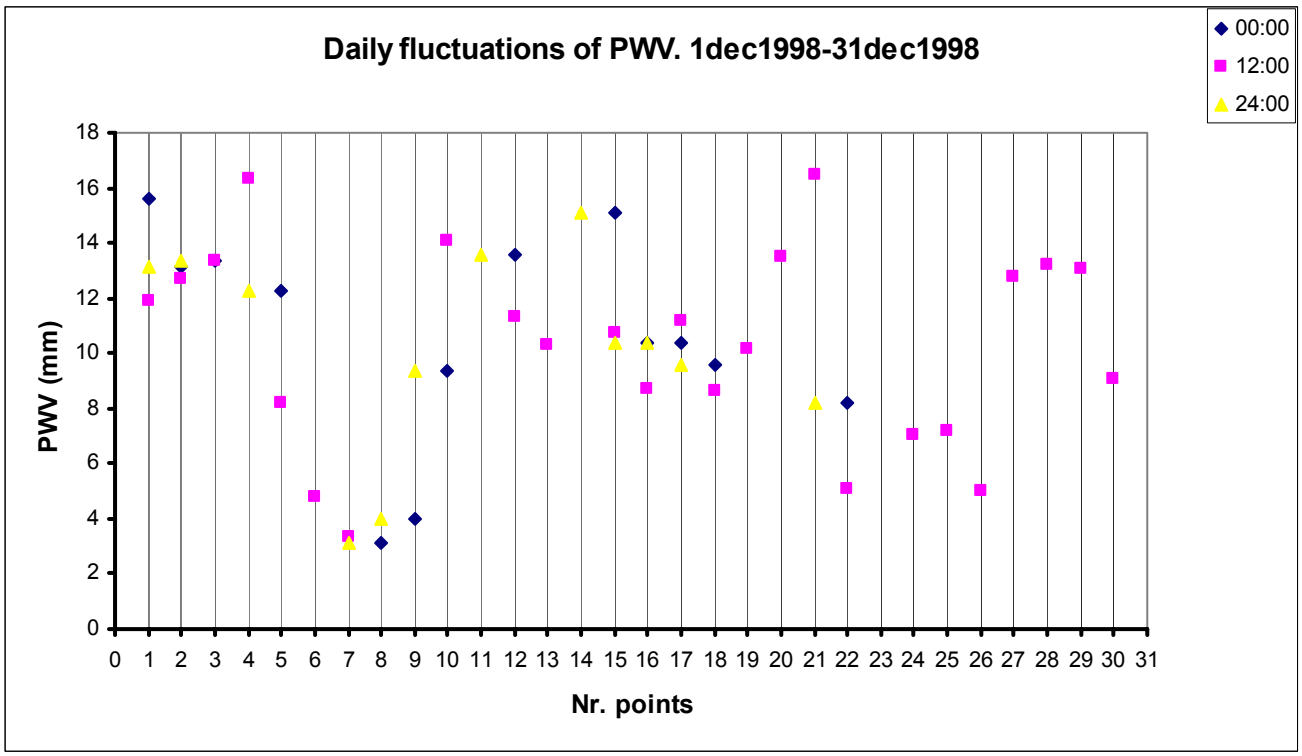

Fig. 3.1.2.1

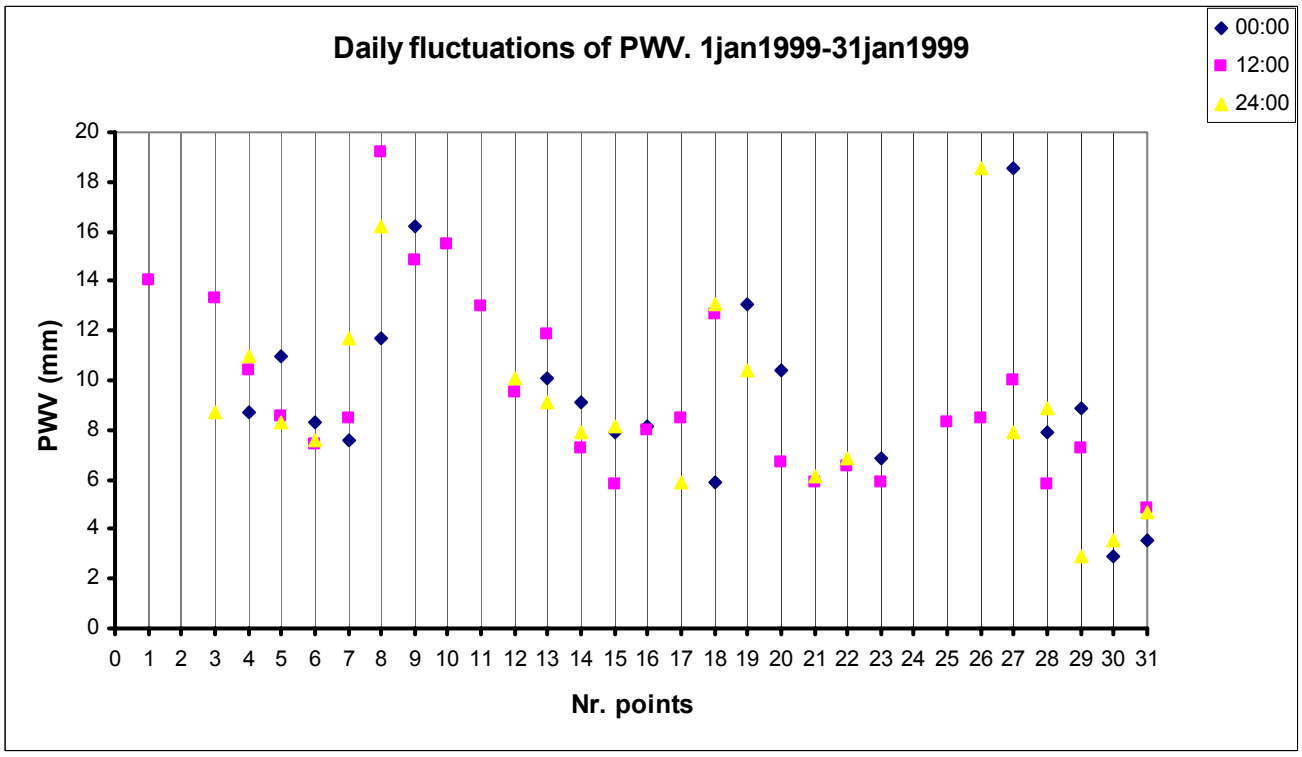

Fig. 3.1.2.2

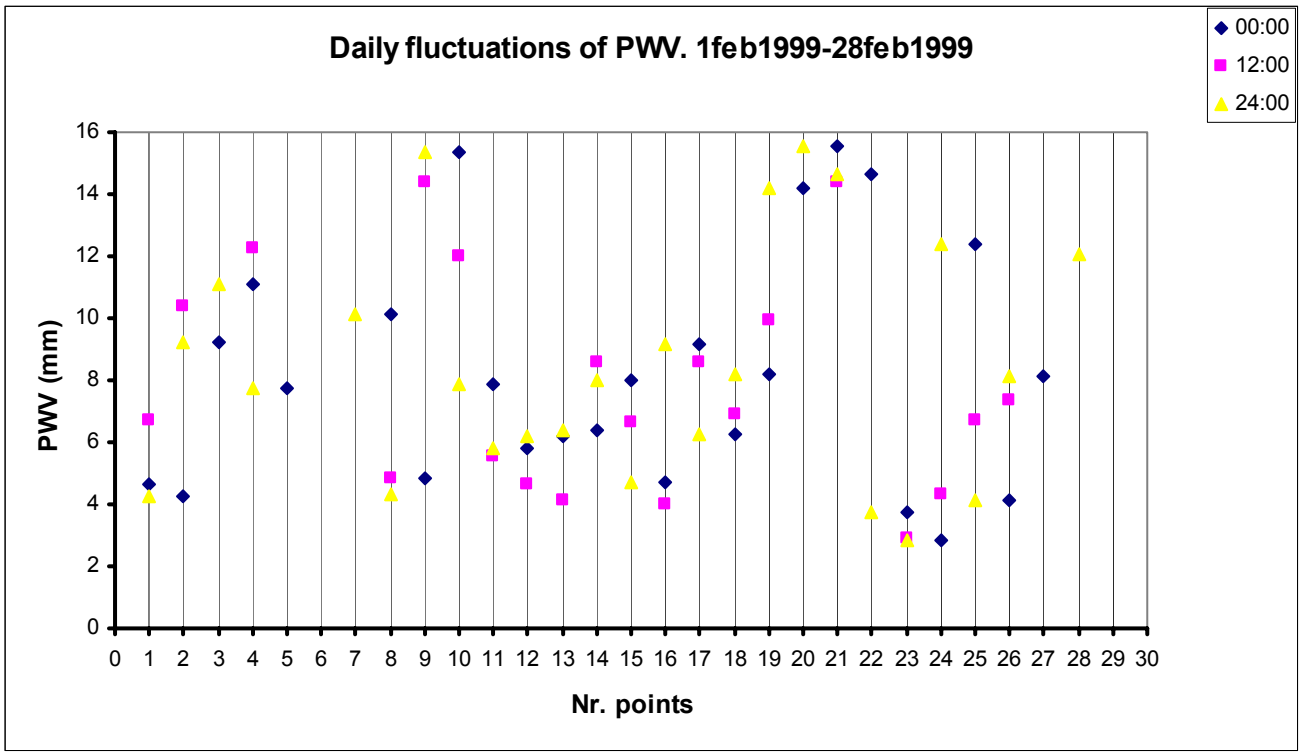

Fig. 3.1.2.3

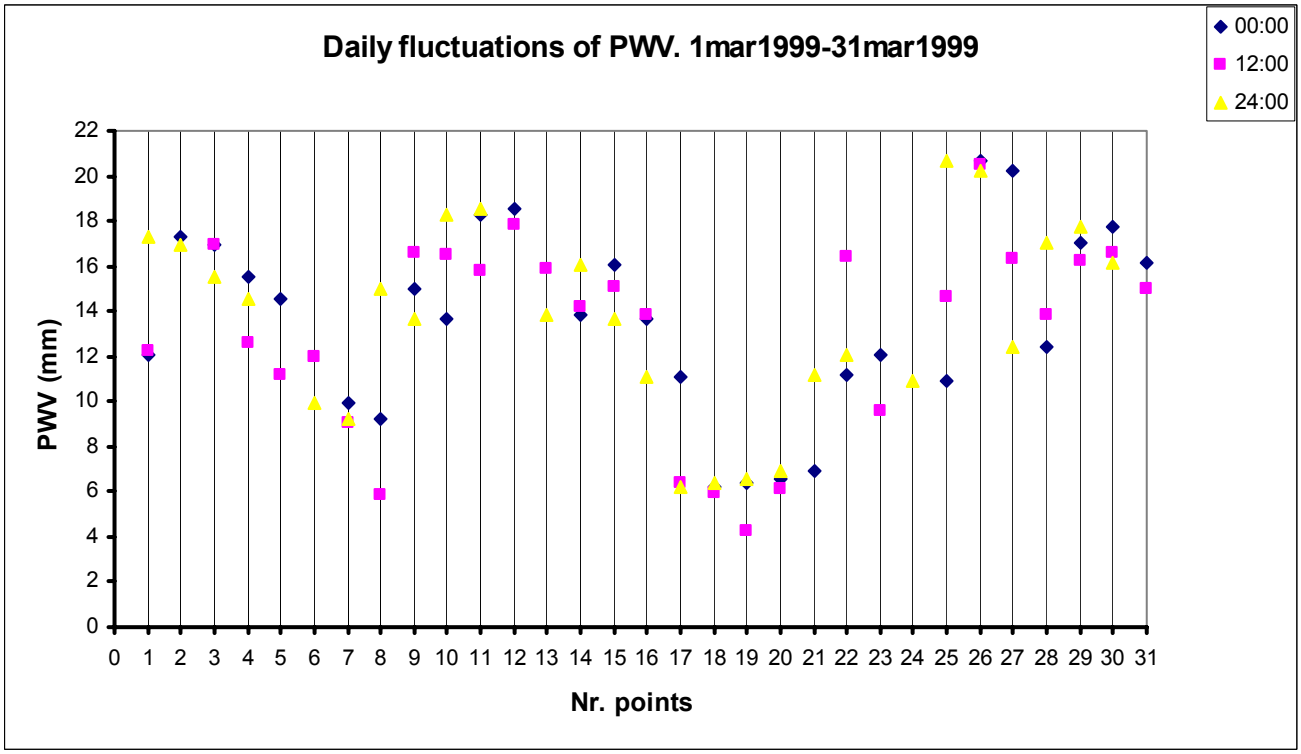

Fig. 3.1.2.4

1999-2000 WINTER

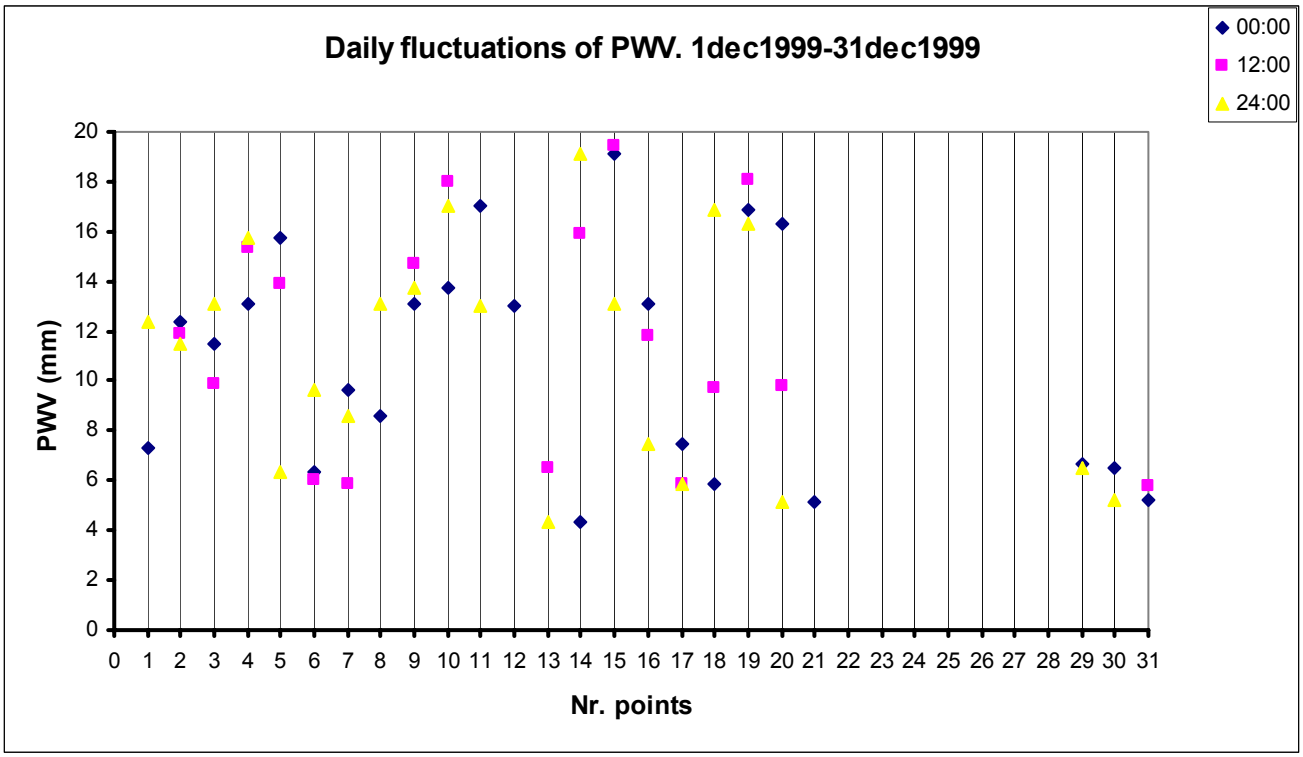

Fig. 3.1.2.5

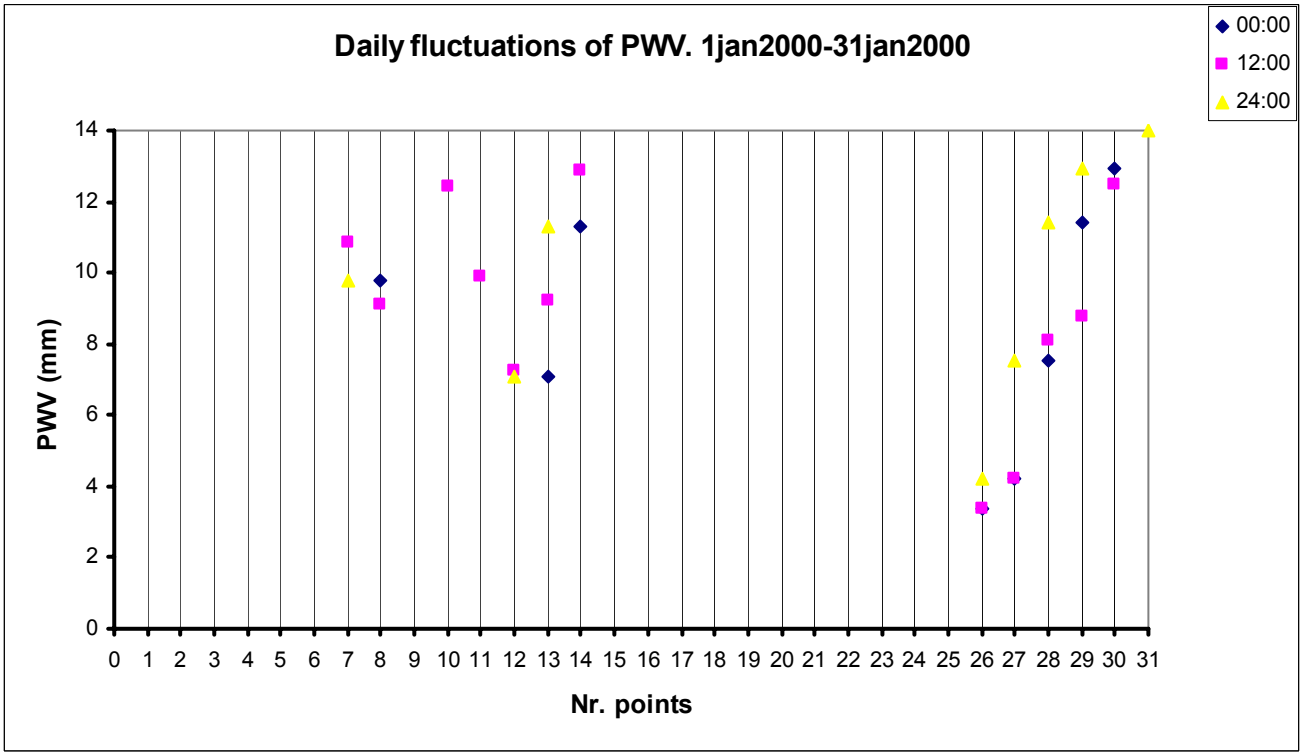

Fig. 3.1.2.6

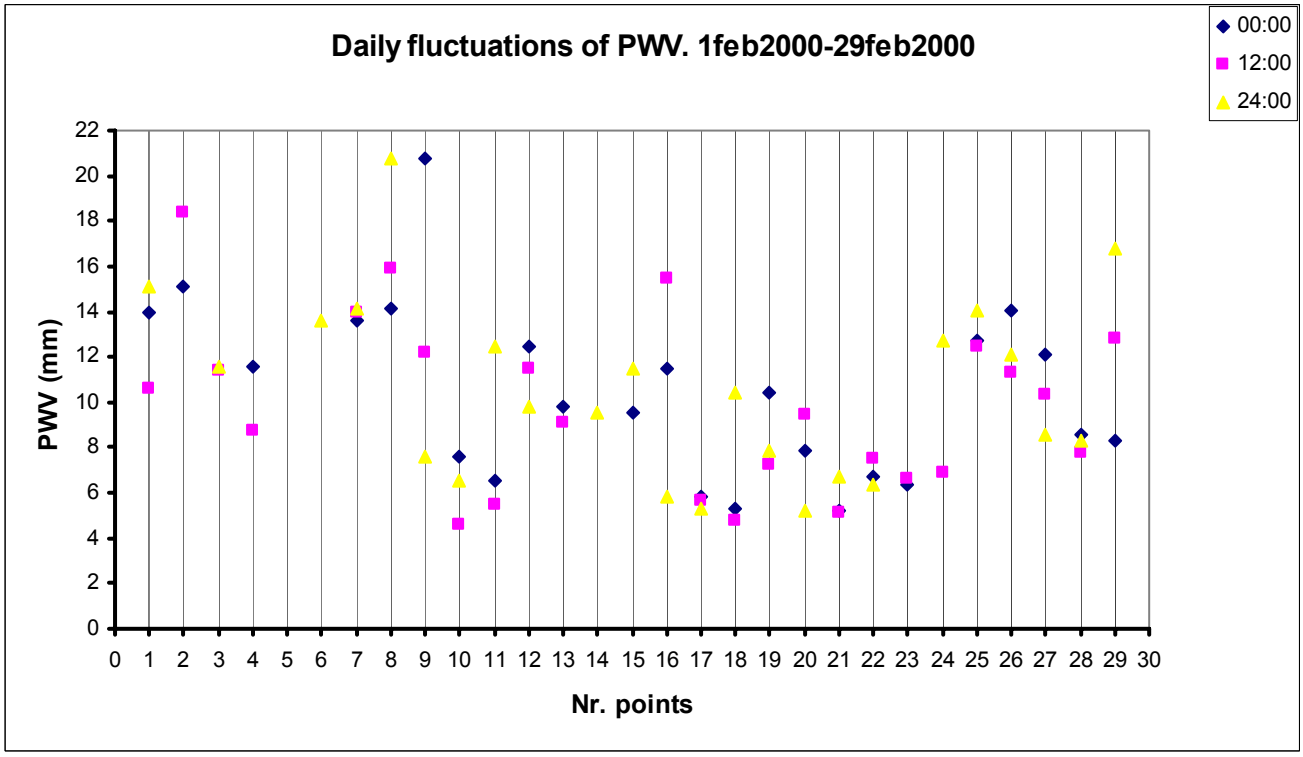

Fig. 3.1.2.7

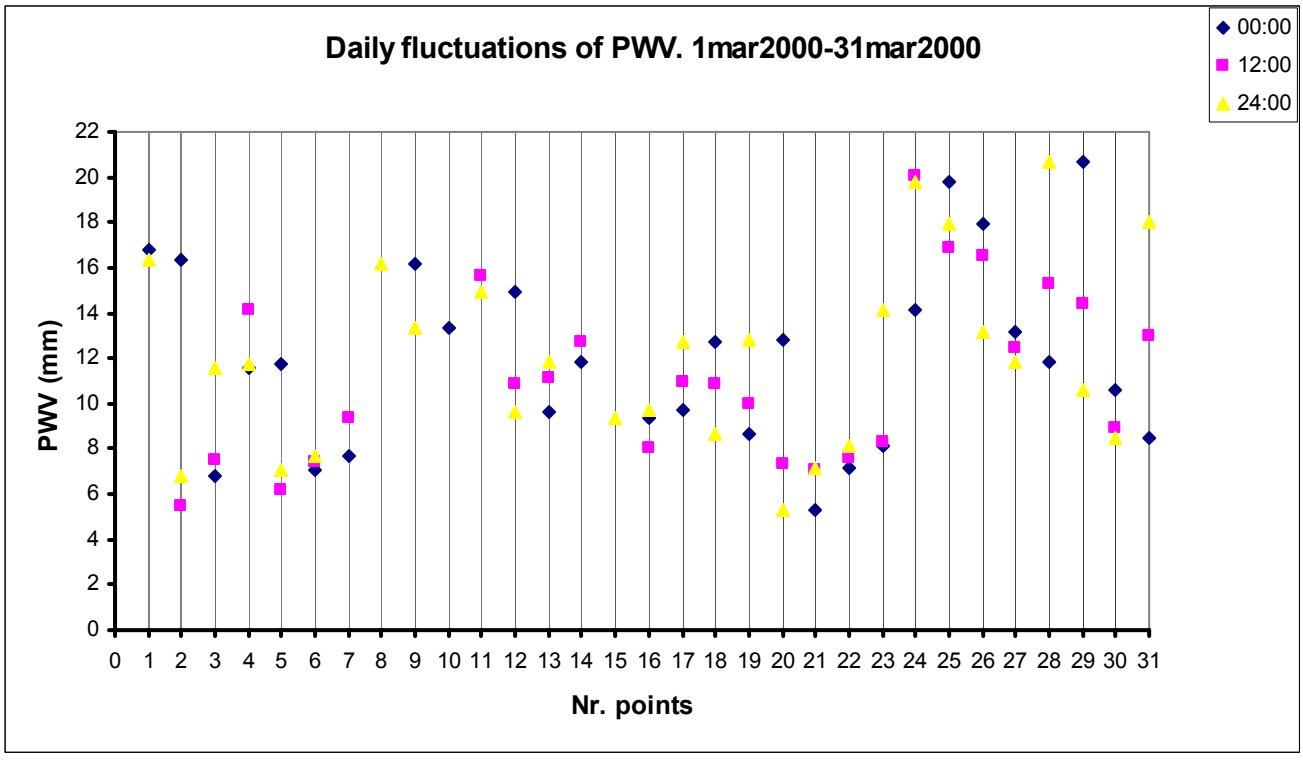

Fig. 3.1.2.8

2000-2001 WINTER

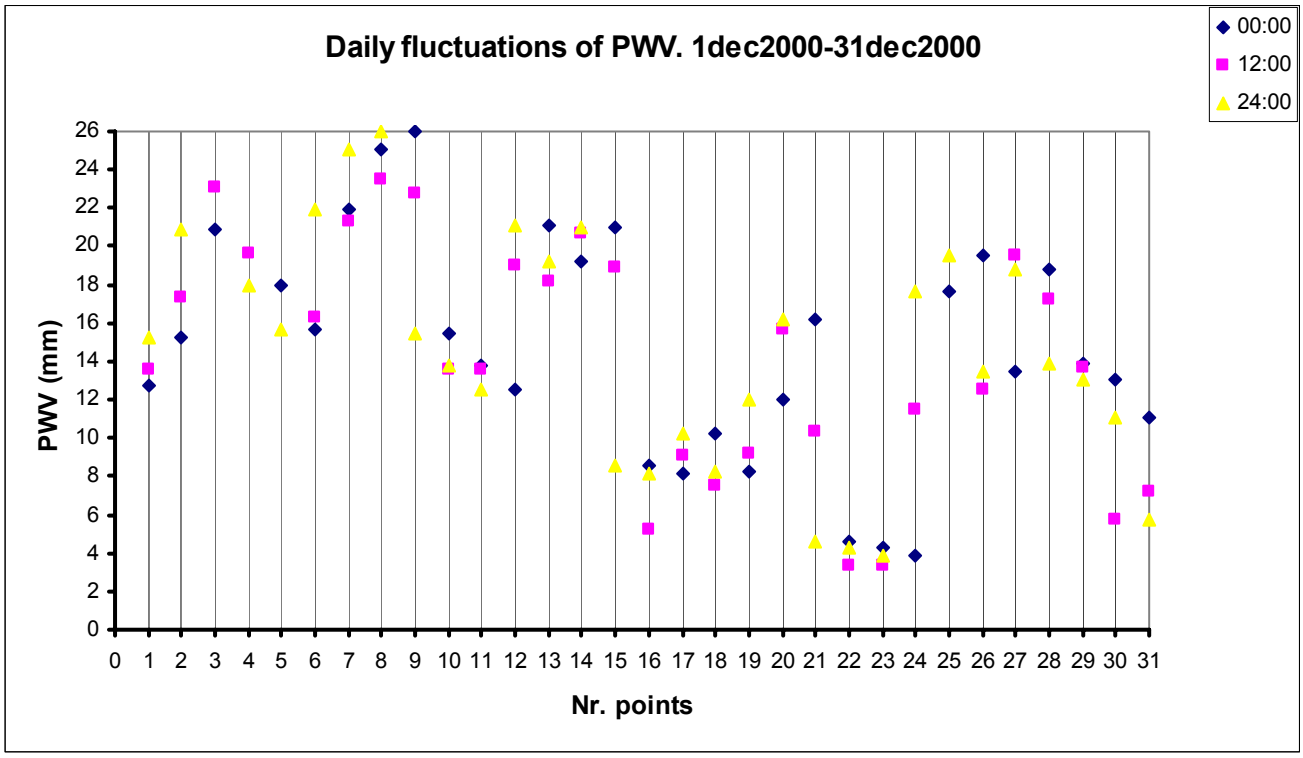

Fig. 3.1.2.9

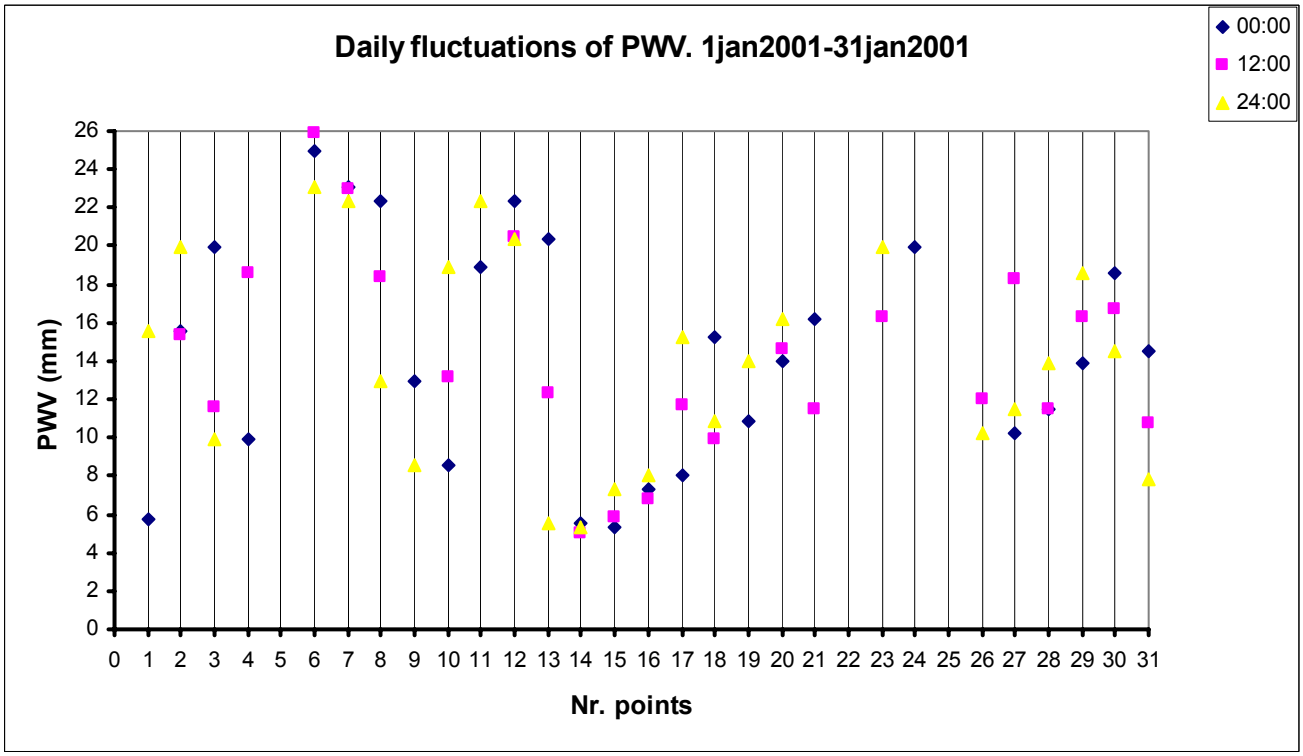

Fig. 3.1.2.10

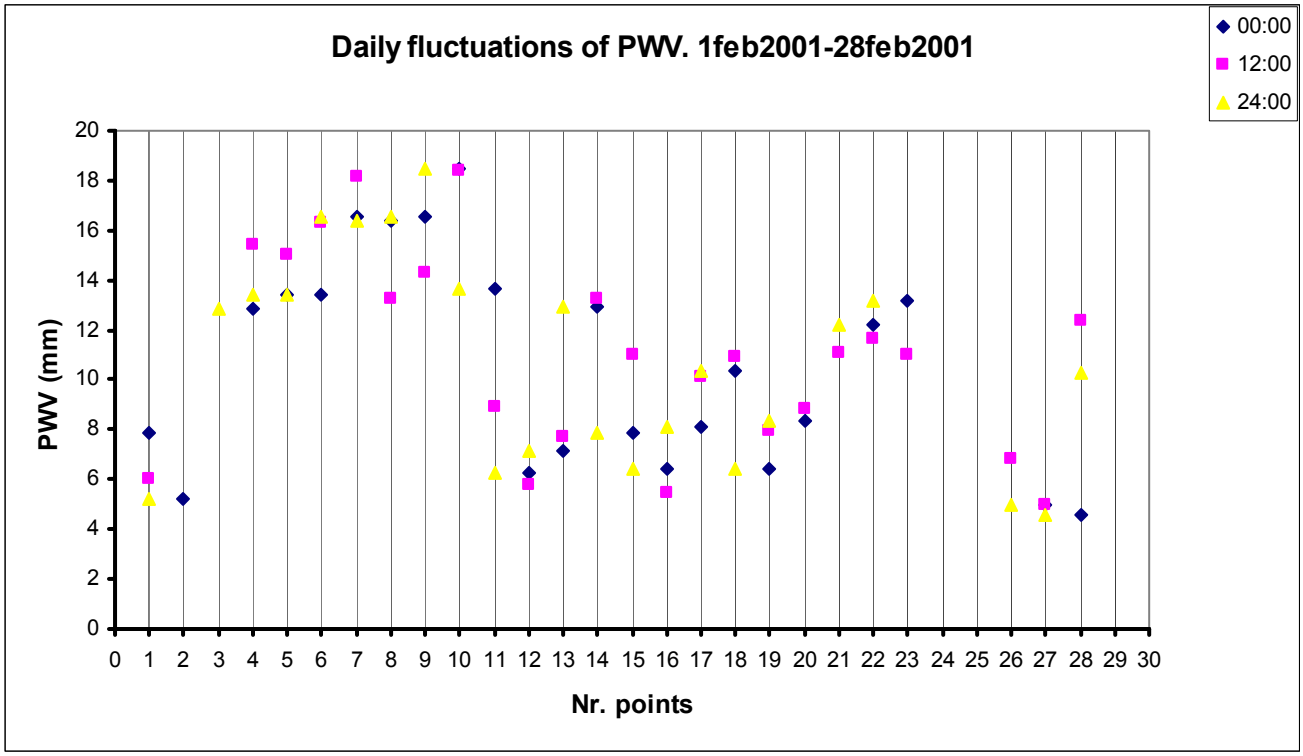

Fig. 3.1.2.11

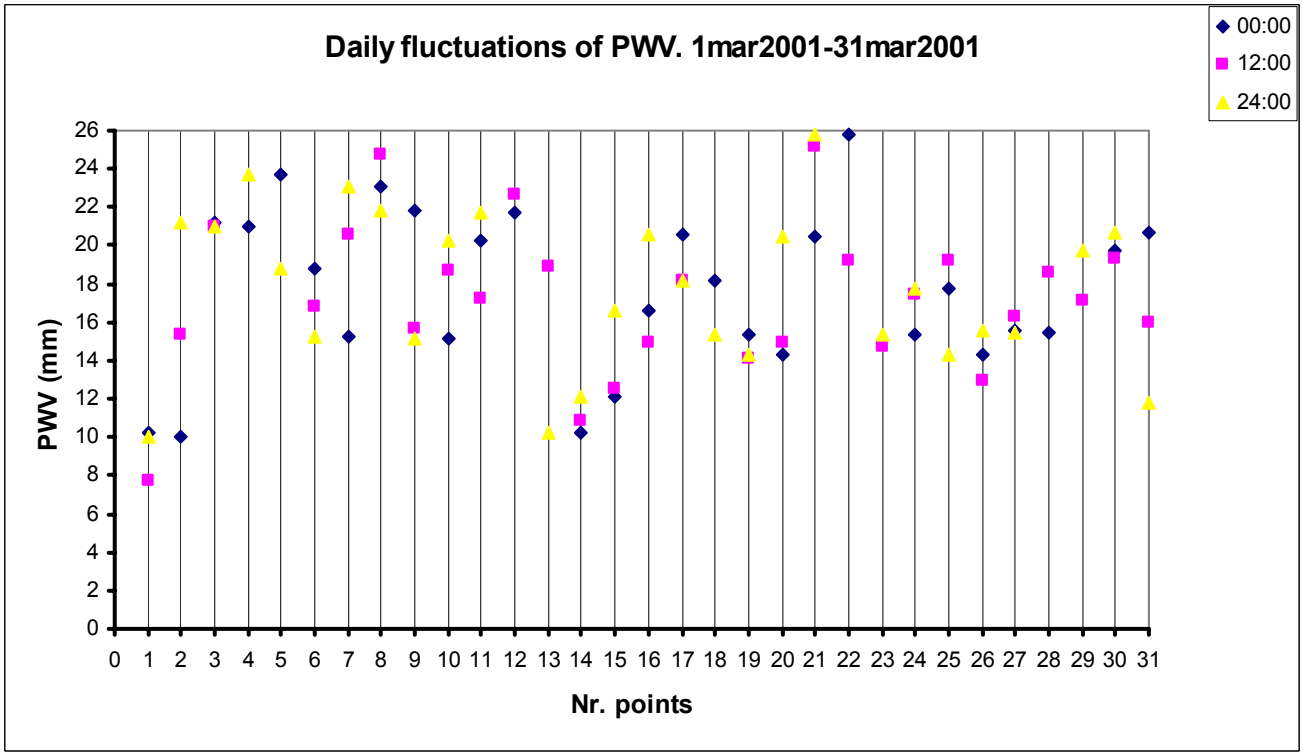

Fig. 3.1.2.12

2001-2002 WINTER

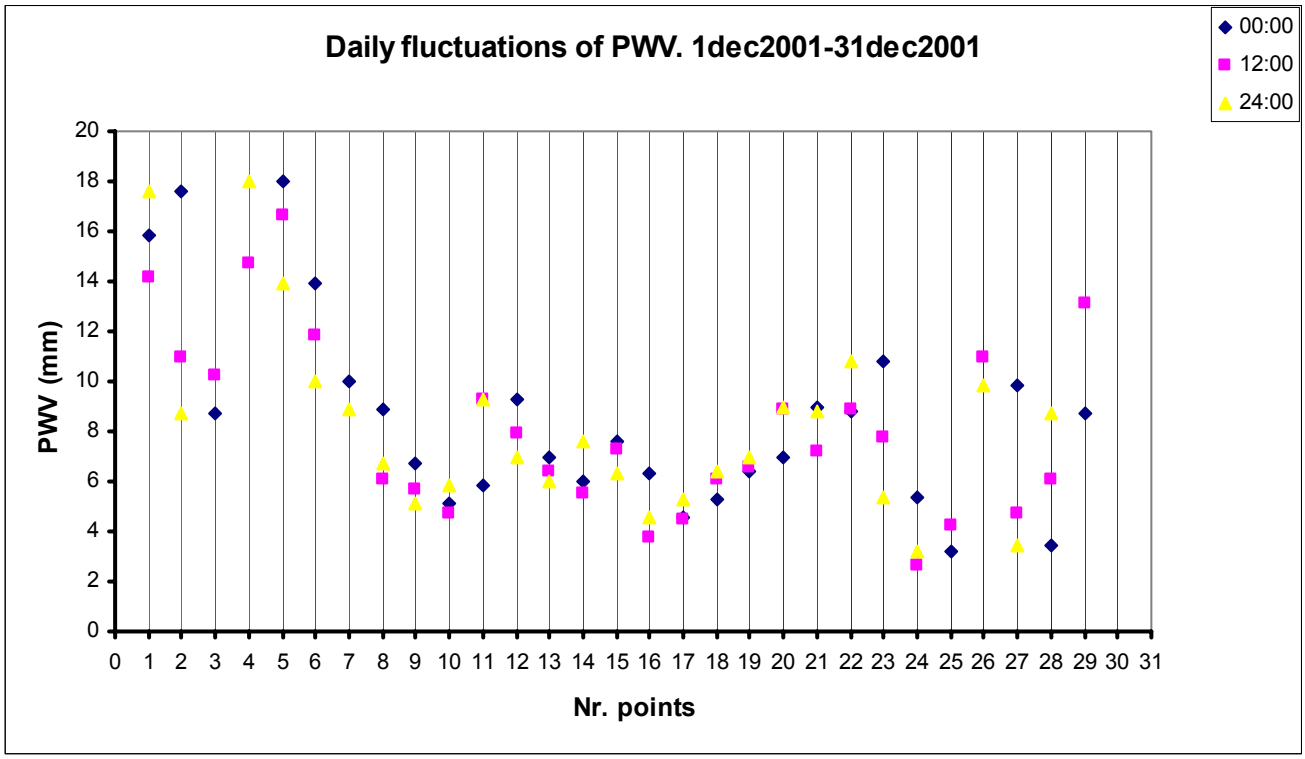

Fig. 3.1.2.13

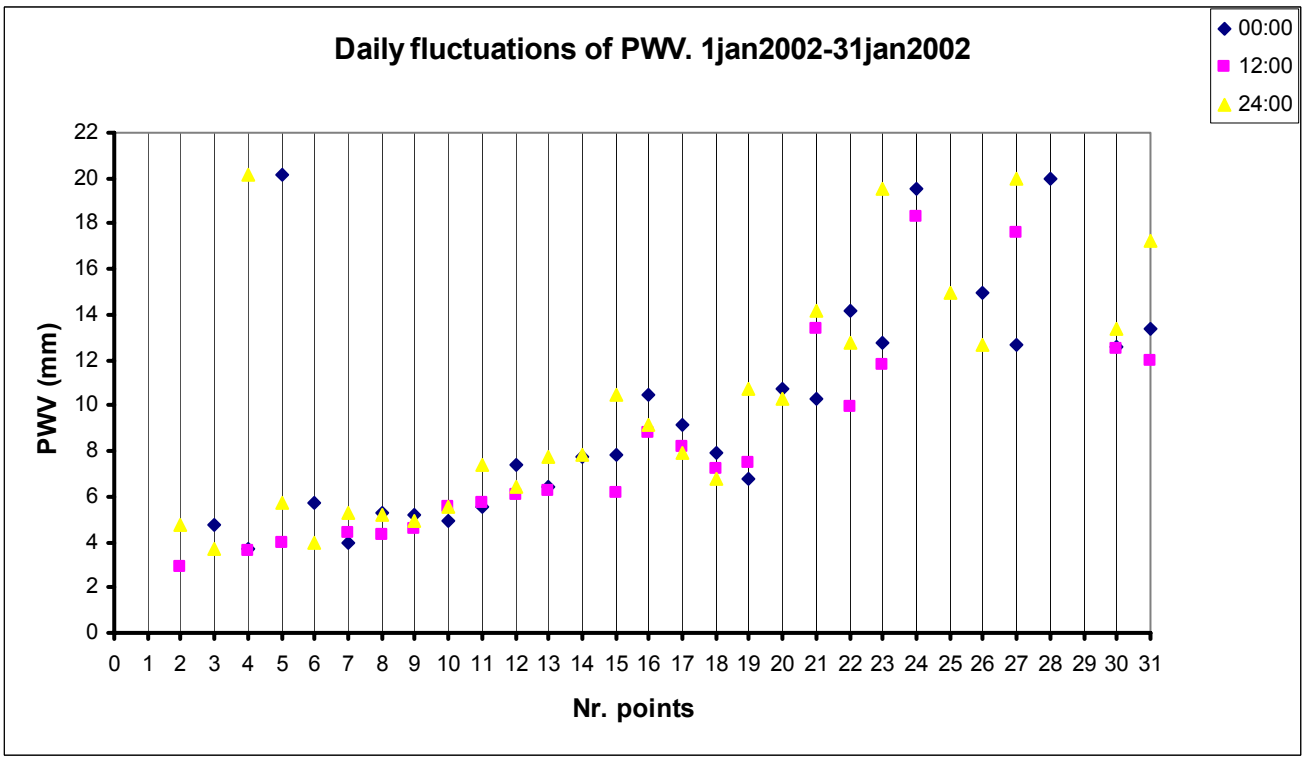

Fig. 3.1.2.14

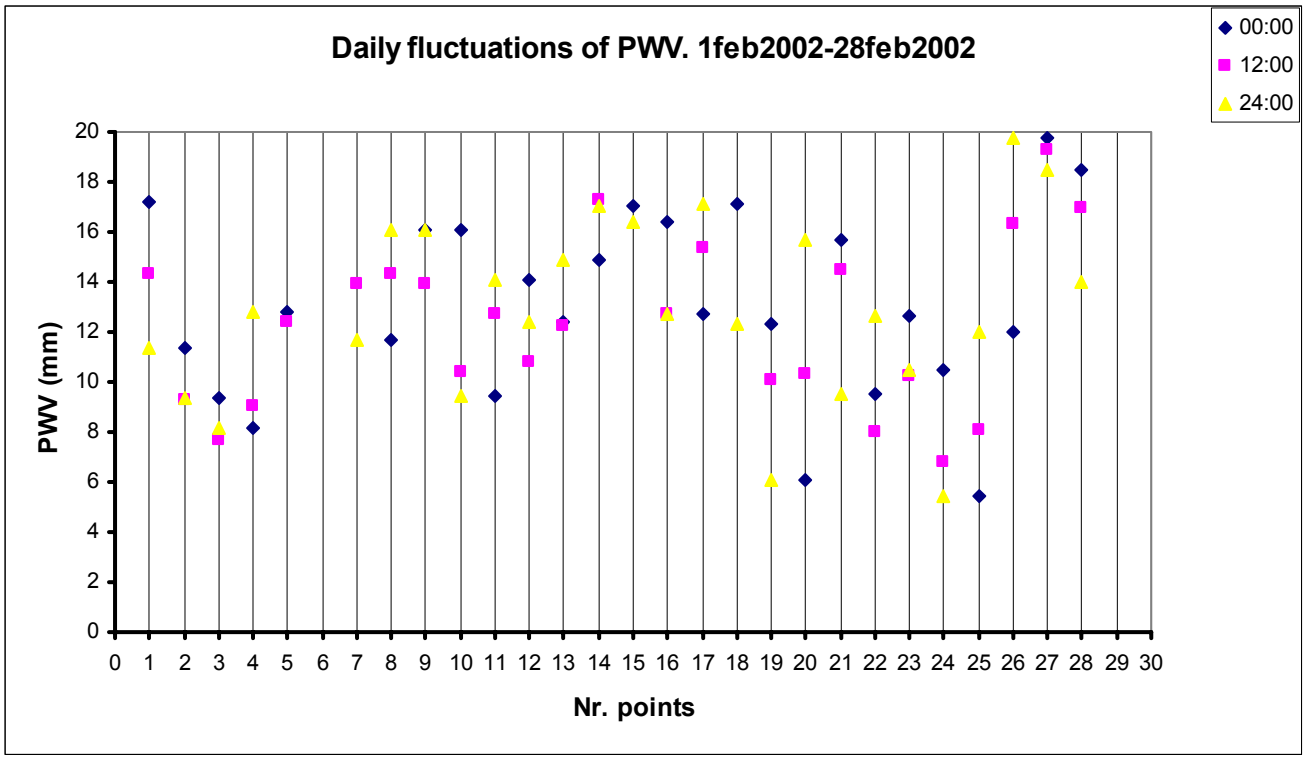

Fig. 3.1.2.15

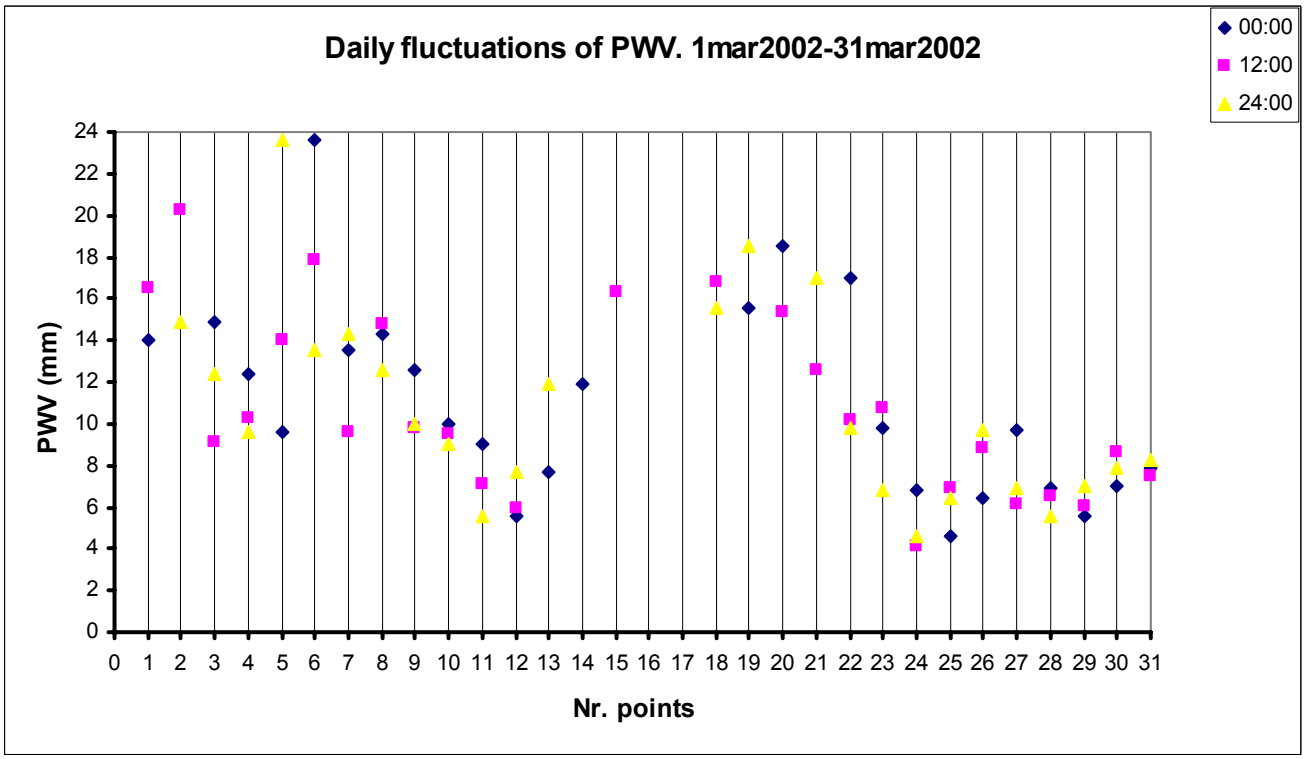

Fig. 3.1.2.16

2002-2003 WINTER

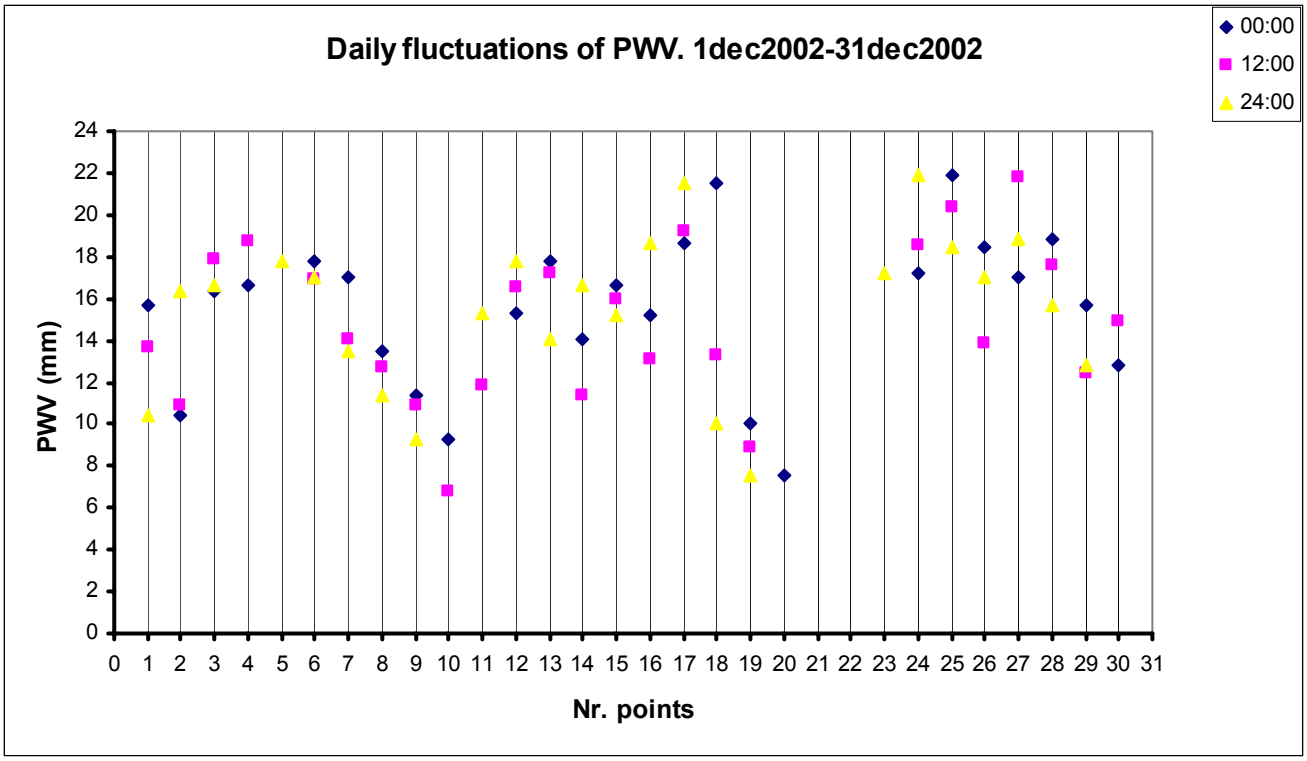

Fig. 3.1.2.17

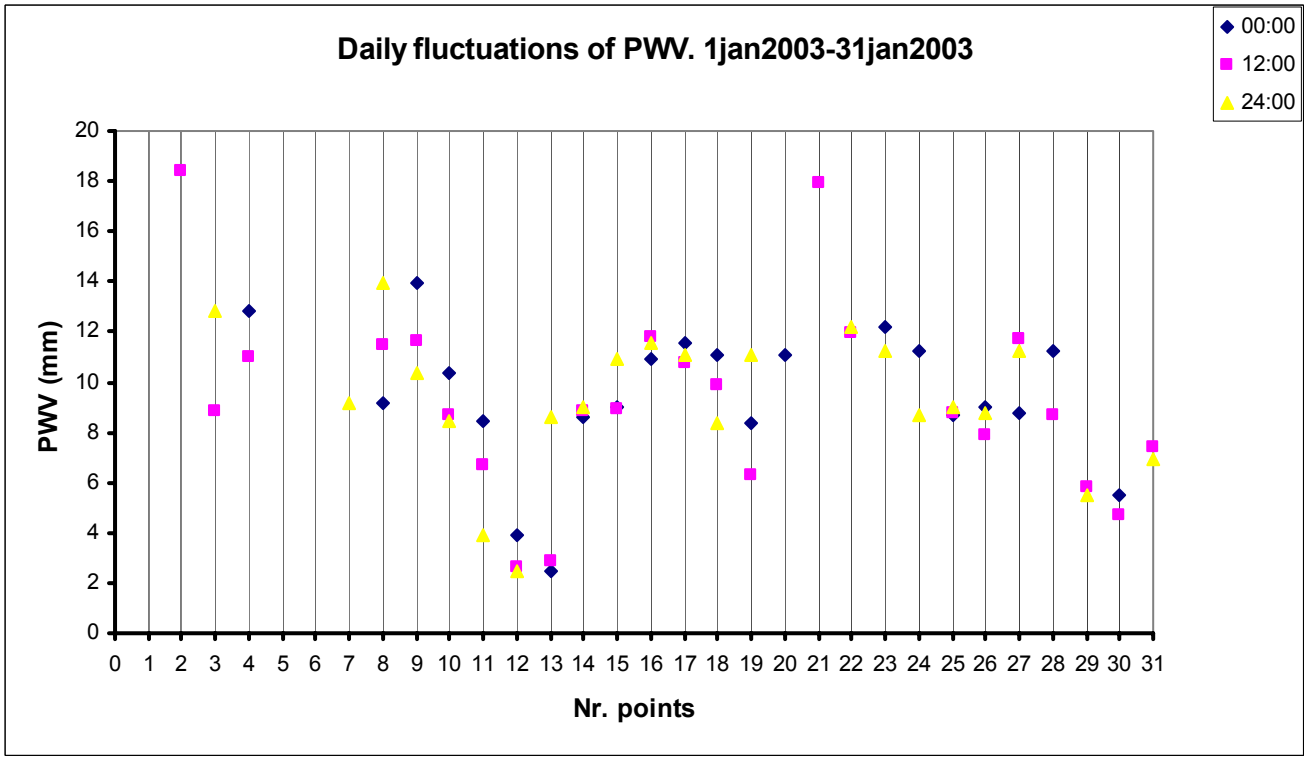

Fig. 3.1.2.18

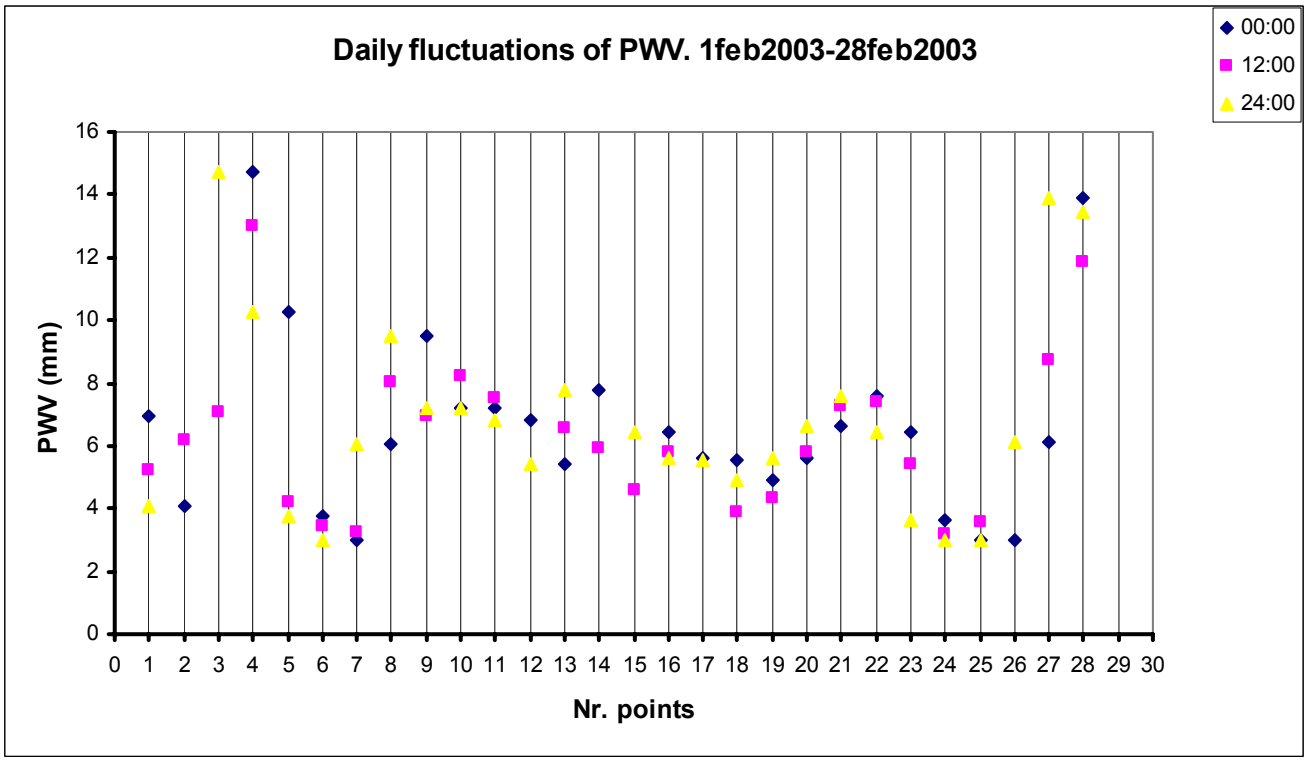

Fig. 3.1.2.19

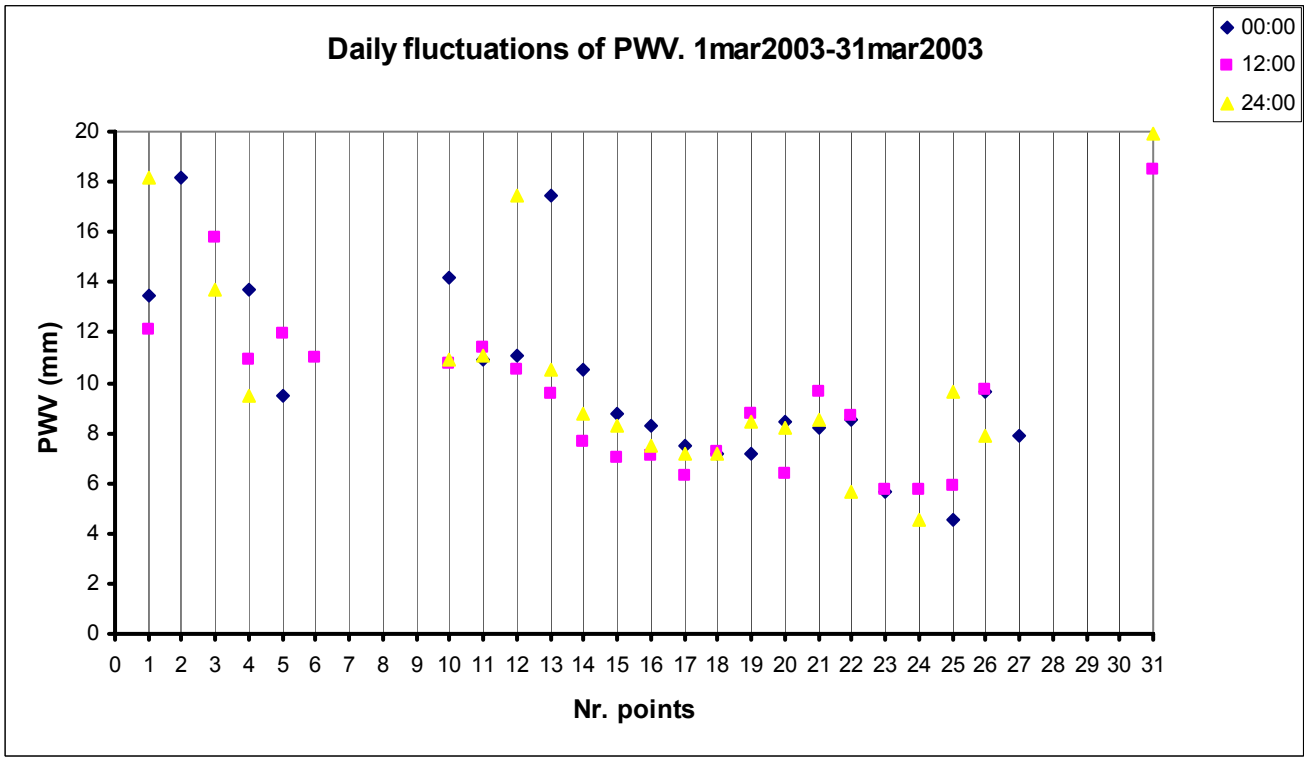

Fig. 3.1.2.20

2003-2004 WINTER

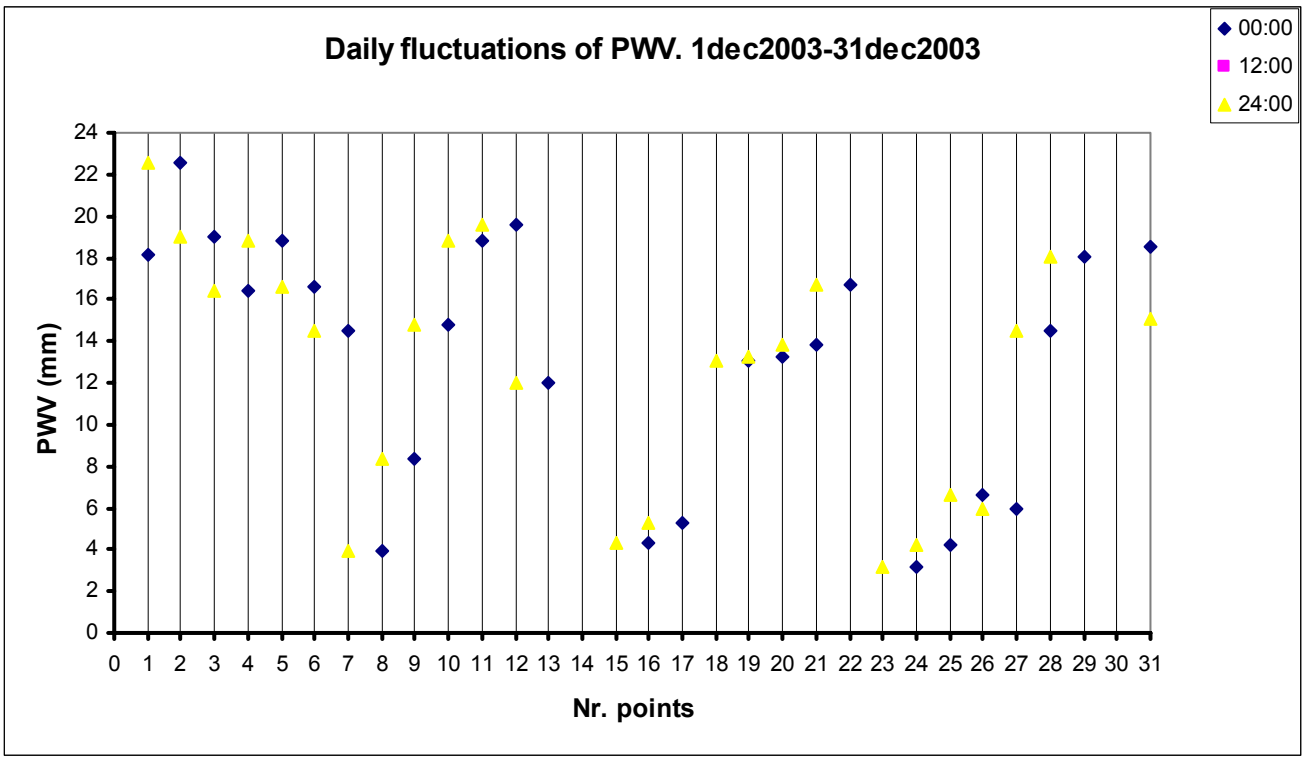

Fig. 3.1.2.21

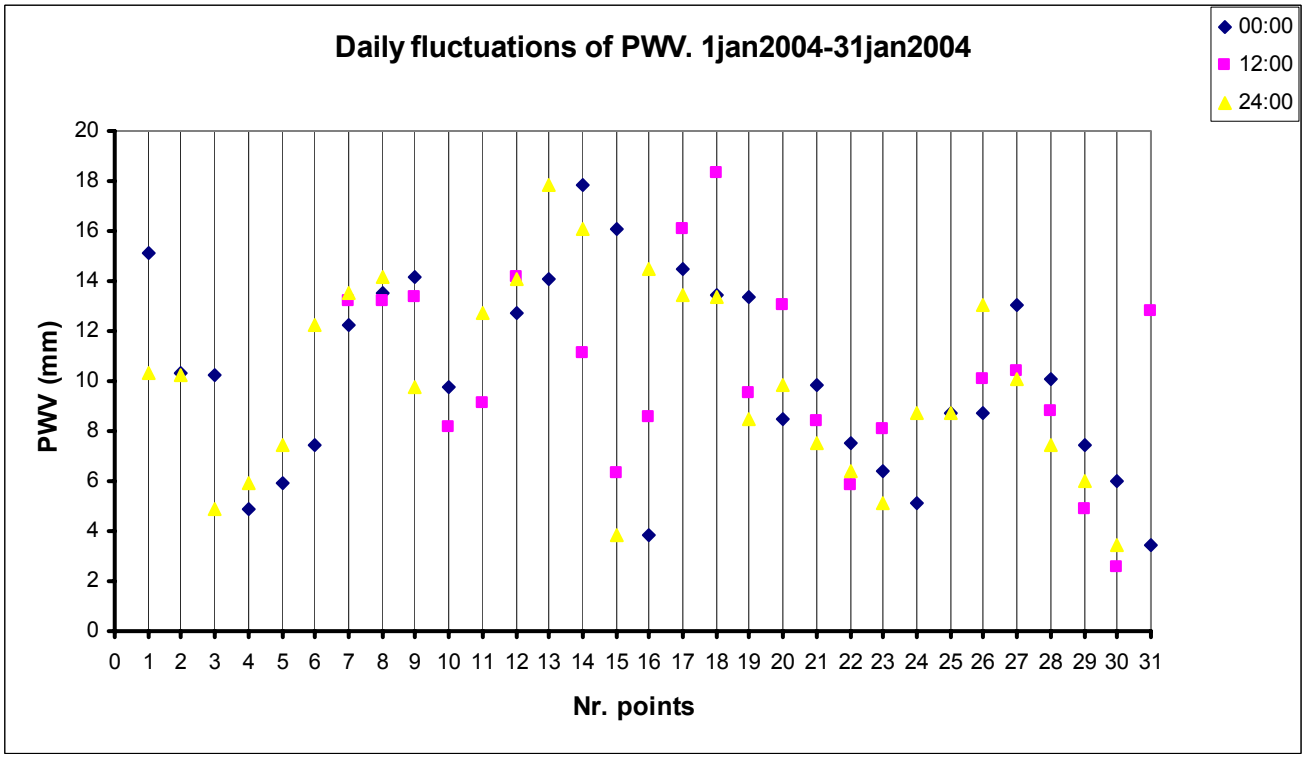

Fig. 3.1.2.22

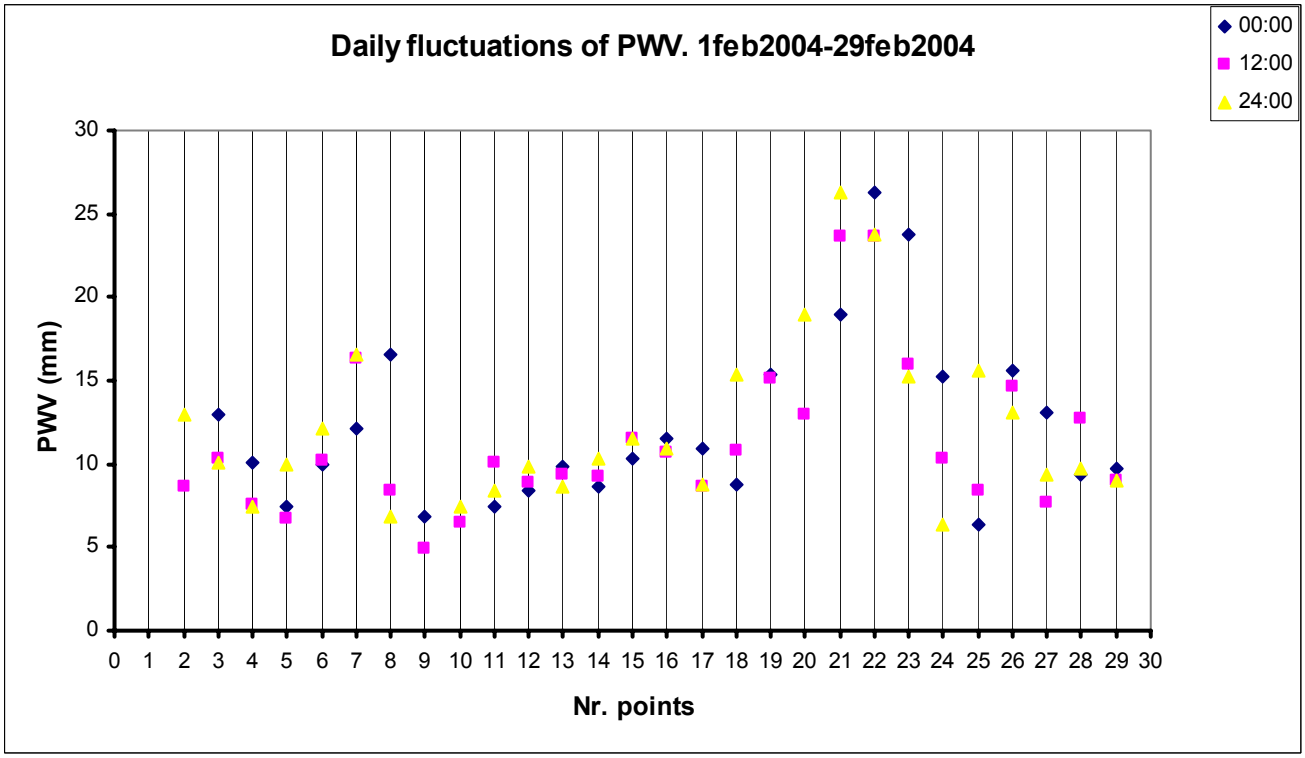

Fig. 3.1.2.23

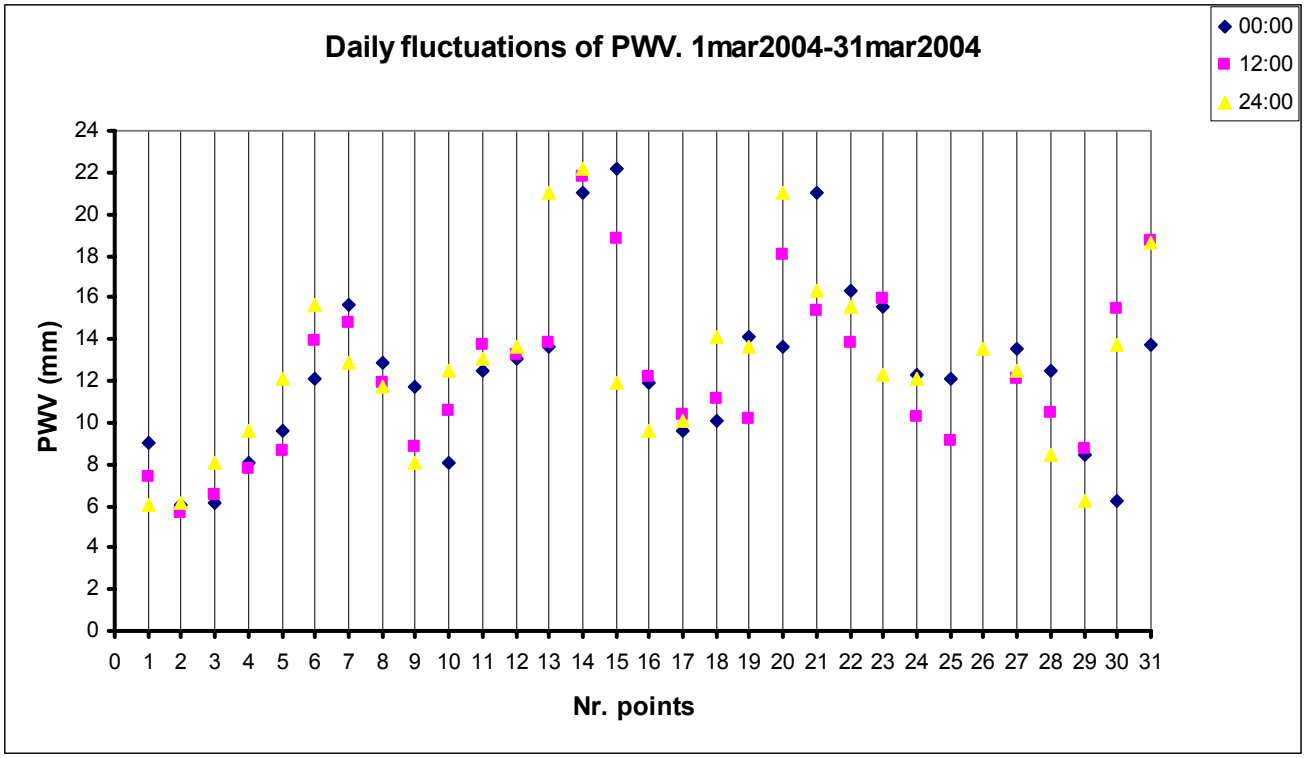

Fig. 3.1.2.24

2004-2005 WINTER

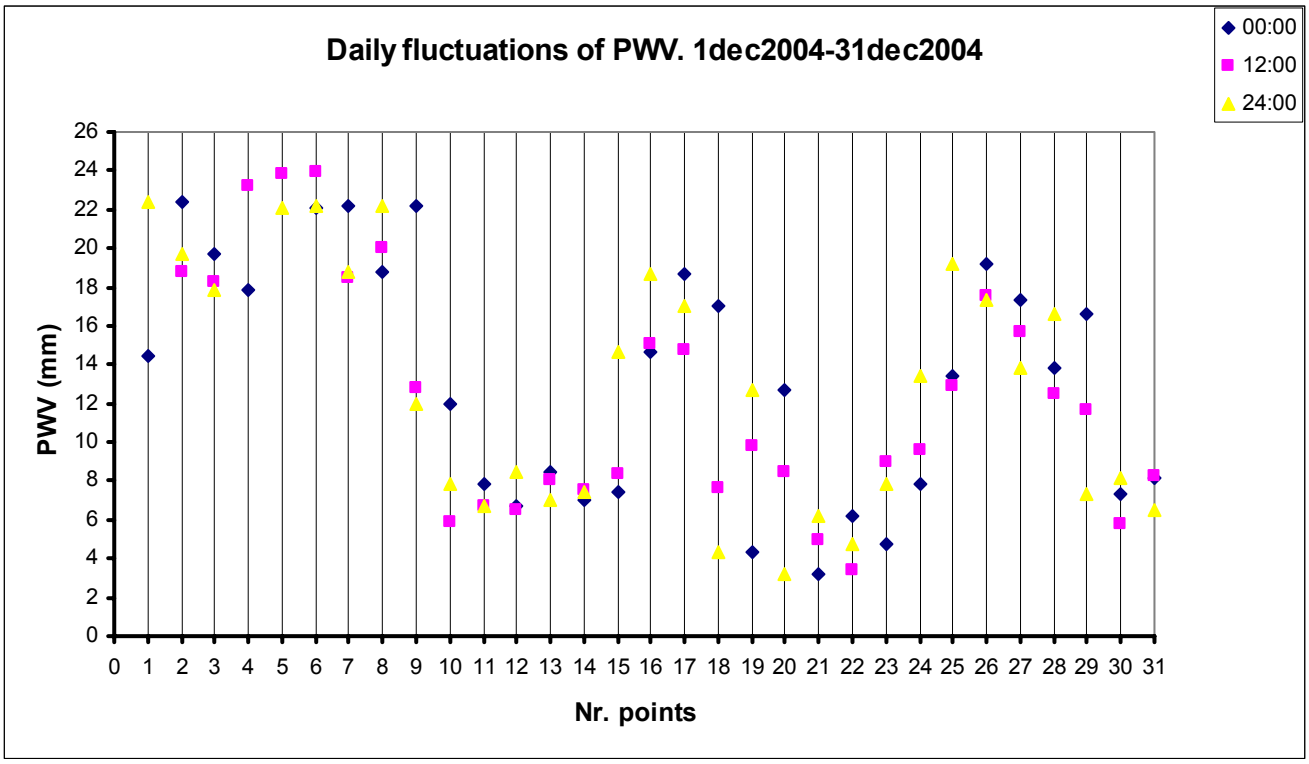

Fig. 3.1.2.25

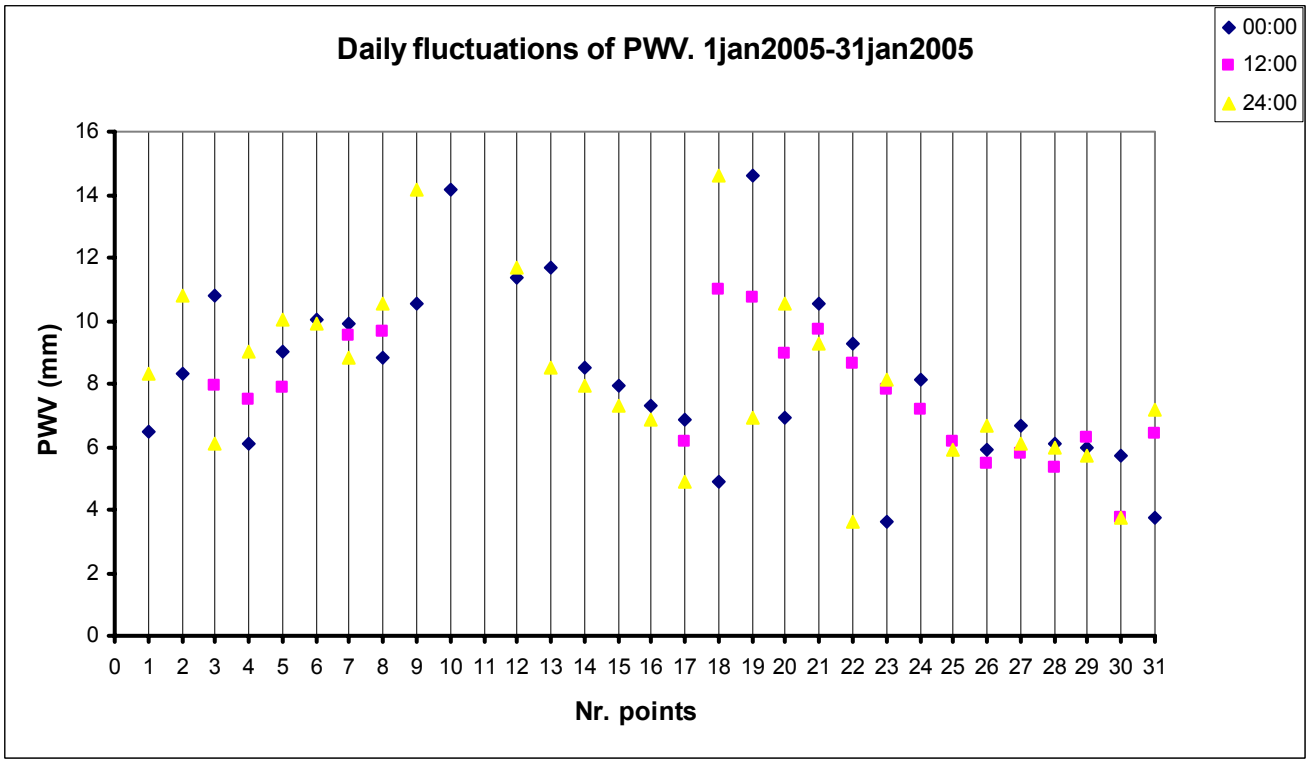

Fig. 3.1.2.26

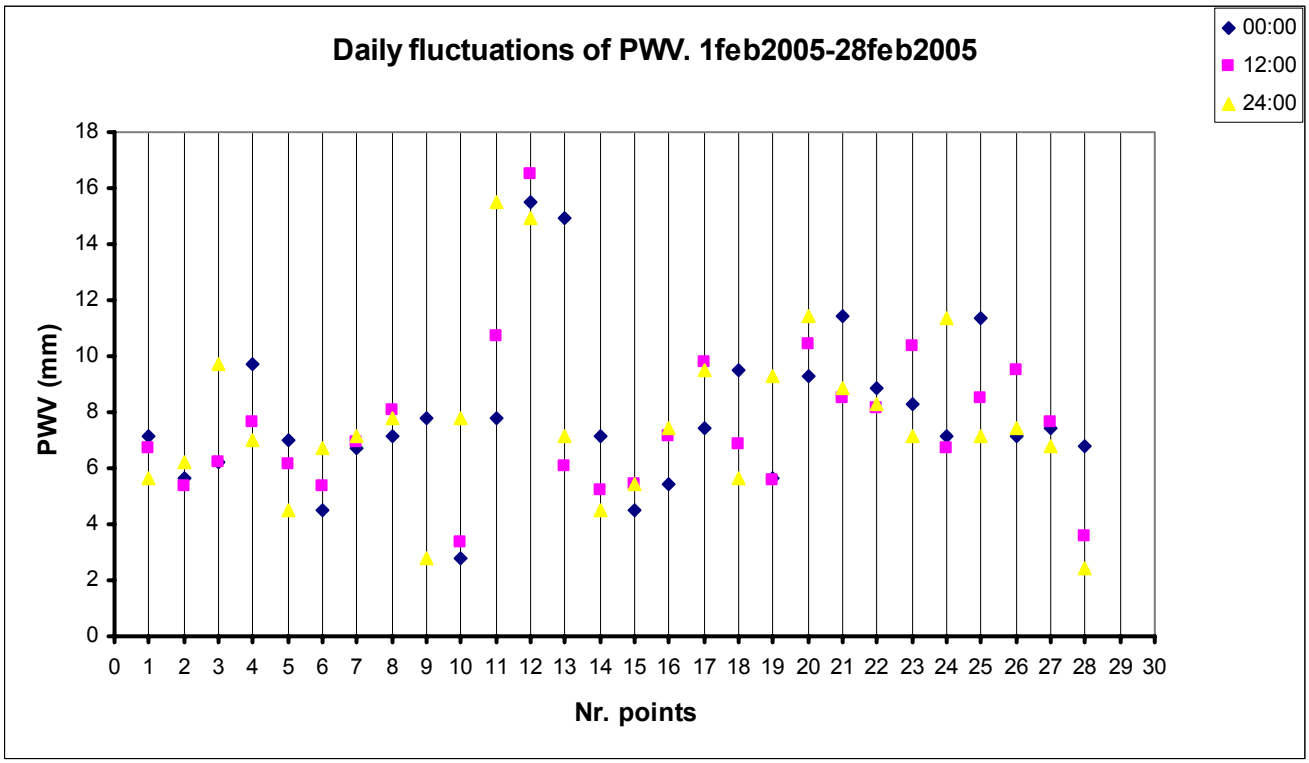

Fig. 3.1.2.27

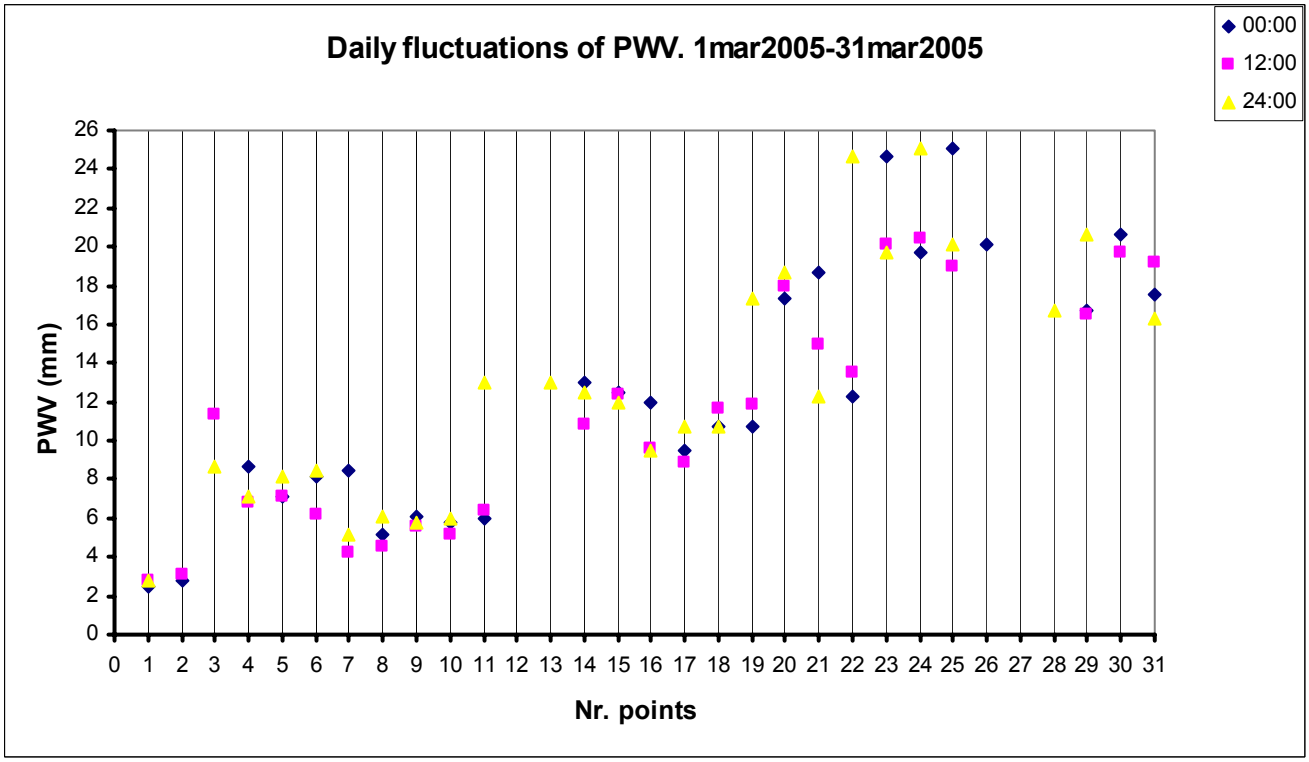

Fig. 3.1.2.28

2005-2006 WINTER

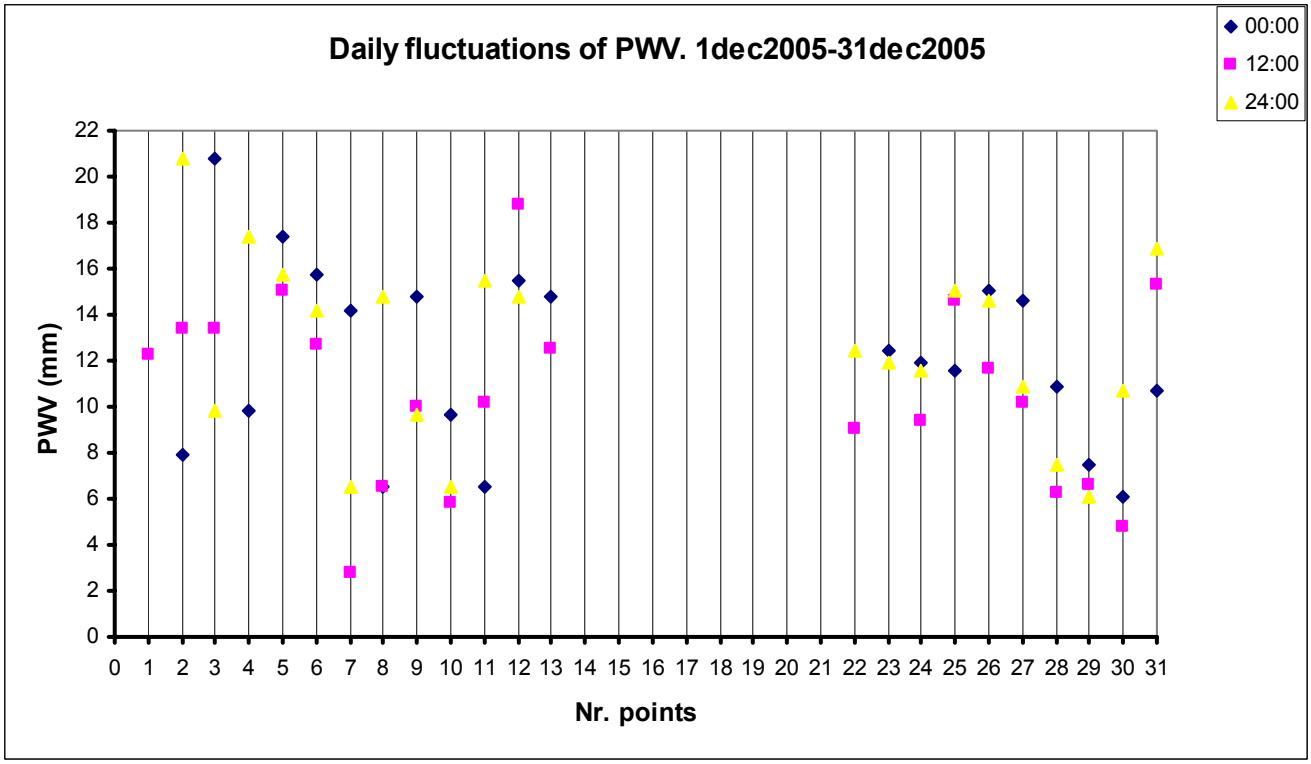

Fig. 3.1.2.29

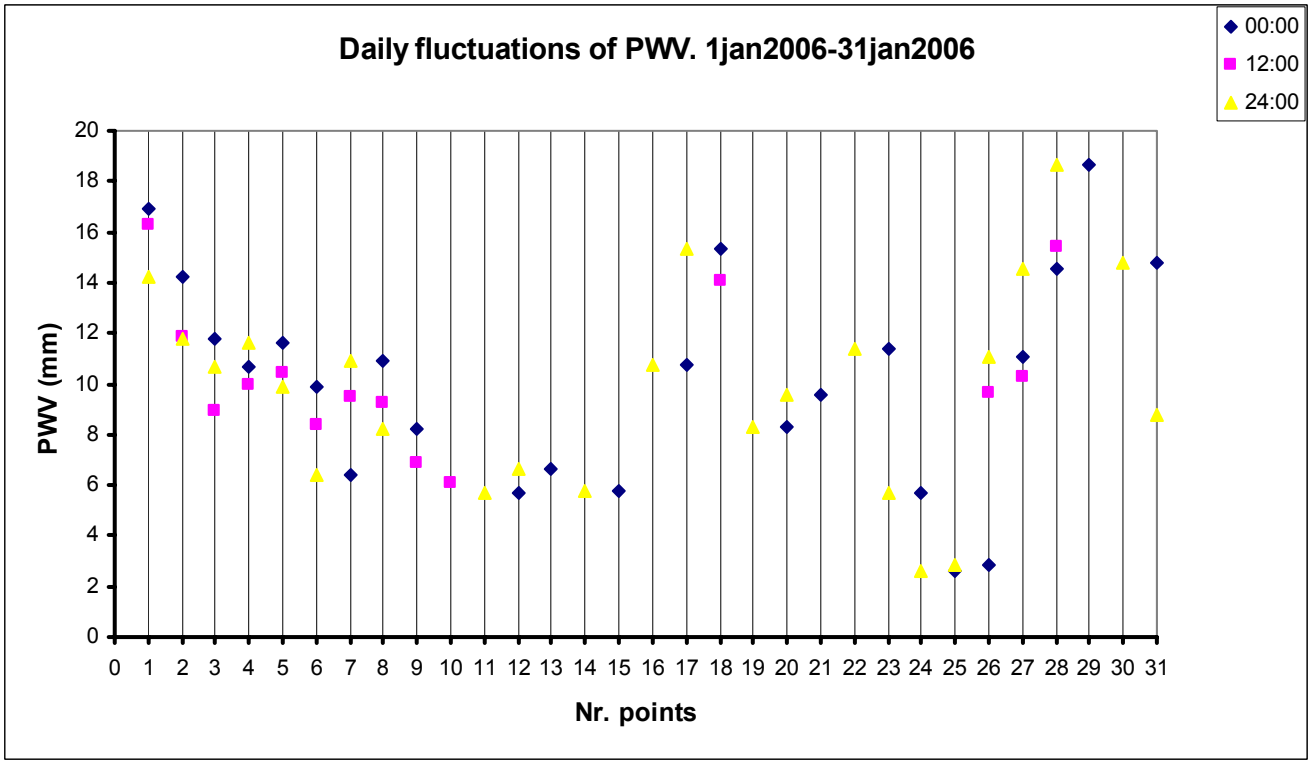

Fig. 3.1.2.30

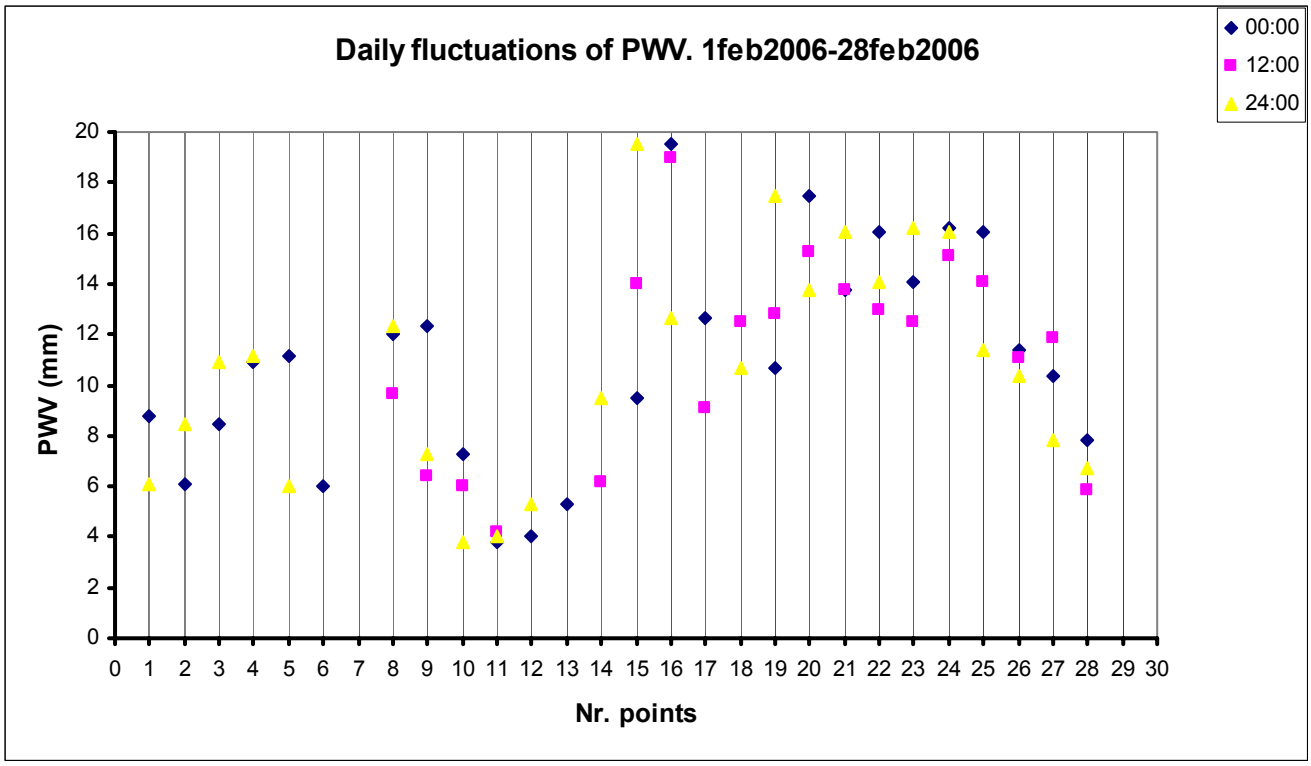

Fig. 3.1.2.31

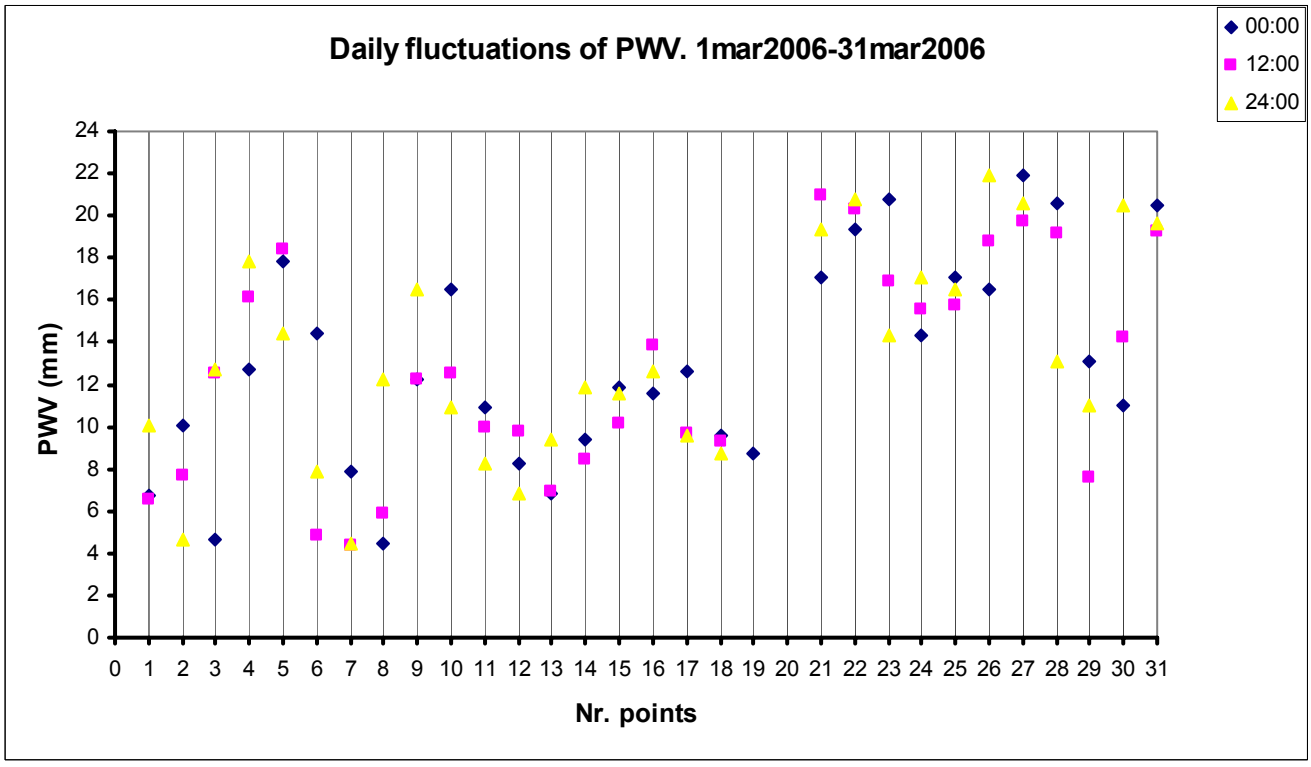

Fig. 3.1.2.32

2006-2007 WINTER

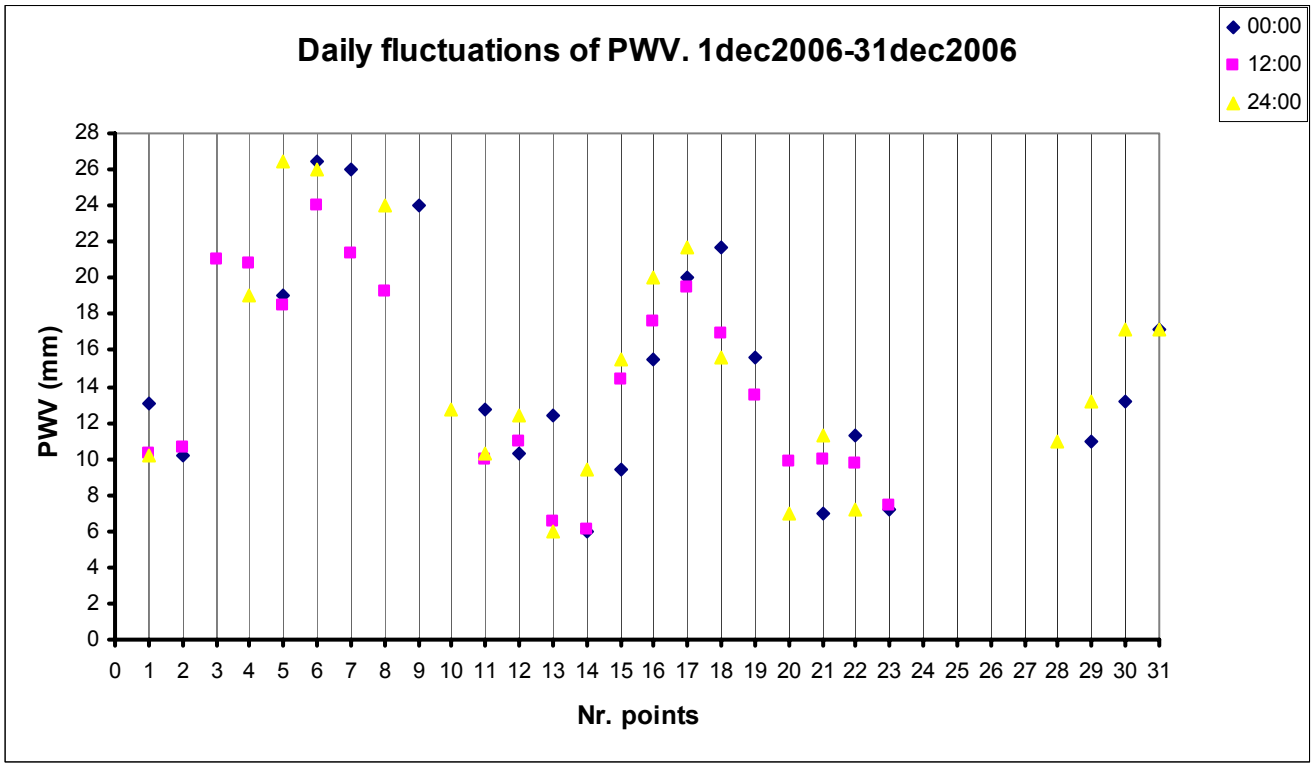

Fig. 3.1.2.33

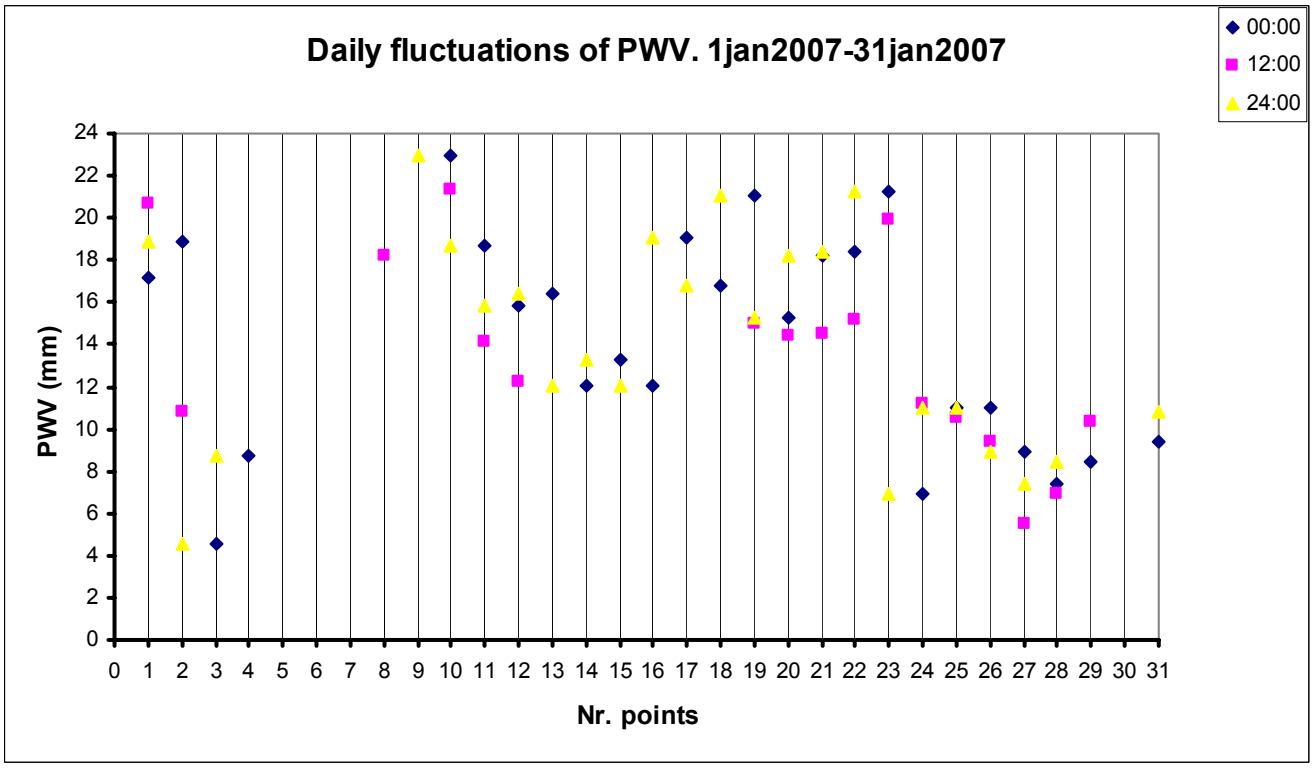

Fig. 3.1.2.34

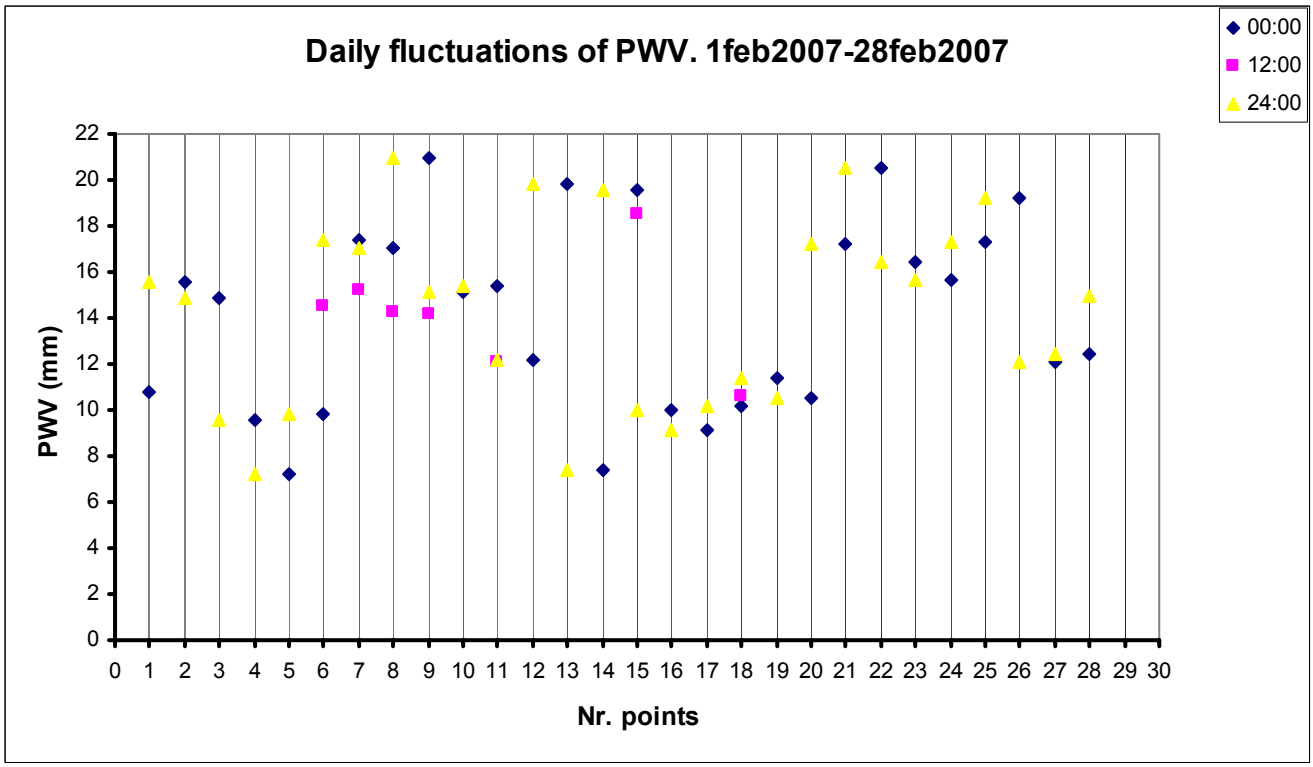

Fig. 3.1.2.35

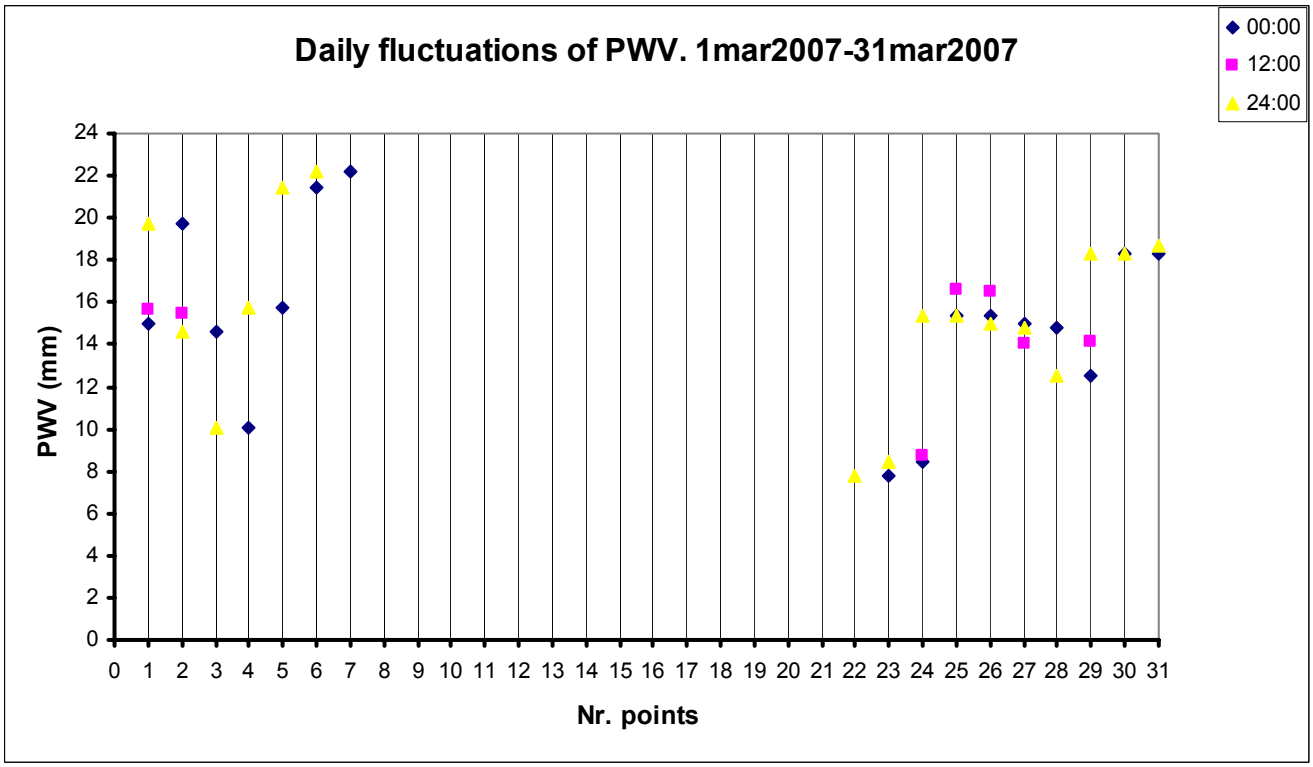

Fig. 3.1.2.36

1998-1999 WINTER STATISTICS

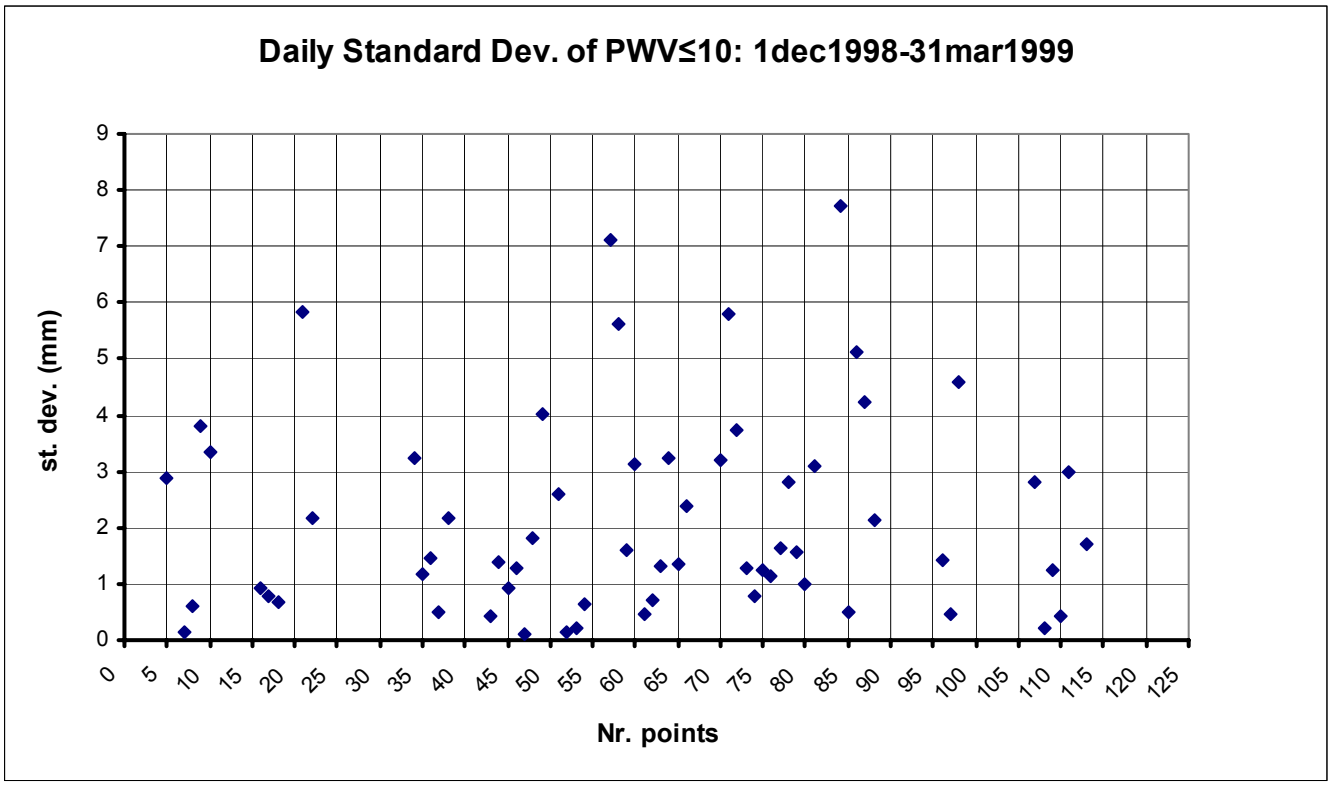

Fig. 3.1.2.37

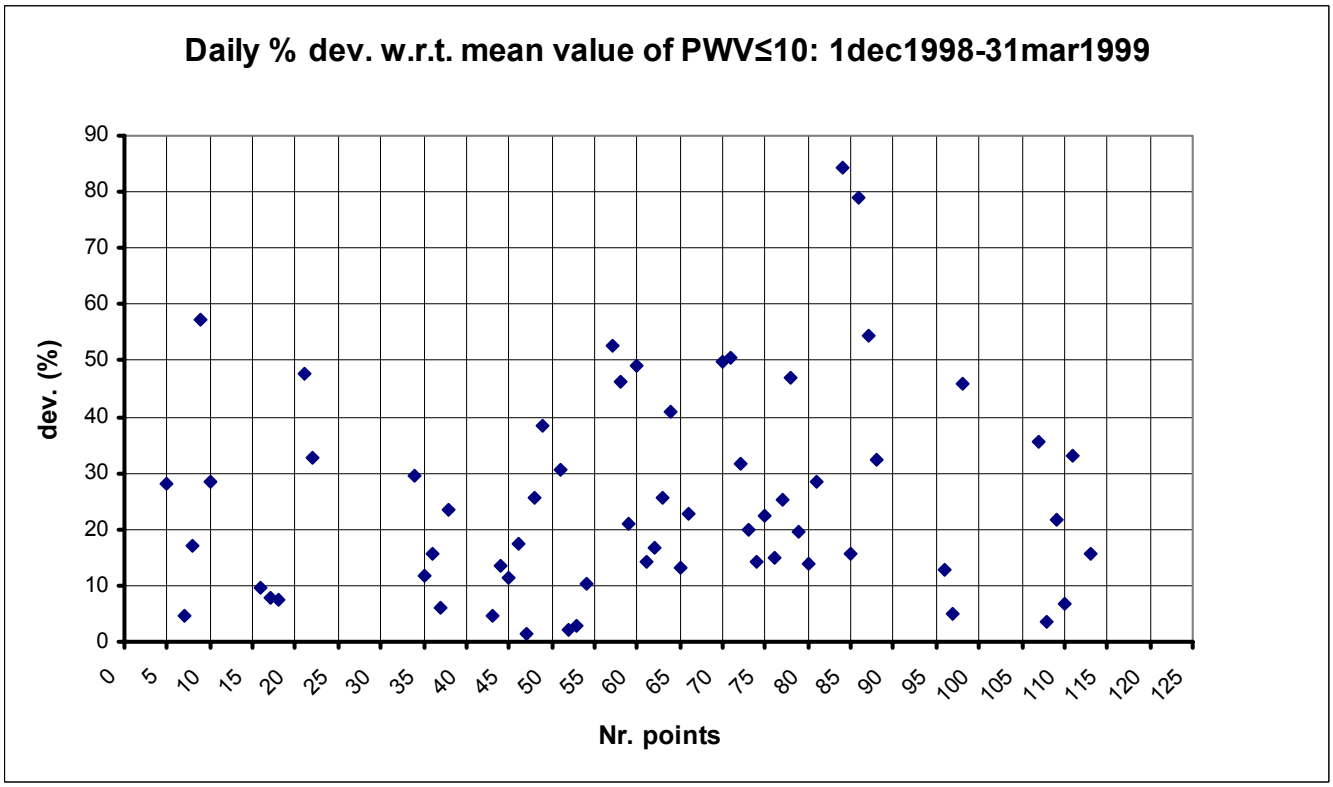

Fig. 3.1.2.38

1999-2000 WINTER STATISTICS

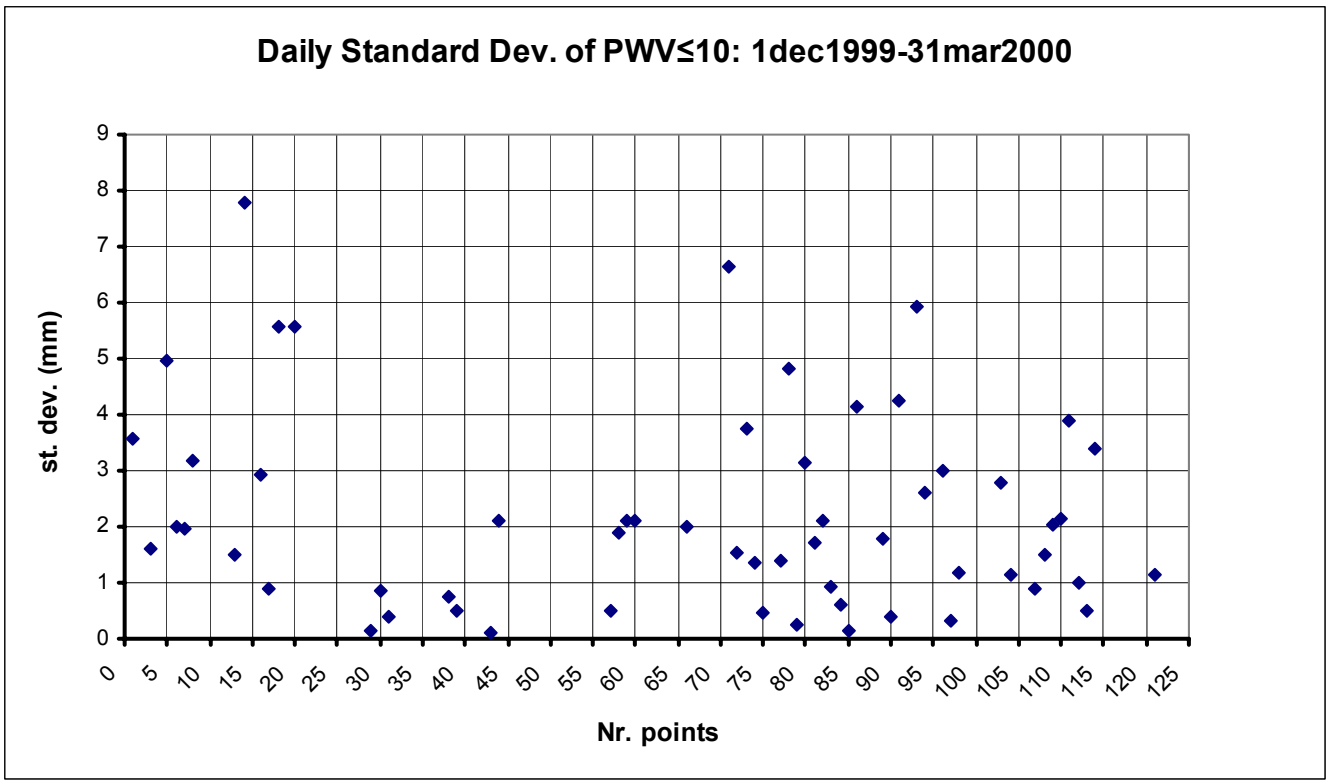

Fig. 3.1.2.39

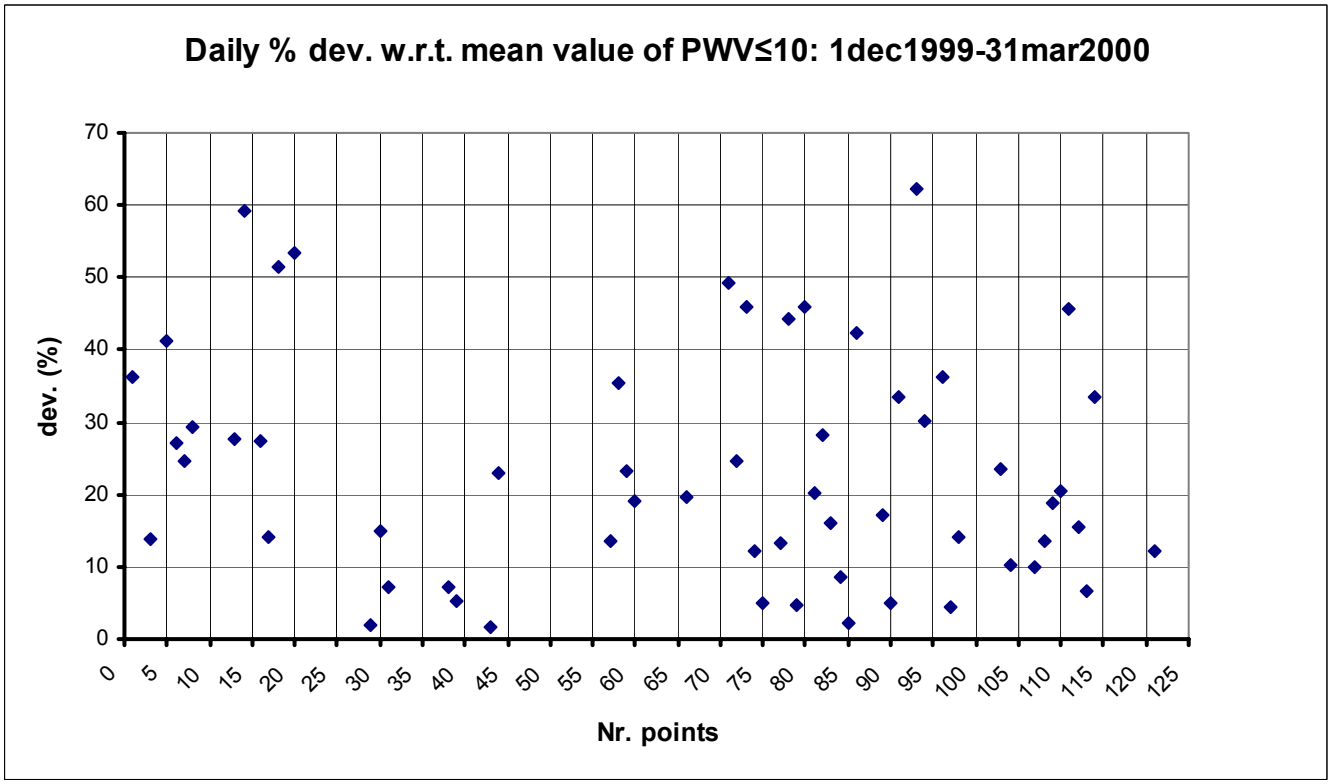

Fig. 3.1.2.40

2000-2001 WINTER STATISTICS

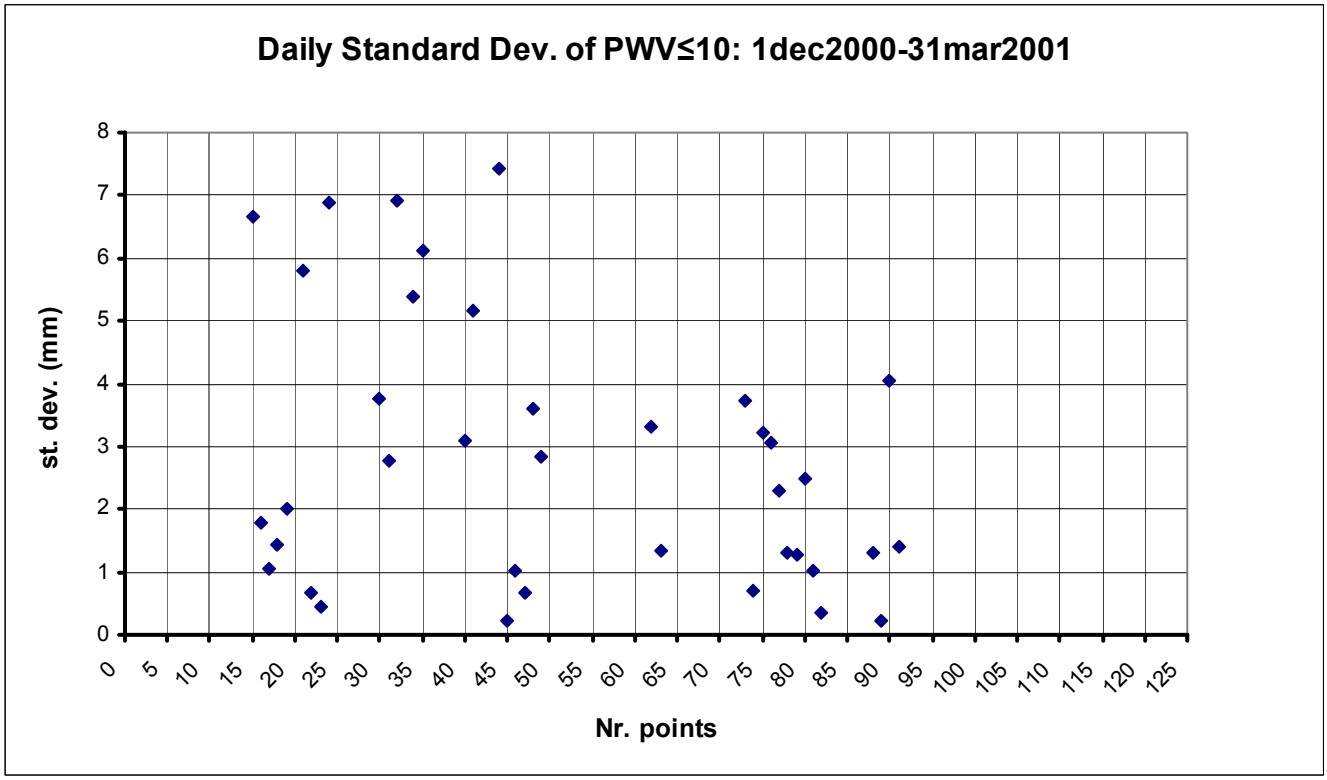

Fig. 3.1.2.41

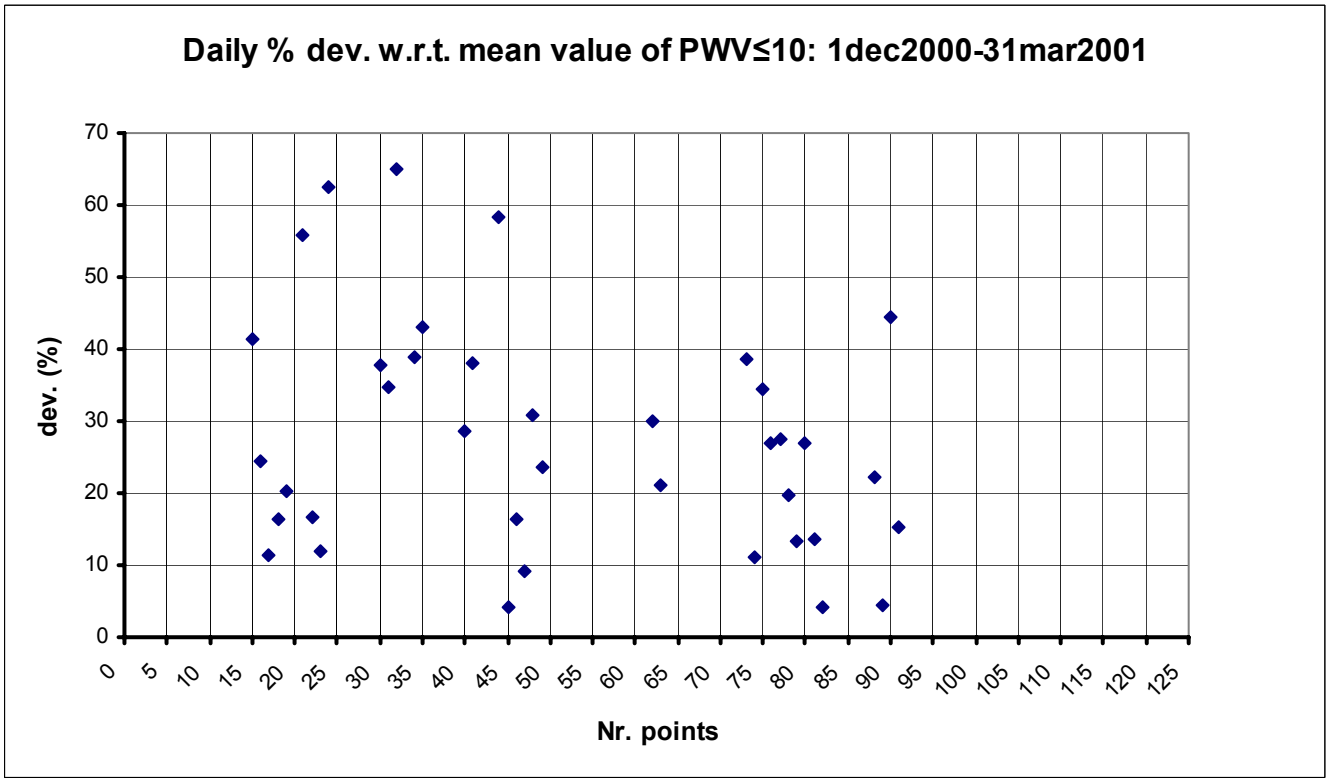

Fig. 3.1.2.42

2001-2002 WINTER STATISTICS

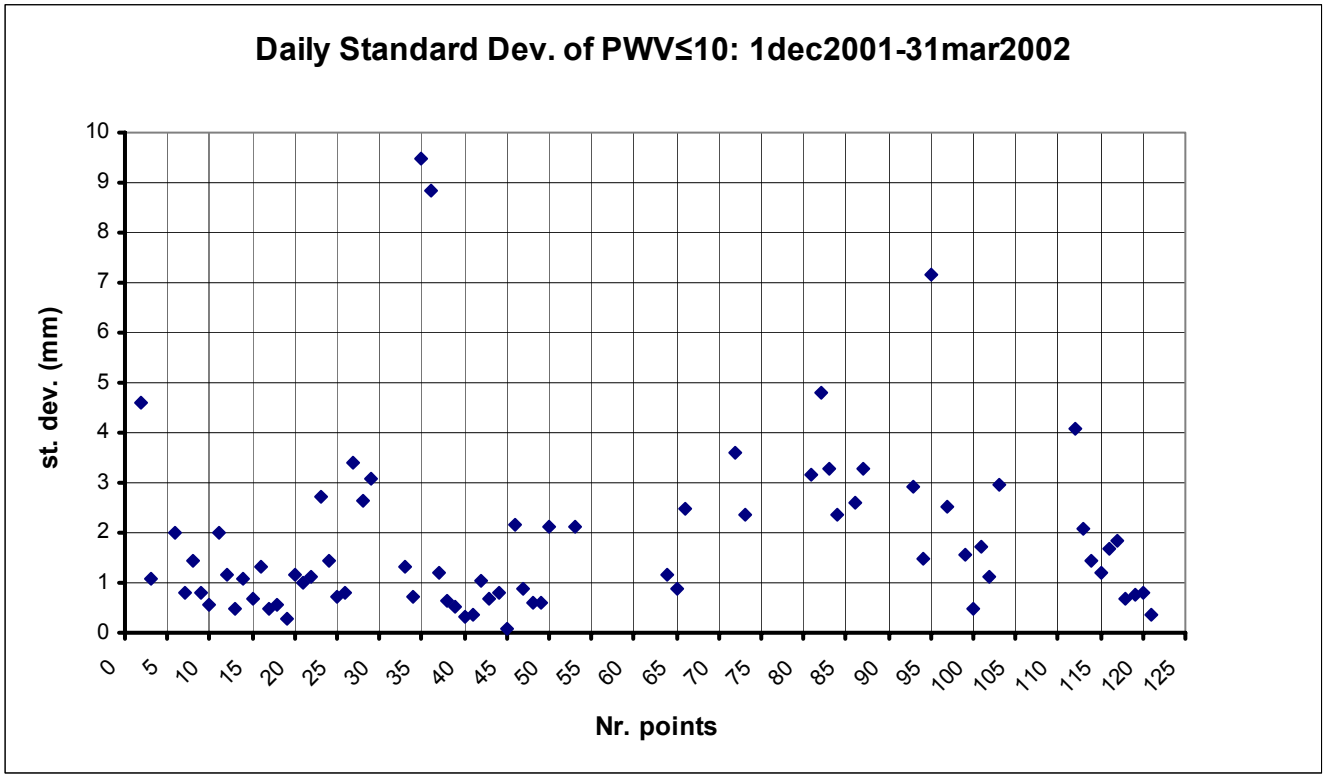

Fig. 3.1.2.43

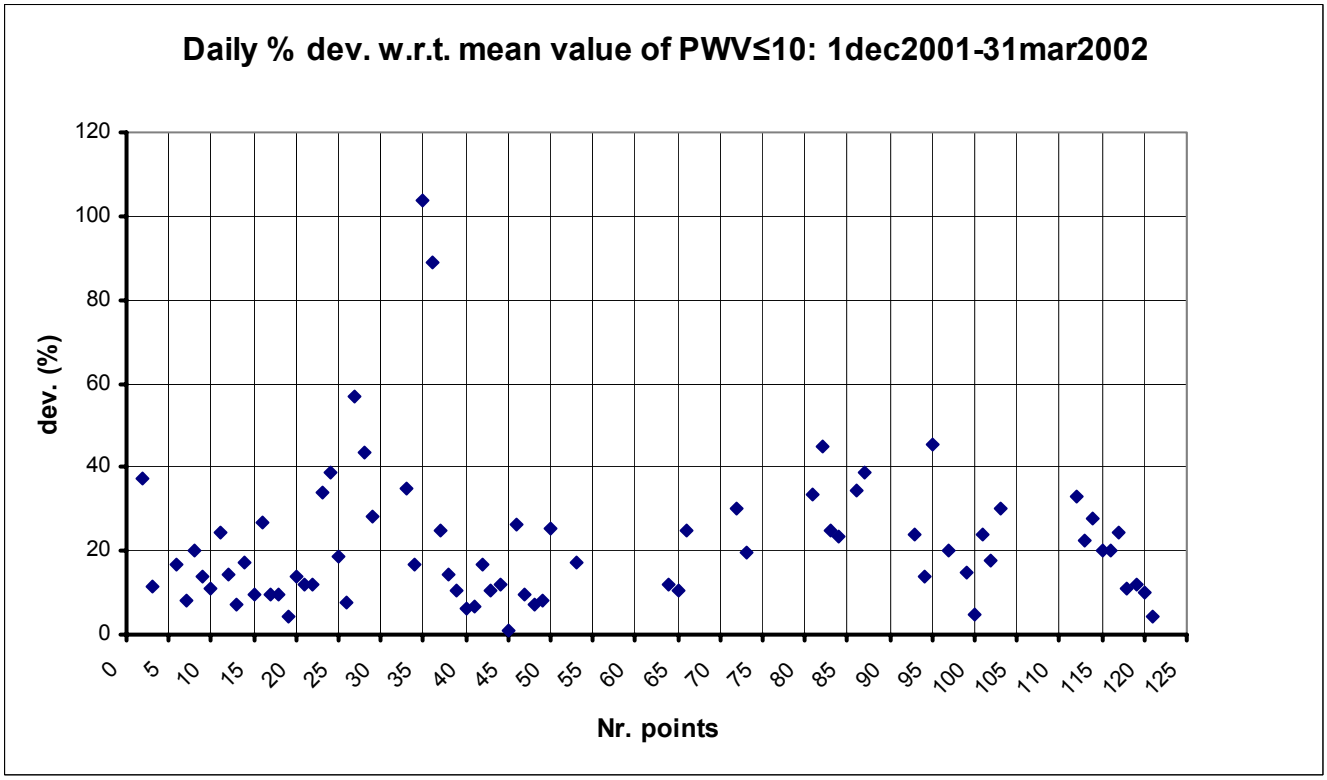

Fig. 3.1.2.44

2002-2003 WINTER STATISTICS

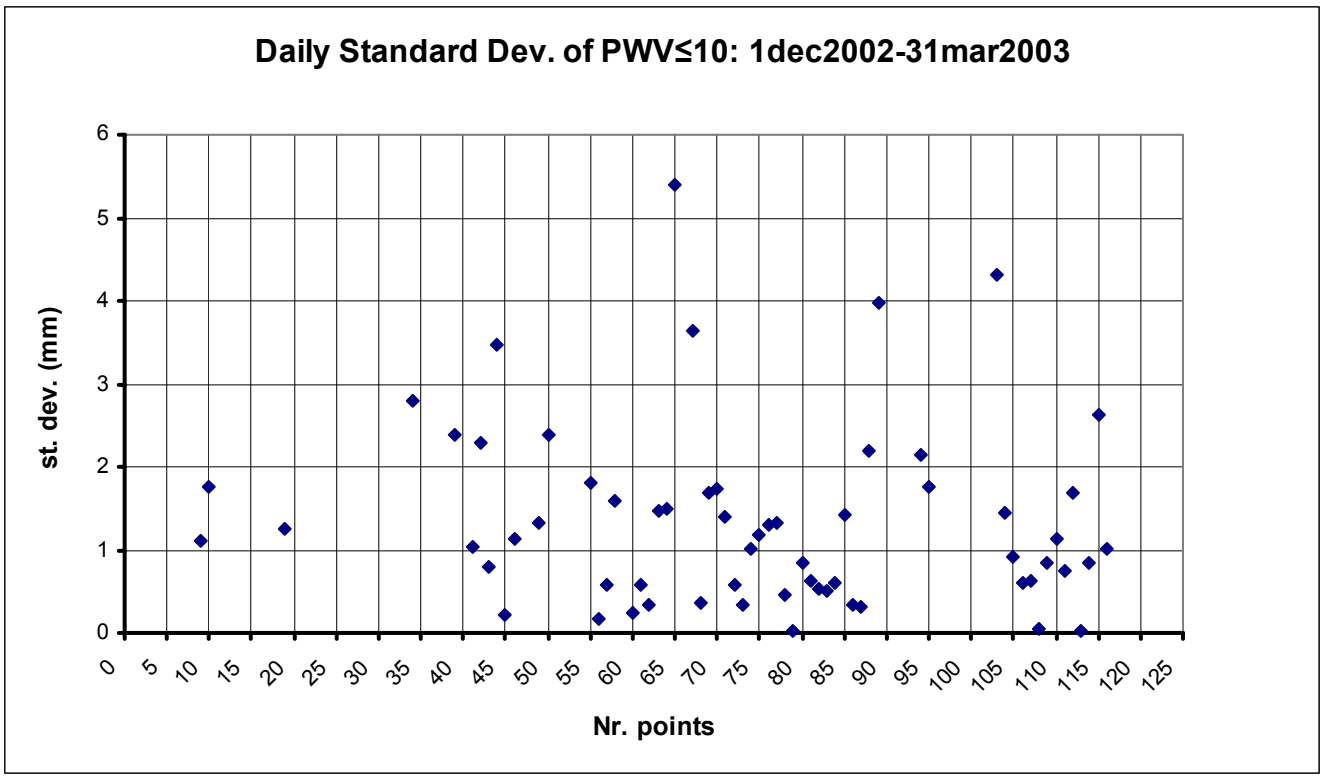

Fig. 3.1.2.45

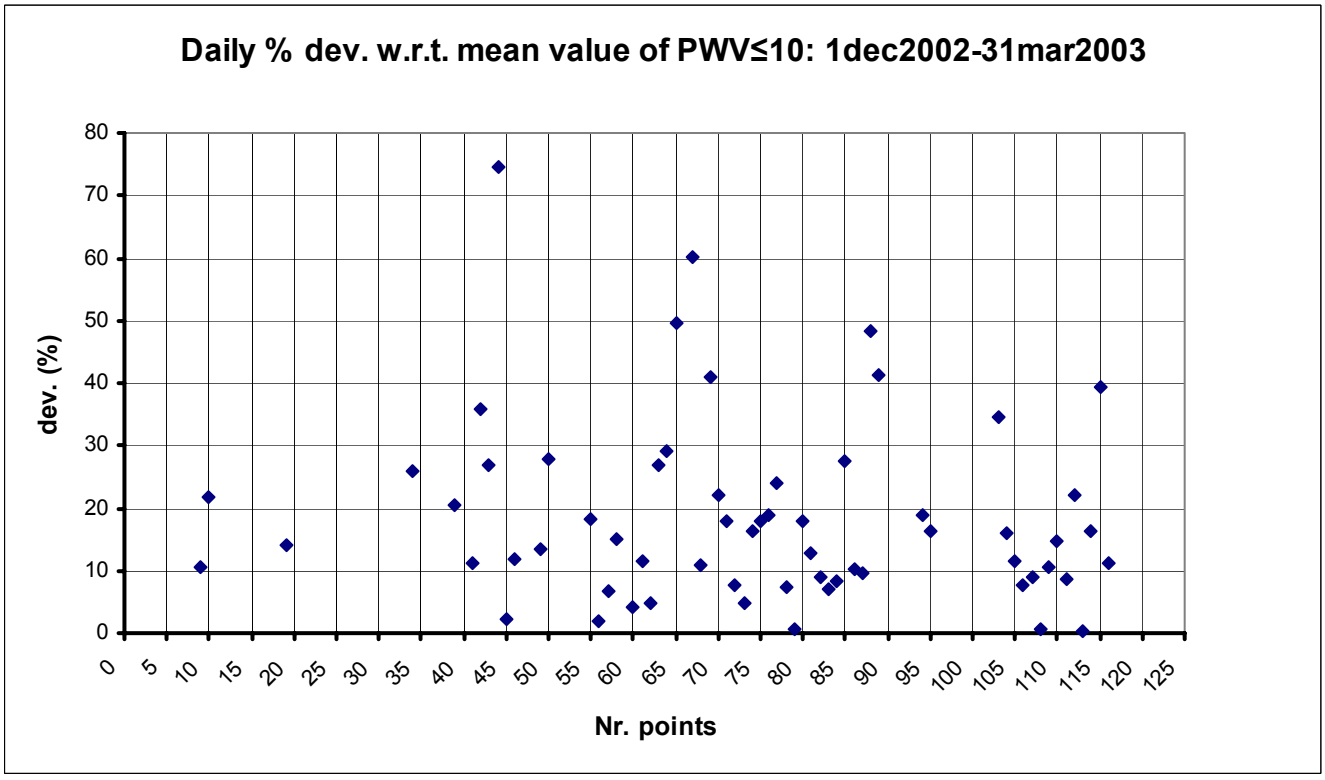

Fig. 3.1.2.46

2003-2004 WINTER STATISTICS

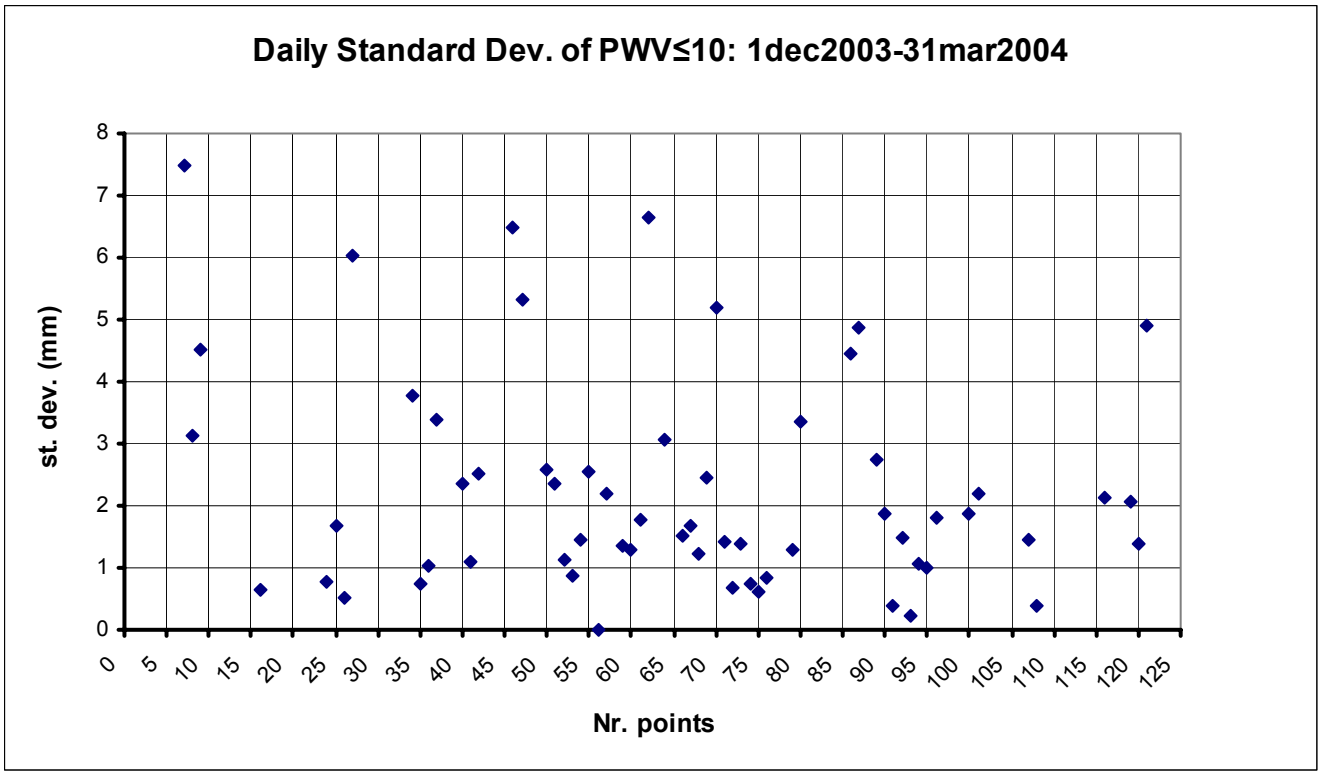

Fig. 3.1.2.47

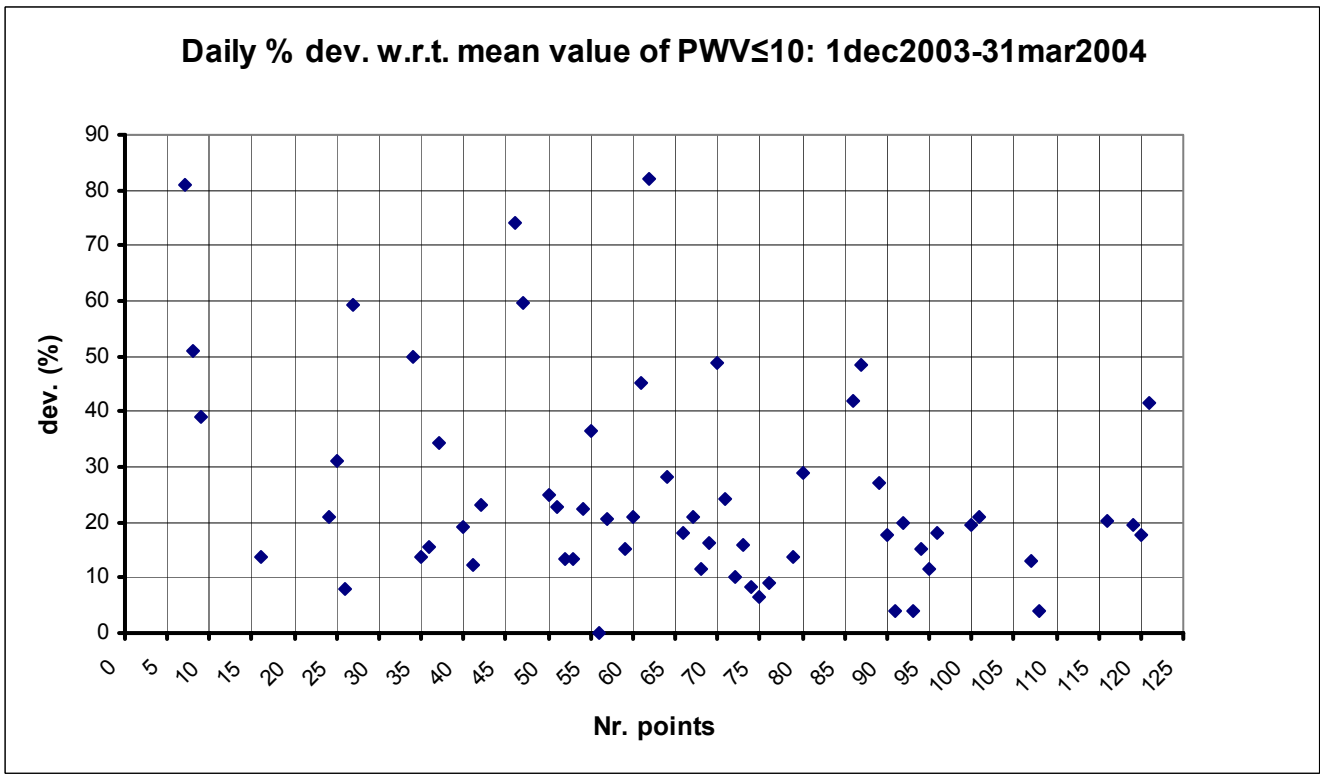

Fig. 3.1.2.48

2004-2005 WINTER STATISTICS

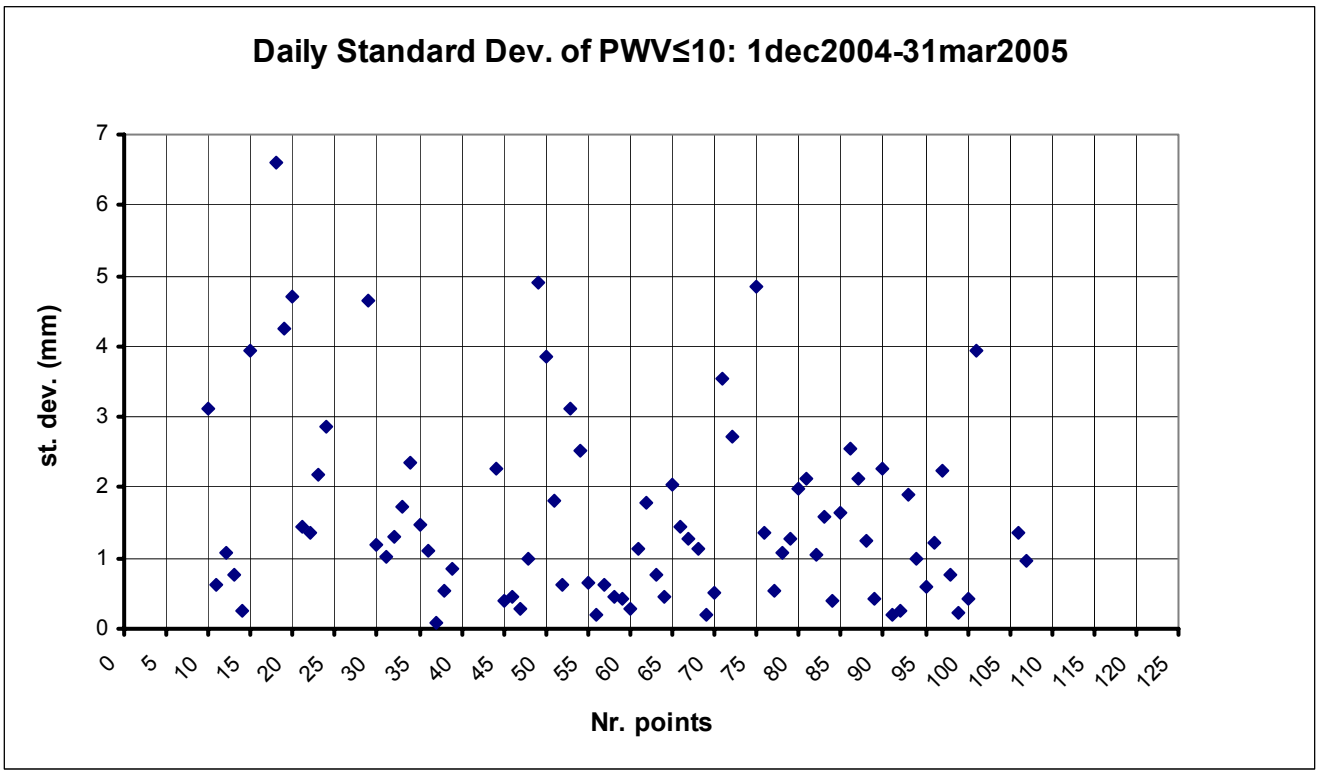

Fig. 3.1.2.49

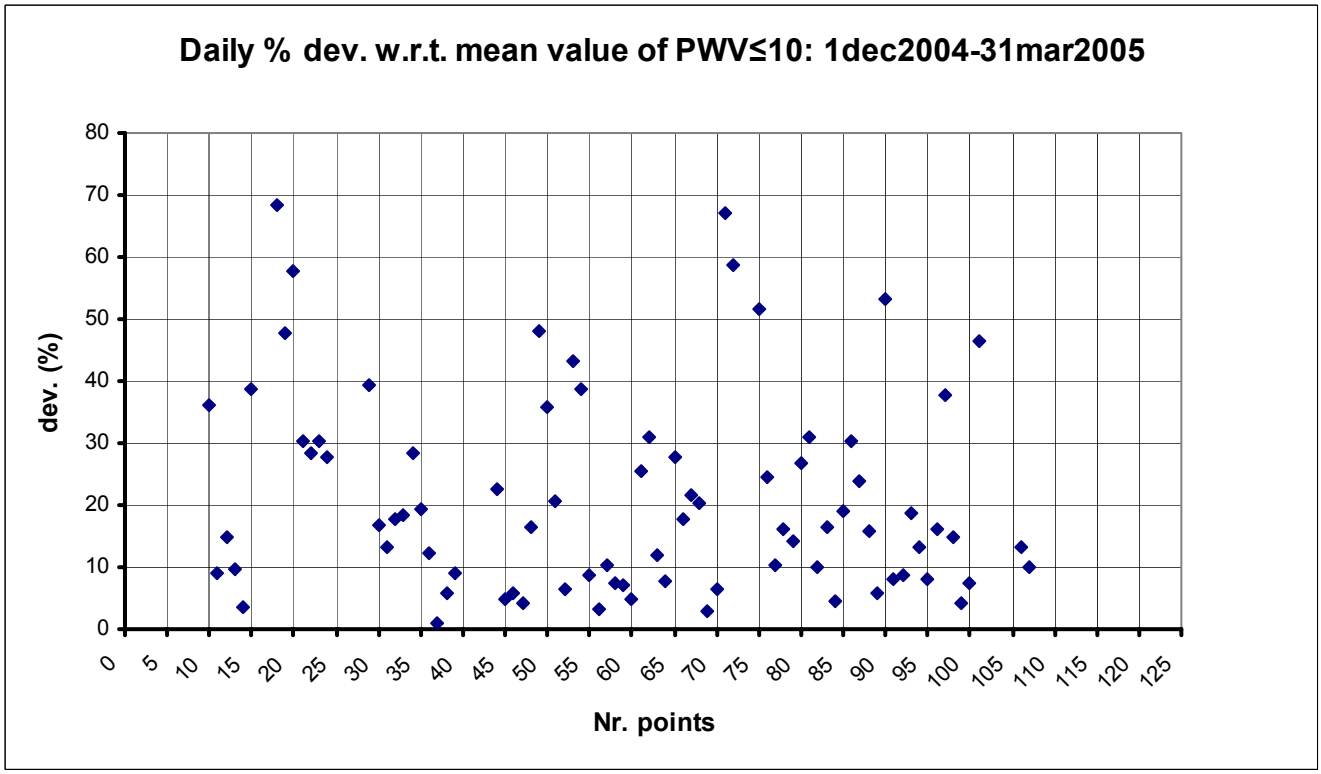

Fig. 3.1.2.50

2005-2006 WINTER STATISTICS

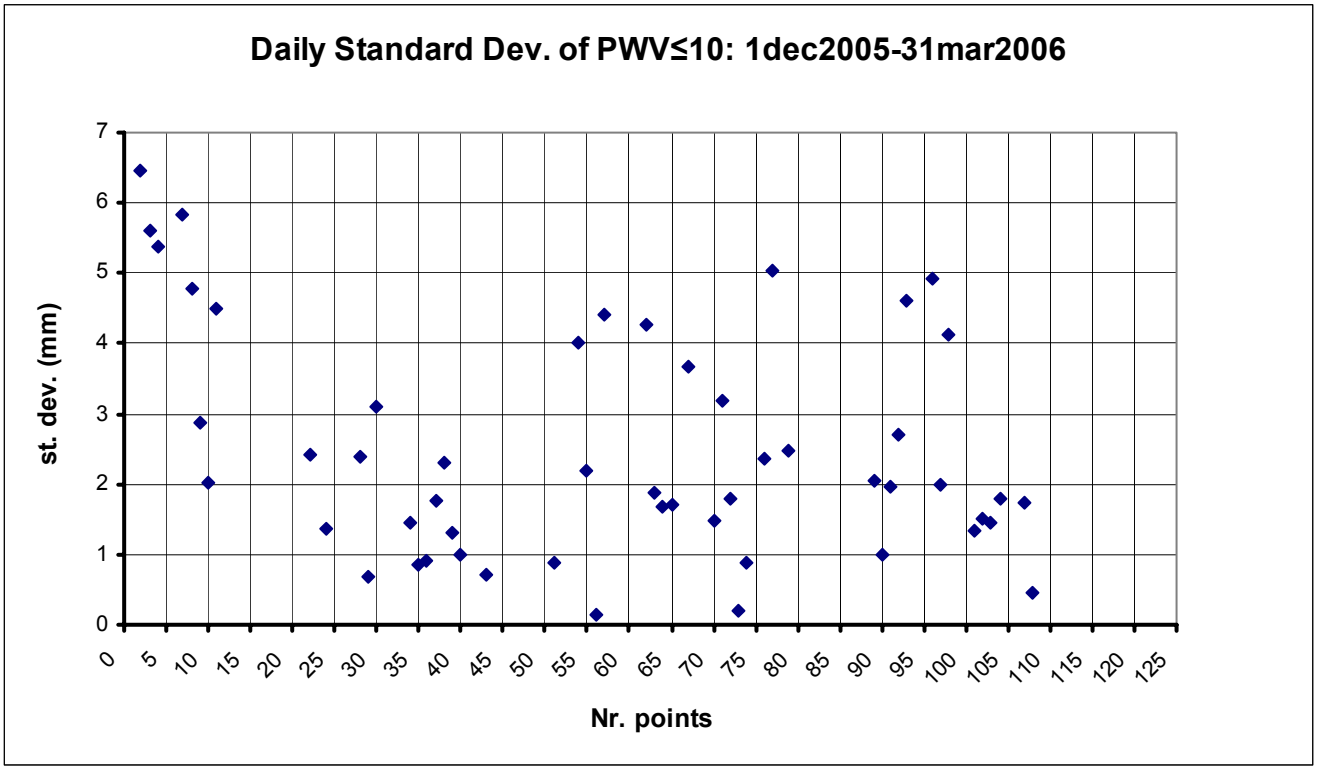

Fig. 3.1.2.51

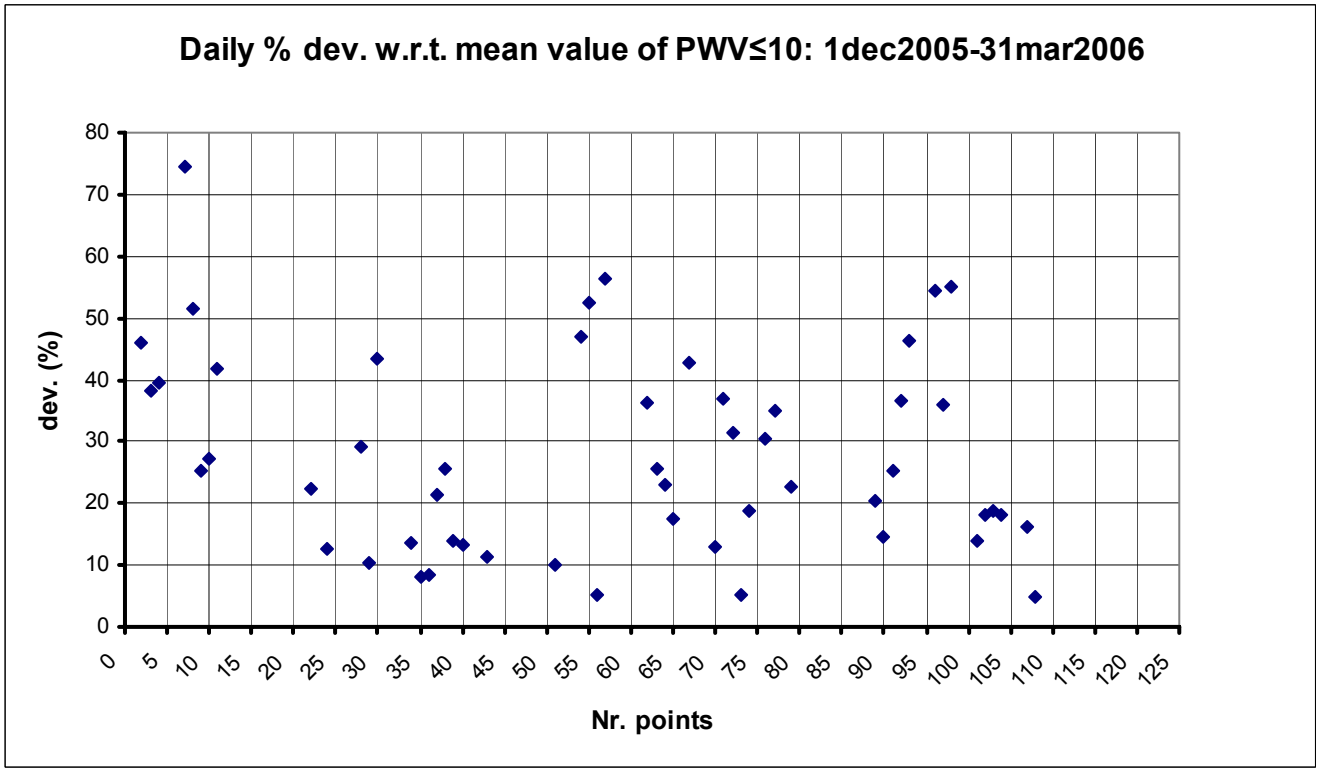

Fig. 3.1.2.52

2006-2007 WINTER STATISTICS

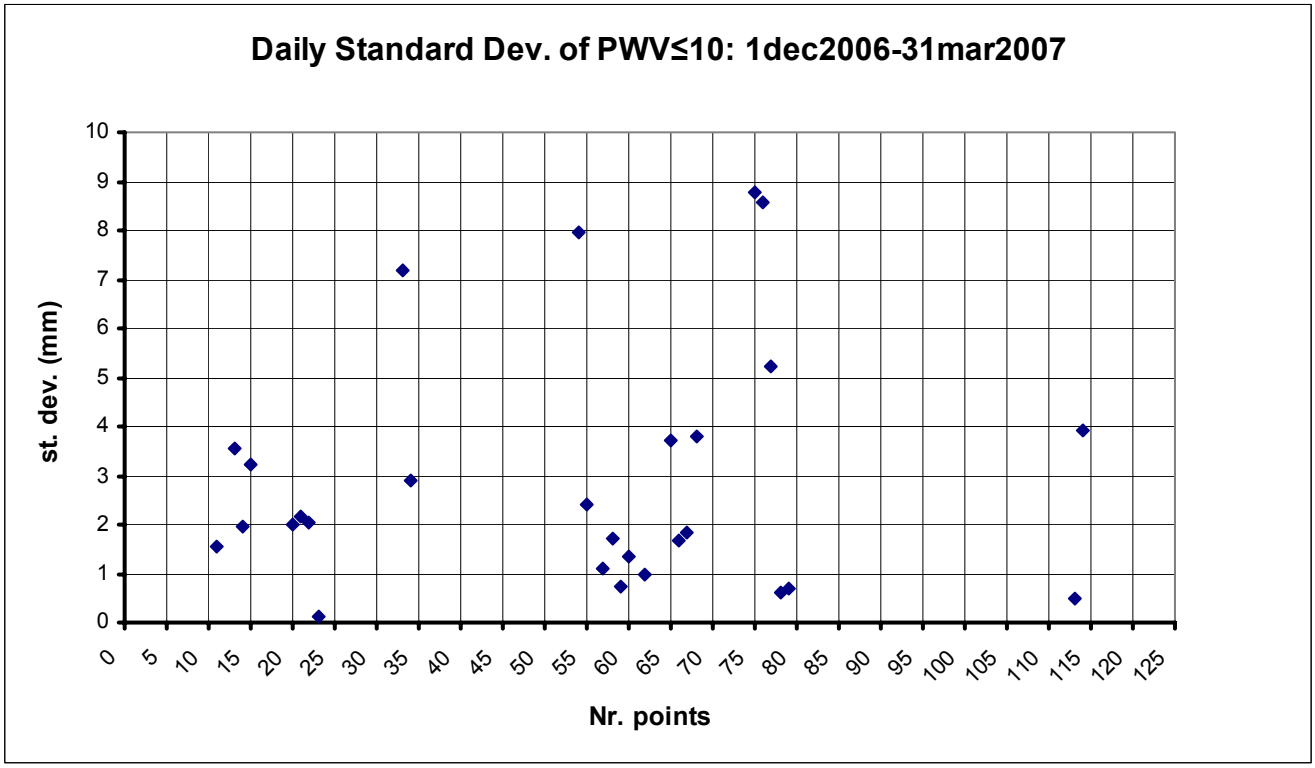

Fig. 3.1.2.53

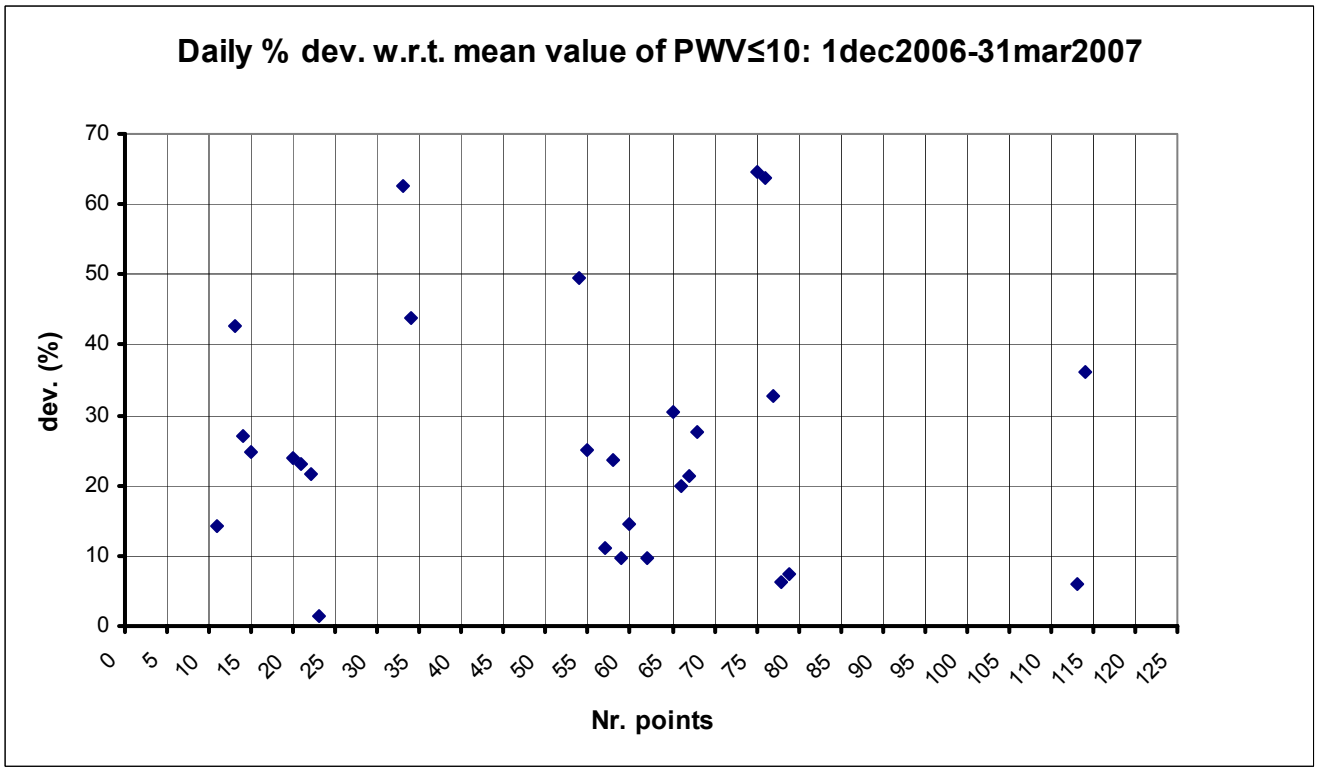

Fig. 3.1.2.54

3.2 Site measurements of τ_o at 22 GHz and its correlation with PWV data

PWV data give a feeling about "good sky" useful for high frequency measurements. However what we are interested in is the attenuation coefficient at zenith, τ_o.
In order to put into relation these two quantities, direct measurements of τ_o were done since the beginning of May 2006 to the end of March 2007. Medicina 32m dish was used to make sky dips, at a frequency of 22 GHz, from which τ_o can be derived.
The number of measurements is not large because of the small amount of spare time without scheduled observations, however about seventy sky dips could be done through the period giving the results plotted in Fig. 3.2.1 and 3.2.2.
τ_o values were put in correlation with PWV data coming both from calculation of weather measurements at the site and data coming from soundings at the Capofiume base.
In the first case the linear correlation is worse than the second case but the differences between the straight line coefficients are low.

$\tau_o = 0.0075 * PWV + 0.0227$ PWVcalculated

$\tau_o = 0.0069 * PWV + 0.0319$ PWVcapofiume

The correlation coefficients are 0.751 and 0.895, respectively, while the rms of the relative residuals with respect to the interpolating line (i.e. $\Delta\tau_o/\tau_o$) are 25% and 20%.
These parameters give the degree of confidence the straight line provides, therefore an *excess factor* of 1.25 could be used in order to take into account the inaccuracy of an interpolation for τ_o estimation.

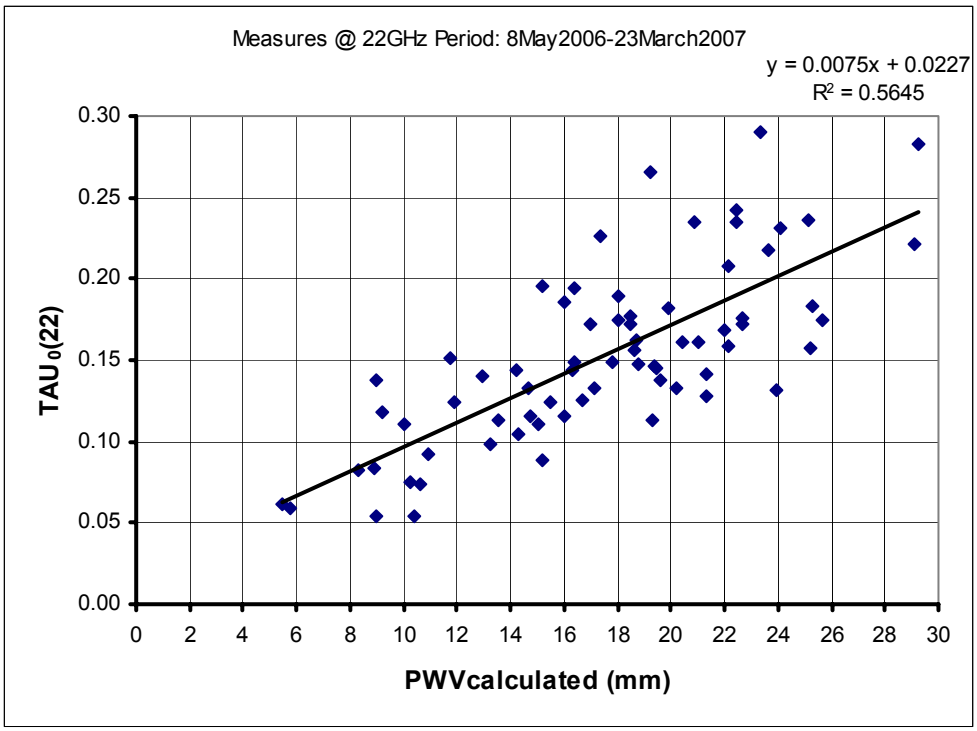

Fig. 3.2.1 Measured τ_o at Medicina observatory site vs PWV from weather data at the site

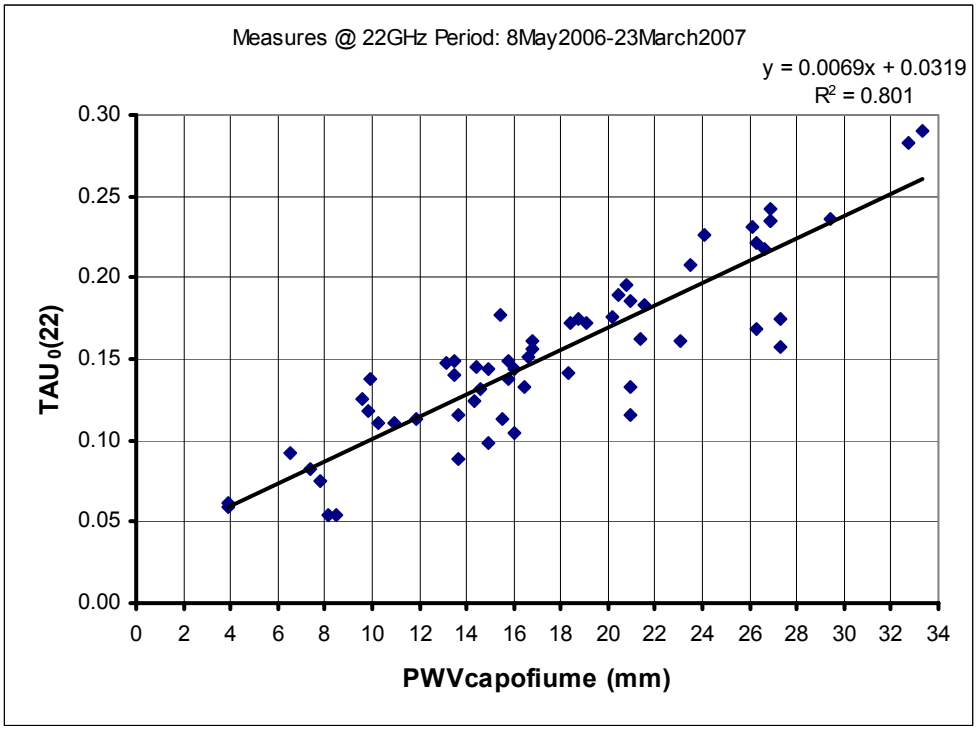

Fig. 3.2.2 Measured τ_o at Medicina observatory site vs PWV from Capofiume base

3.3 Inaccuracy of the PWV data: its effect on attenuation and brightness temperature

Once stated the uncertainty and fluctuations of the PWV data, expressed as *excess factors*, it is interesting to determine how these affect the uncertainty and variations of the derived quantities. These quantities are the atmospheric attenuation and brightness temperature provided by the terms $e^{-\tau o}$ and $(1- e^{-\tau o})$.
Using the derived formula of the previous paragraph and applying the excess factors the outcome is simple to derive.
Only PWV≤10mm will be used as border value for using antennas at high frequencies.
Table 3.3.1 shows how much the attenuation and brightness temperature increases when excess factors are applied to PWV nominal values. The table shows the worst case only, the one for the highest value of water vapour.

PWV = 10mm		
Excess factor	*1.25*	*1.4*
Attenuation increase factor	1.02	1.03
Brightness Temp. increase factor	1.16	1.26

Table 3.3.1

An increase of the water vapour by 25% and 40% increases much less the attenuation and noise produced by the atmosphere.

3.4 Empirical relationships between τ_o at 22 GHz and τ_o at 90 GHz at the site

The last step before to proceed further with calculations of the antenna performance is to derive an estimation of τ_o at 90 GHz from the knowledge of $\tau_o(22)$.

In [1] Tables 3.2a,b,c,d give values of both parameters using ATM software package applied to Medicina site.

Moreover in [6], Figure 2 together with Table A-1, one more example is reported at sea level and for standard atmosphere. Rearranging Table A-1 values at 90 and 22 GHz for different elevations, values of τ_o can be calculated.
Based on the data reported in Table 3.4.1 an interpolation curve can be derived (Fig. 3.4.1),

PWV(mm)	2	3.4	5.4	5.6	9.2	10.2	15	15	17.2	28	30	48
$\tau_o(90)/\ \tau_o(22)$	3.13	2.82	2.59	2.31	2.1	1.98	2	1.76	1.82	1.76	1.64	1.62

Table 3.4.1

$$\frac{\tau_o(90)}{\tau_o(22)} = 3.4593 * \mathrm{PWV}^{-0.2136}$$

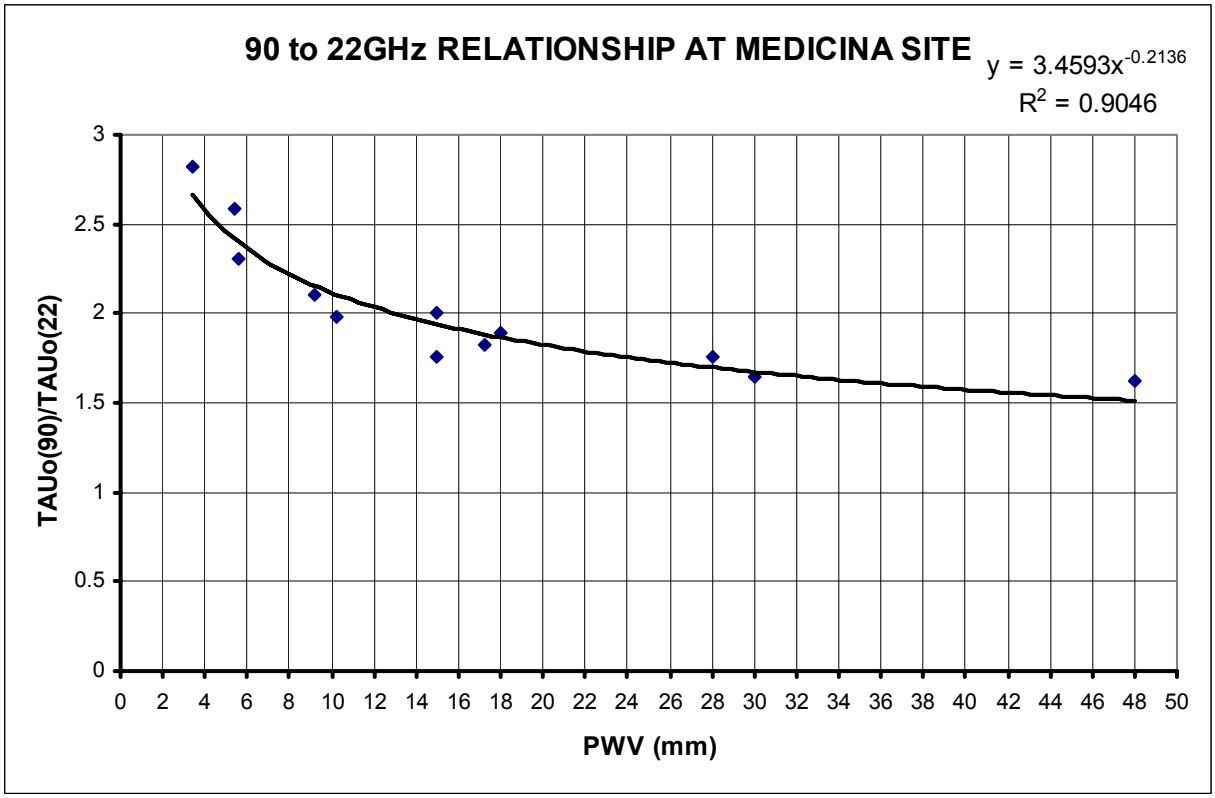

Fig. 3.4.1

It must be noted that for PWV approaching zero the ratio $\tau_o(90)/\tau_o(22)$ must assume a finite value, corresponding to the effect of the oxygen line only. Instead the interpolation curve goes to infinite for PWV→0, therefore it must not be used for data extrapolation.
In view of the calculation to be done in the next paragraph it is useful to give a comparison between $\tau_o(22)$ as obtained by the data measured and as given by ATM. This is shown in the following table 3.4.2, from which one can see that ATM systematically underestimates τ_o the more the lower PWV is, i.e. right in the range this study is dealing with. That is one more reason to use ATM only to get the ratio $\tau_o(90)/\tau_o(22)$.

τ_o 22 GHz COMPARISON			
PWV (mm)	τ_o by ATM	τ_o by formula from measured data	ratio
2	0.030	0.046	1.52
3.4	0.040	0.055	1.38
5.4	0.054	0.069	1.28
5.6	0.054	0.071	1.31
9.2	0.080	0.095	1.19
10.2	0.084	0.102	1.22
15	0.120	0.135	1.13
15	0.115	0.135	1.18
17.2	0.135	0.151	1.12
18	0.127	0.156	1.23
28	0.210	0.225	1.07
30	0.220	0.239	1.09
48	0.340	0.363	1.07

Table 3.4.2

3.5 Atmospheric attenuation and brightness temperature @ 3.3mm

Using the formulae in 2.1.3 and in 2.2.2 the attenuation and brightness temperature of the atmosphere at 90 GHz can be calculated versus antenna elevation.
Graphs 3.5.1 and 3.5.2 show the results by considering both the mathematical expressions of $\tau_o(22)$ (paragraph 3.2), its relationship with $\tau_o(90)$ (paragraph 3.4) and both the excess factors.
The case with no excess factor (excess factor equal to 1) is also given in order to show the effects coming from the nominal value of PWV (Fig. 3.5.3 and 3.5.4).
In order to avoid too many curves appearing in the graphs only two water vapour conditions are considered, PWV=5mm and PWV=10mm.
One result is worthwhile to mention: in the philosophy to get approximate values, essentially we have two really distinct groups of curves, identified by the PWV value only.
The various curves in each group, arising from different excess factor and from Medicina or Capofiume data, show values very close each other, at least at the level of the approximation we are dealing with.

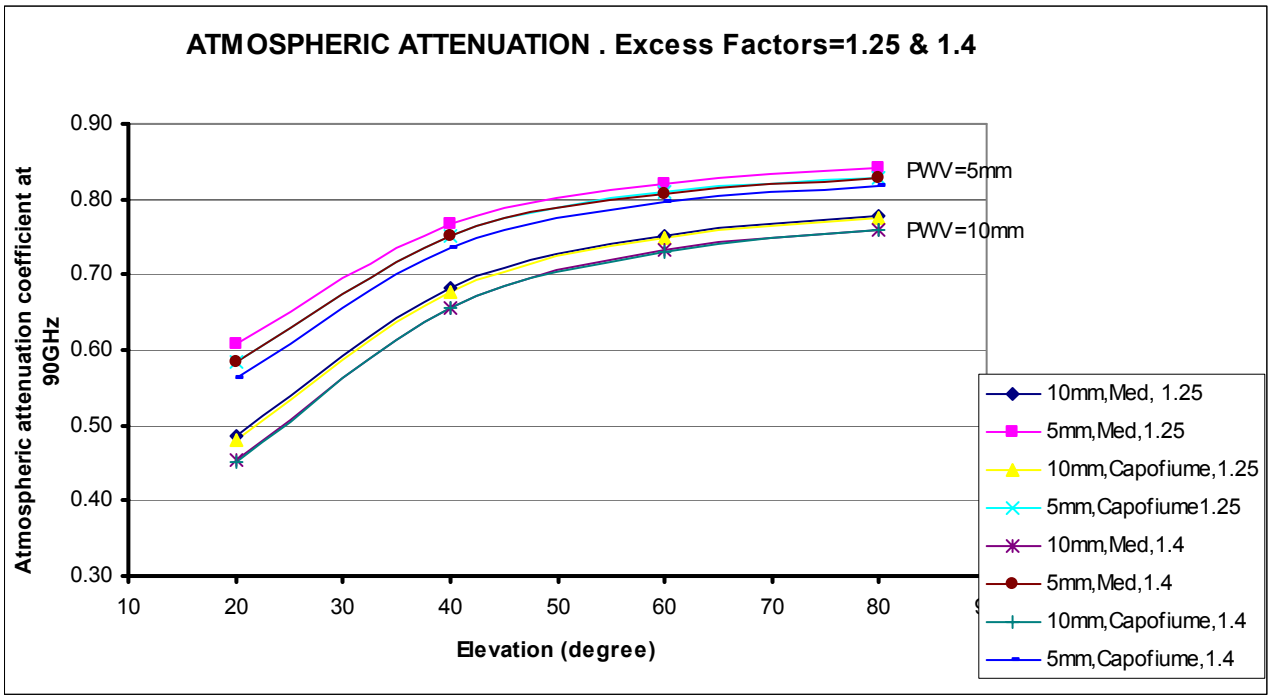

Fig. 3.5.1

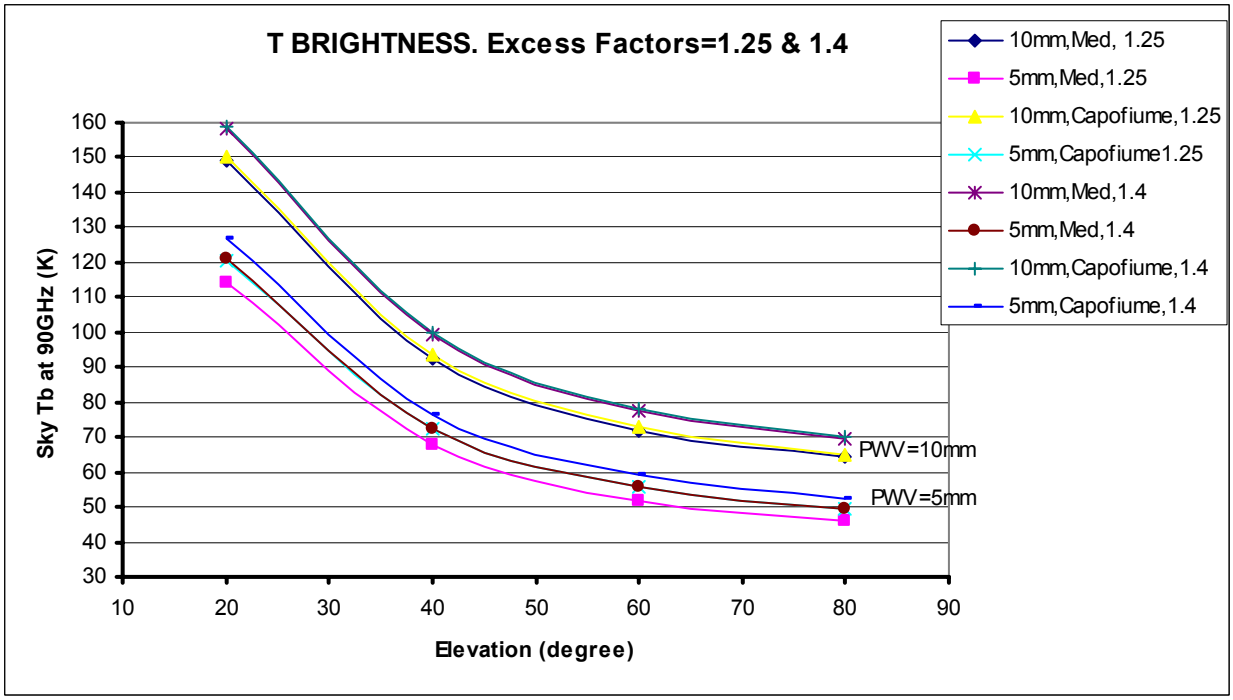

Fig. 3.5.2

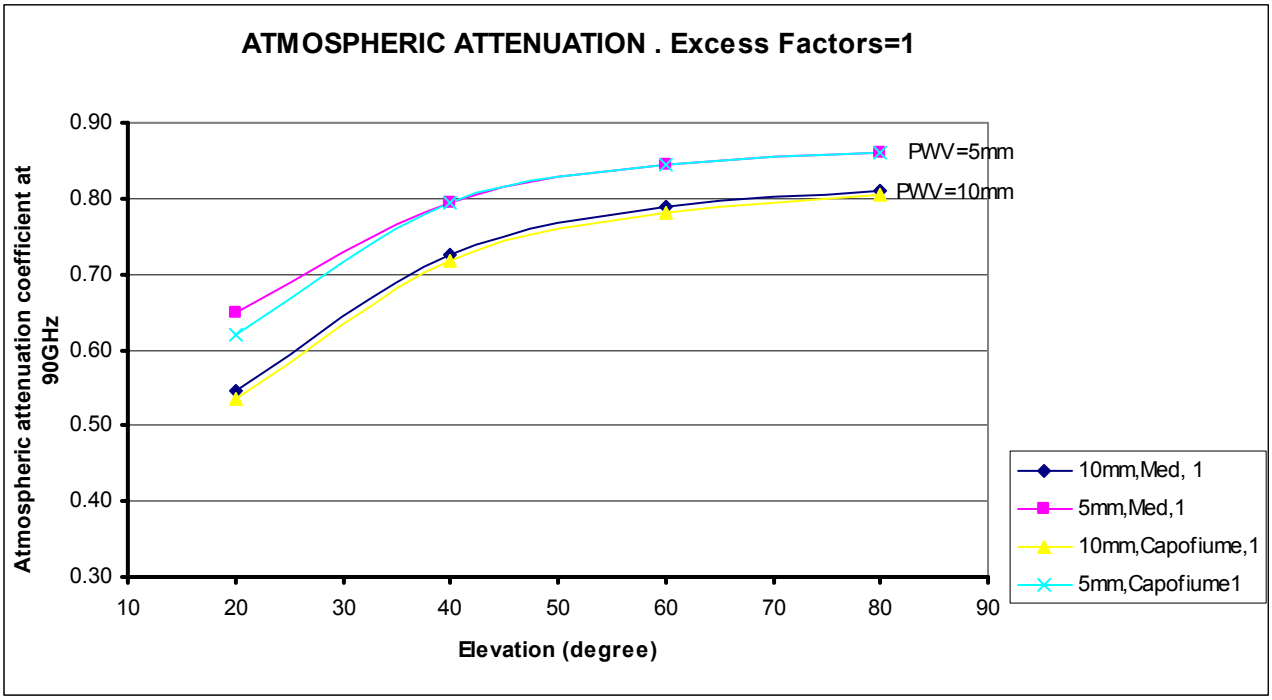

Fig. 3.5.3

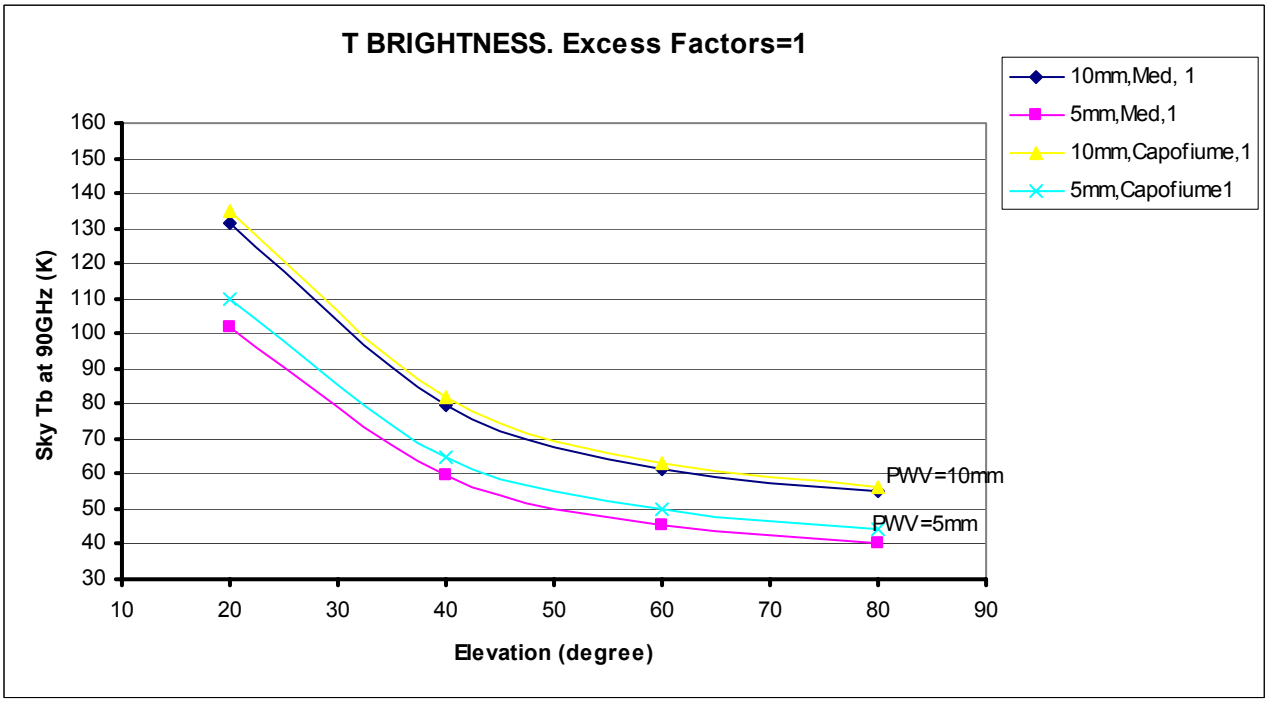

Fig. 3.5.4

3.6 SEFD calculations @ 3.3 mm

Accordingly to Fig. 1.4 and its parameters description given in Chapter 2 it holds,

$$G(K/Jy) = A * \eta_{surf} * \eta * \frac{Ag * 10^{-26}}{2 * k}$$

$$T_{sys}(K) = T_{rx} + T_{spill}$$

k=Boltzmann constant, $1.38*10^{-23}$ $m^2kg/(s^2K)$.
The term $Ag*10^{-26}/2k$ is the maximum antenna gain ideally available, strictly related to the antenna area only. For a 32 m dish antenna it is 0.29 K/Jy. Note that in doubling the diameter of the antenna this value is multiplied by four (1.16 K/Jy for SRT).

Realistic values of η can be assumed from already available receivers of the Medicina antenna. The illumination of the dish changes with respect to the focus location (primary focus receivers illuminate in a different manner than Cassegrain ones, in order to avoid picking up too much ground noise) but it is fairly the same for all receivers placed at the same focus.
A proper mounting of a 90 GHz receiver would be in the Cassegrain focus, so the efficiency components of the secondary focus 4.3-5.8 GHz receiver can be used. They are summarized in Table 3.6.1 [7].

η	$\eta_{cross}*\eta_{diffr}$	η_{phase}	η_{taper}	$\eta_{blockage}$	η_{spill}	η_{prim}	η_{sub}
components	0.98	0.97	0.82	0.89	0.846	0.987	0.857

Table 3.6.1 Antenna efficiency components

The last two terms η_{prim} and η_{sub} are already included in η_{spill} ($=\eta_{prim} * \eta_{sub}$) but they are made clear because they enter in the calculation of the spillover noise.

An usable antenna at 90 GHz needs a refurbishment of the overall surface accuracy. Present value of Medicina should give an antenna efficiency equal to zero. Subreflector and panels were manufactured for a usable antenna gain at 22 GHz, even though degraded with respect to the peak gain at 5 GHz. Moreover, gravity deformations of the back-up structure have to be overcome, otherwise the efficiency at elevations other than 45^o (usually the elevation where the panels of the primary mirror are aligned) drops dramatically. This is the reason why putting better panels and subreflector is a waste of money if an active surface is not installed as well.
For this reason in the calculation of SEFD at 90 GHz the antenna is assumed to be completely refurbished (new panels, new subreflector, active surface installed) with the best achievable performance in terms of surface accuracy components. As a consequence the antenna gain vs elevation will be considered constant and therefore the variation of SEFD vs elevation will be ascribed to Tsys only.
In Table 3.6.2 η_{surf} components are reported [8] taking as state-of-the-art the achievements we expect to obtain in SRT. The performance with respect to wind, thermal and gravity deformations of panels and subreflector are thought as rms'ed over elevation and in precision condition of the weather environment. Two values of η_{surf} are considered corresponding to two possible performance in terms of alignment of the primary mirror, 150 and 50 micron.
In summary, the graphs of SEFD take into account:

a) two values of receiver noise temperature (chapter 2)
b) two values of total rms surface accuracy (table 3.6.2)

c) pair of excess factor 1.25 and 1.4 (PWV worst case)
d) pair of excess factor 1 and 1 (PWV nominal case)

This subdivision aims at setting limits of a realistic range of actual SEFD values at 90 GHz for a well refurbished antenna.

η_{surf} components (micron)		
Subreflector, wind	negligible	negligible
Subreflector, thermal	negligible	negligible
Subreflector, gravity	negligible	negligible
Subreflector, meas. error	15	15
Panel, wind	4	4
Panel, thermal	11	11
Panel, gravity	29	29
Panel, meas. error	25	25
Panel, manufacturing	65	65
Subreflector, manufacturing	50	50
Alignment	150	50
TOTAL η_{surf} (RSS)	*176*	*105*

Table 3.6.2 Antenna surface efficiency components

Results coming from Fig. 3.6.1 to 3.6.8 are very encouraging. SEFD range vs elevation spans from 1000÷2000 Jy in the nominal case, to 2000÷5000 Jy at worst.

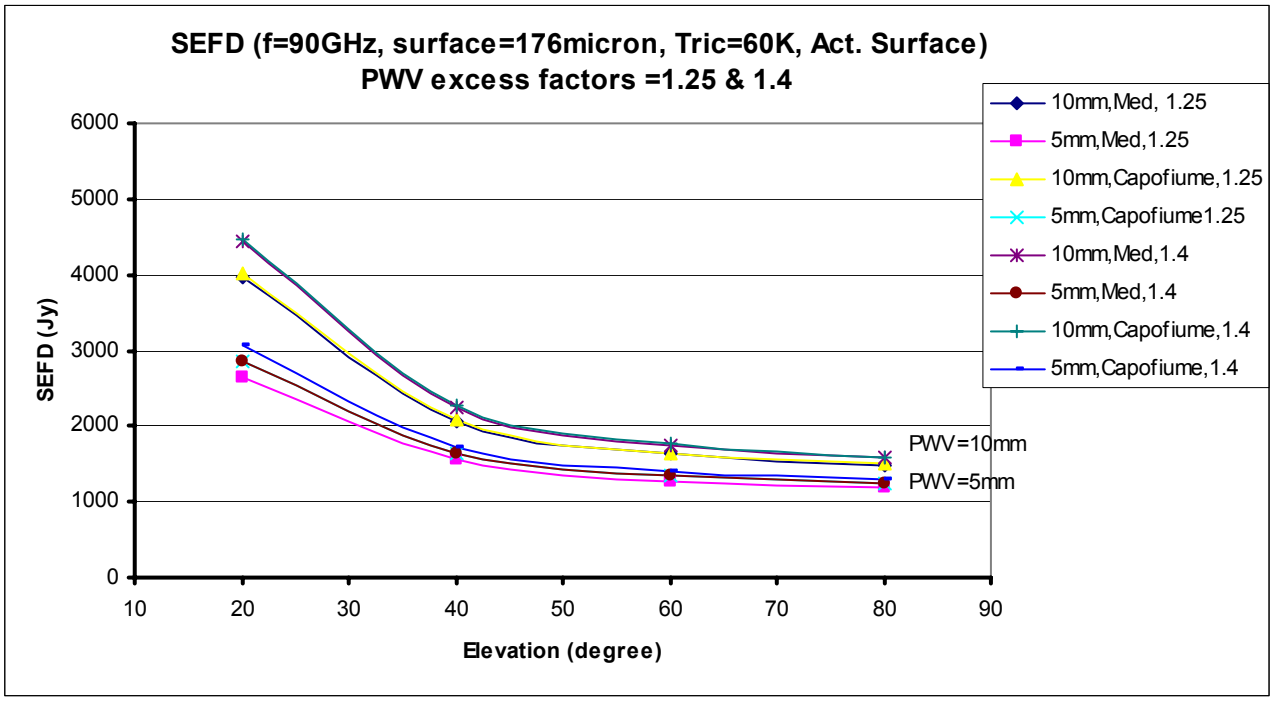

Fig. 3.6.1

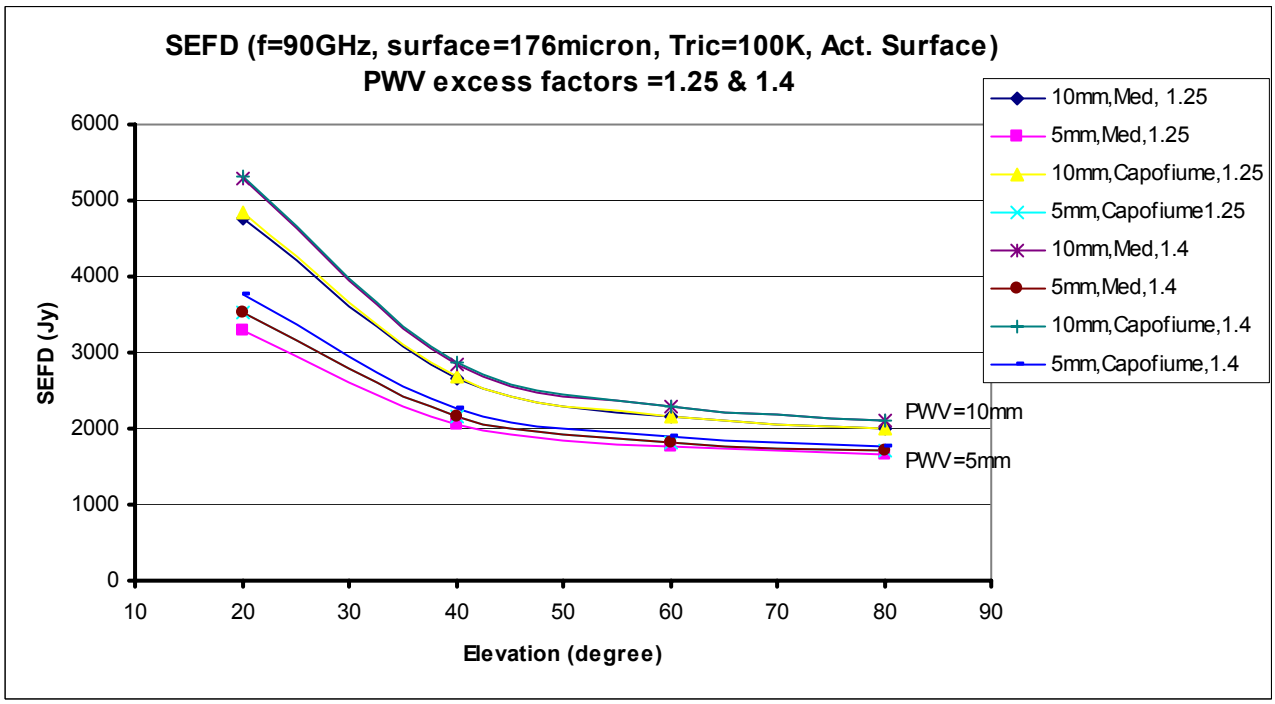

Fig. 3.6.2

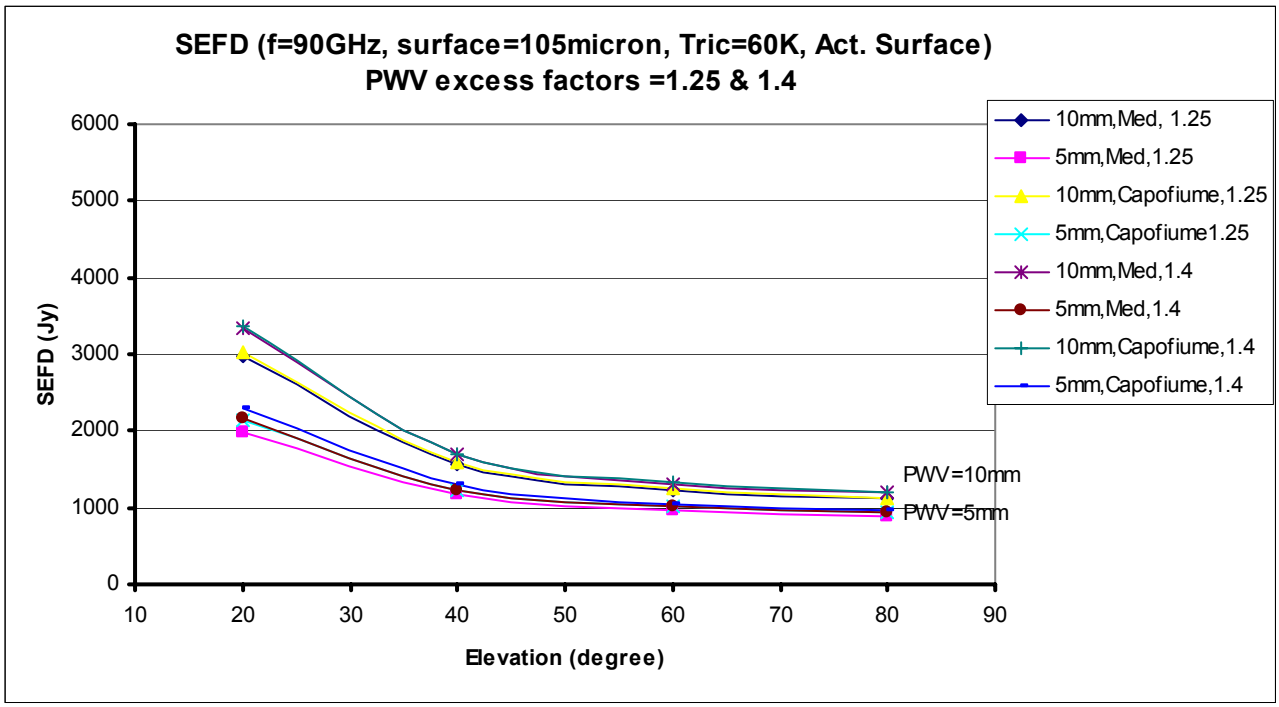

Fig. 3.6.3

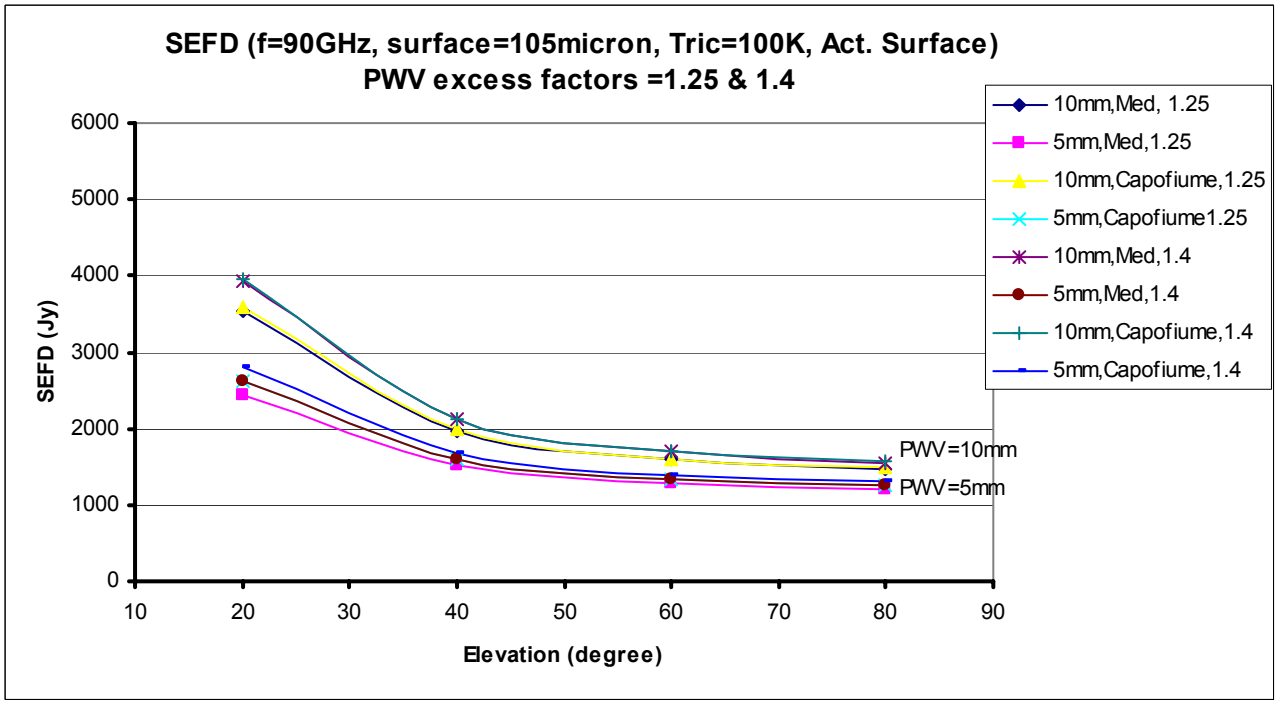

Fig. 3.6.4

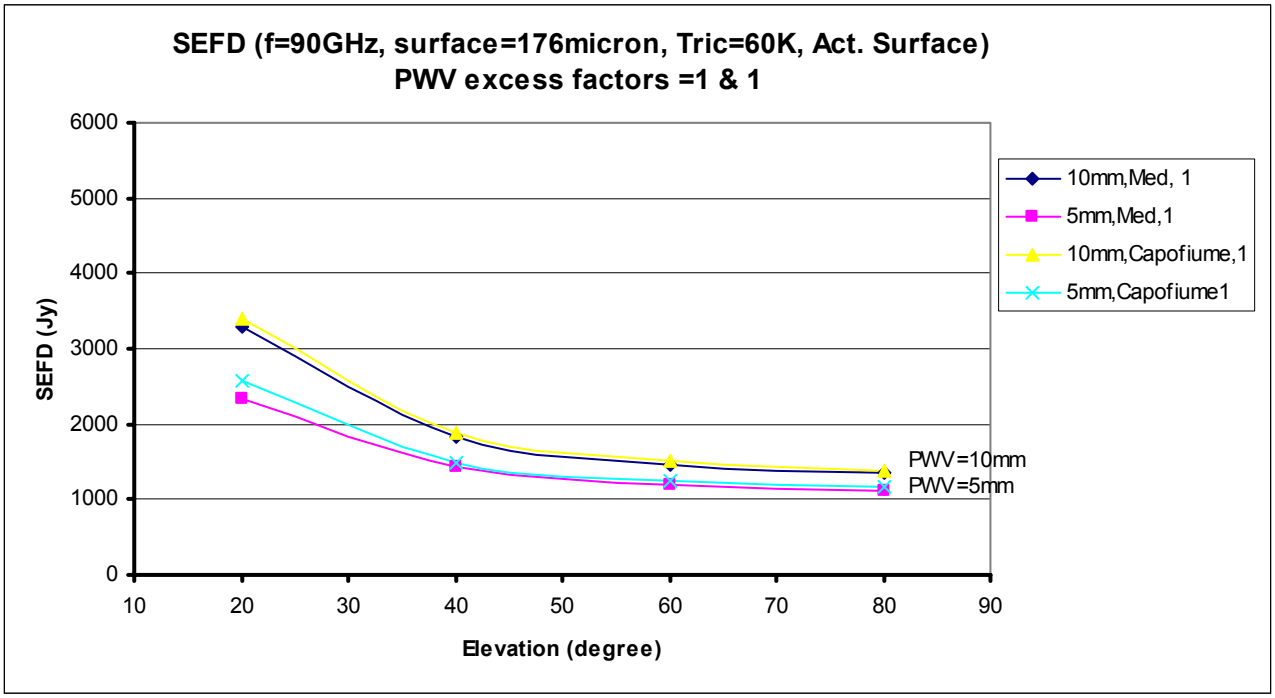

Fig. 3.6.5

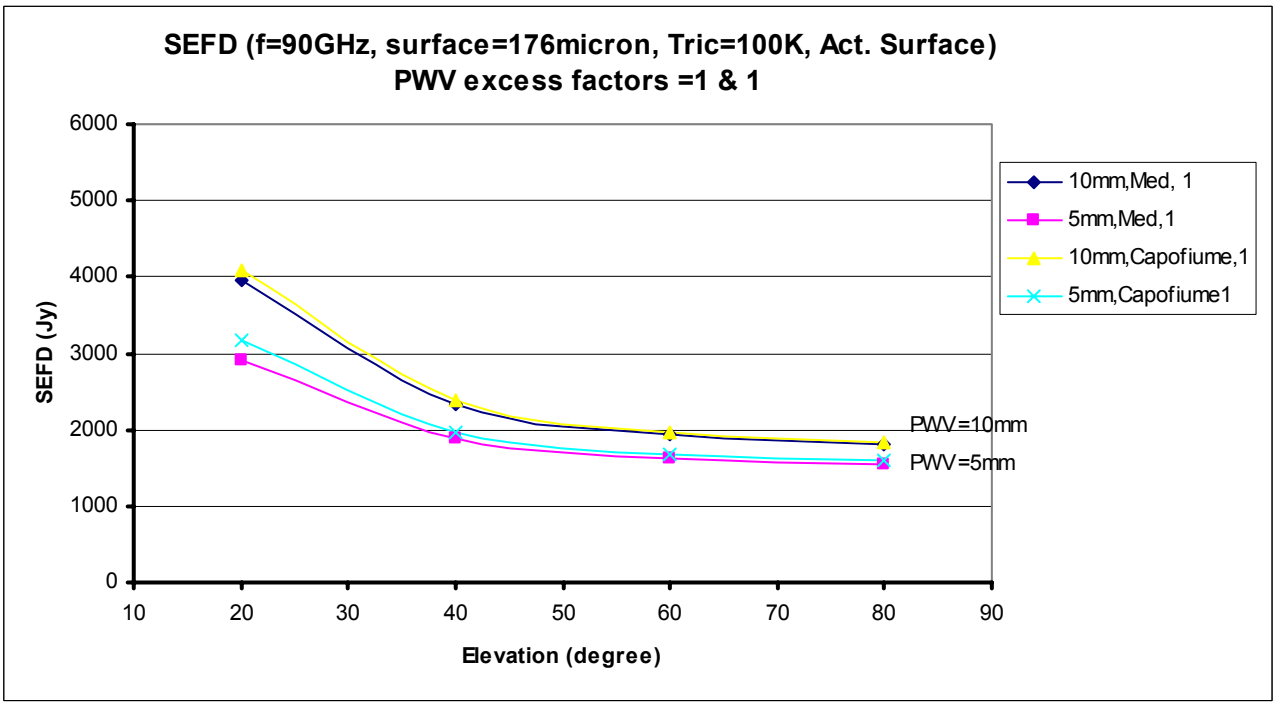

Fig. 3.6.6

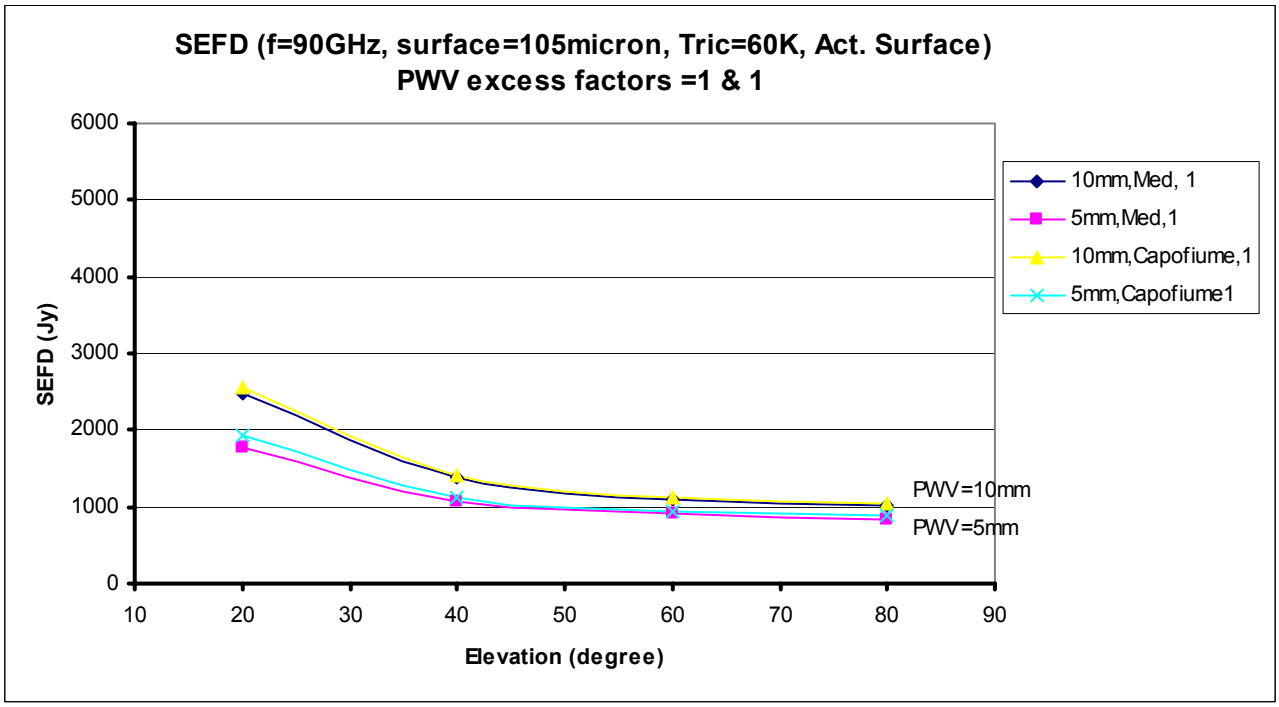

Fig. 3.6.7

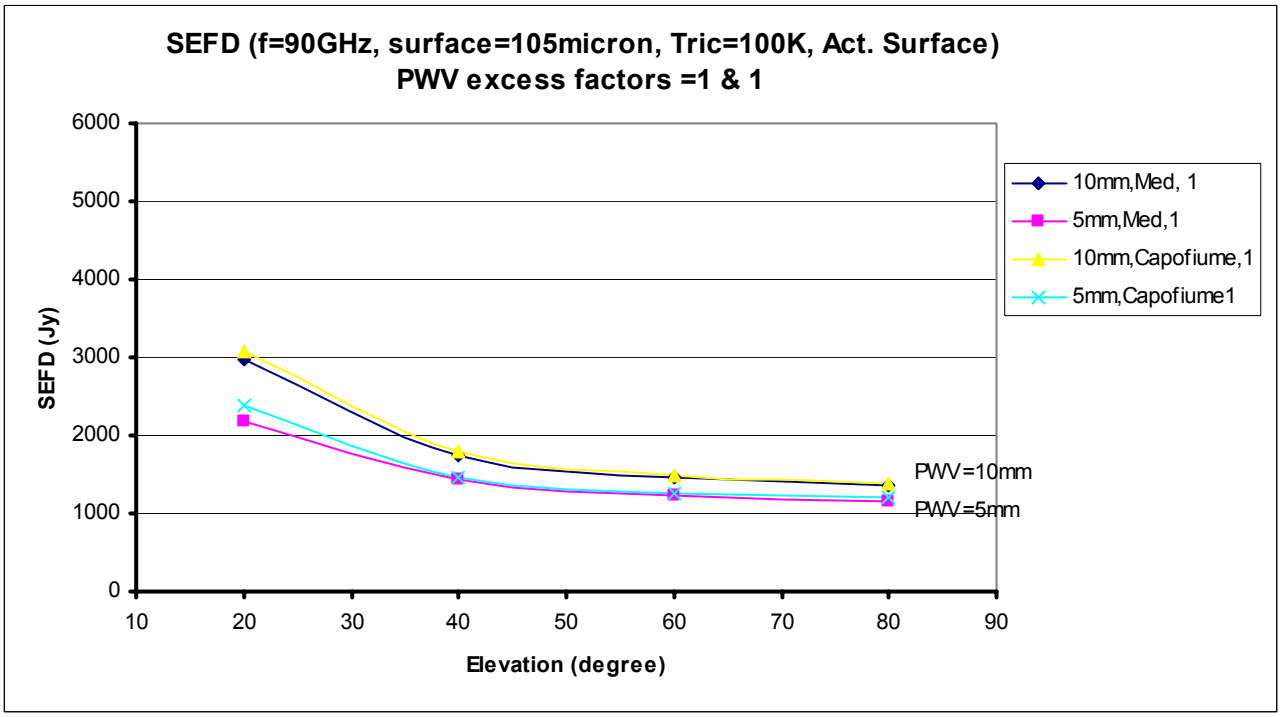

Fig. 3.6.8

3.7 Comparison between large diameter antennas placed at sea level and small diameter antennas placed at high altitude

Usually the use of sea level antennas at high frequencies is considered odd and silly because of the high water vapour column. However it is rarely realized that mm and sub-mm antennas placed at high altitude are of smaller diameter with respect to sea level antennas. The reason is because mm/sub-mm antennas work at very high frequencies, some hundred of GHz, so the surface accuracy they need, some tens of micron or less, is not reachable for medium and large diameter antennas. The opposite holds for sea level antennas, generally from 20 to 100 m in diameter, where 100 GHz is the highest frequency they use.
Table 3.7.1 shows this remark; apart from some exceptions most antennas have a diameter less than 16m.
This means that the Medicina antenna has on average four times collecting area of mm/sub-mm antennas.

LIST	D (m)	equivalentD (m)	Altitude (m)	Number of antennas	Location
HHT	10		3186	1	Az,USA
JCMT	15		4092	1	Hawai,US
Kitt Peak	12		1914	1	Az,USA
Sest	15		2400	1	Chile
SMA	6	16.4	4000	8	Hawai,US
FCRAO	14		314	1	MA,USA
Ovro	10.4	24.3	1222	6	CA,USA
Hat Creek	6.1	17.8	1009	9	CA,USA
Metsahovi	14		100	1	Finland
Nobeyama	45		1300	1	Japan
Pico Veleta	30		2920	1	Spain
Plateau de Bure	15	35.1	2550	6	France
CARMA	10.4 + 6.1		2400	6+10	CA,USA
CSO	10.4		4000	1	Hawai,US
ALMA	12	95.6	5400	64	Chile
LMT	50		4580	1	Mexico
Apex	12		5100	1	Chile
Taeduk	14		200	1	Korea
Delingha	14		3200	1	China
ASTE	10		4800	1	China

Table 3.7.1 Characteristics of mm/sub-mm antennas

This factor could be used to recover the loss due to a lower antenna surface efficiency and higher water vapour column, i.e. higher $\tau_o(90)$. It is interesting to disclose the net amount of this effect by making two different calculations (both of them done for two cases of receiver temperature performance):

a) supposing an optimized illumination (same efficiency factors other than η_{surf} and the same temperature picked up from the ground) and the same receiver for both a 16 m high altitude and the Medicina antenna at 90 GHz, calculate the SEFD ratio between the two receiving systems,

b) supposing an optimized illumination (same efficiency factors other than η_{surf} and the same temperature picked up from the ground) and the same receiver, calculate $\tau_o(90)$ which Medicina can tolerate so that it has the same SEFD as the 16 m high altitude antenna

The results are in Table 3.7.2, highlighted in bold, from which we see Medicina has almost half SEFD of a high altitude antenna (0.531 and 0.629). On the other hand, a similar SEFD value is obtained if Medicina site experiences $\tau_o(90)$ values equal to 0.383 or 0.507! These last values imply that Medicina could observe at 90 GHz, with performance comparable to a high altitude antenna of 16 m in diameter, not only in winter.

case		Tric (K)	Tatm (K)	Tground (K)	t_o	e^{-to}	η_{surf}	Area factor	SEFD ratio: seaLevel/High alt.
A	Sea level antenna	60	52.6	10	0.2	0.819	0.850	4	**0.629**
	High altitude antenna	60	0	10	0	1	1	1	
B	Sea level antenna	100	52.6	10	0.2	0.819	0.850	4	**0.531**
	High altitude antenna	100	0	10	0	1	1	1	
C	Sea level antenna	60	92.3	10	**0.383**	0.682	0.850	4	1
	High altitude antenna	60	0	10	0	1	1	1	
D	Sea level antenna	100	115.3	10	**0.507**	0.602	0.850	4	1
	High altitude antenna	100	0	10	0	1	1	1	

Table 3.7.2 Comparison between sea level and high altitude antennas in the 3mm band

There is also a further consideration that makes Table 3.7.2 really interesting. For mm/sub-mm antennas 90-100 GHz is the lowest frequency used and the best PWV values measured at high altitude antennas are devoted to observe at the highest frequencies. This means the Tatm contribution reported as zero in the column is not true, making even better the comparison quoted.

4. CONCLUSIONS

The main conclusion of this investigation is that Medicina site, and Noto, shows enough number of days with convenient water column and τ_o values, that makes worthwhile the use of the antennas in the 3 mm band.
A summary of the environment, usable as a rule of thumb, is in Table 4.1. These are rough mean values in the period,

Period	τ_o/T_{bo}	
	22 GHz	*90 GHz*
all year	≤ 0.2/52K	≤ 0.4/96K
winter	≤ 0.1/28K	≤ 0.2/52K

Table 4.1 Medicina (and Noto) atmosphere summary

The results of the SEFD calculations, also in the worst combination of parameters, clearly show that acceptable values of sensitivity can be achieved.
The worst SEFD outcome is around 5000 Jy (El = 20°, excess factor = 1.4, T_{rx} = 100 K, surface rms = 176 micron, PWV = 10 mm), giving 5 mJy of sensitivity for 10 GHz bandwidth and 100 sec of integration time.
However achieving this figures is the result of many antenna refurbishments. The calculations show that a good SEFD comes from a careful development of receiver noise, surface rms upgrade (including a well working active surface), pointing (not considered in this study but very important for avoiding loss of antenna gain) and observation management (dynamic scheduling is requested, in order to exploit 3 mm condition whenever possible).
Any of these have to be met but SEFD is particularly sensitive to the total surface rms value, as can be seen in the summary reported in table 4.2: SEFD vs elevation is calculated for two couples of each parameter variation while maintaining their ratio (2 for PWV, 1.7 for Trx and Surface rms and 1.4 for excess factor). Then a mean of the ratios between SEFDs corresponding to the two parameter values is taken. For example, while SEFD ratios show a mean of 1.3 for PWV changing from 5 to 10 mm and 1.51 for the couple 10 to 20 mm, the mean ratio changes from 1.33 to a factor 2.31 for surface rms dependence. A total surface rms of 300 micron worsens more than twice the sensitivity performance of the 90 GHz receiving system with respect a performance of 176 micron (see fig. 4.1 and 4.2 for values to be compared with fig. 3.4.1 and 3.4.2 respectively).

SEFD dependence to parameters variation					
Parm Ratio		PWV dependence	Trx dependence	Surface rms dependence	Excess factor dependence
	Parameter Variation	SEFDs ratio mean value			
2	5mm to 10mm	1.3			
2	10mm to 20mm	1.51			
1.7	60K to 100K		1.28		
1.7	100K to 170K		1.38		
1.7	105µm to 176µm			1.33	
1.7	176µm to 300µm			2.31	
1.4	1 to 1.4				1.19
1.4	1.4 to 1.96				1.39

Tab. 4.2

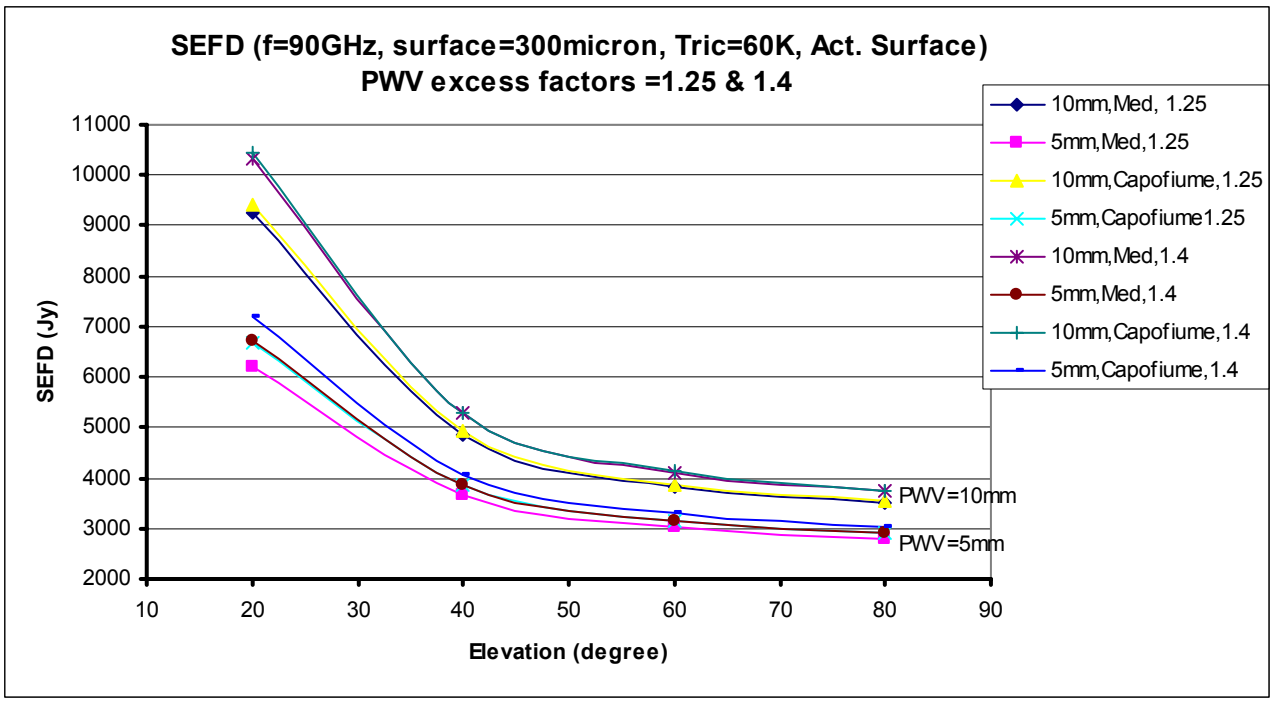
SEFD (f=90GHz, surface=300micron, Tric=60K, Act. Surface)
PWV excess factors =1.25 & 1.4
SEFD (Jy)
Elevation (degree)
PWV=10mm
PWV=5mm
10mm,Med, 1.25
5mm,Med,1.25
10mm,Capofiume,1.25
5mm,Capofiume1.25
10mm,Med,1.4
5mm,Med,1.4
10mm,Capofiume,1.4
5mm,Capofiume,1.4

Fig. 4.1

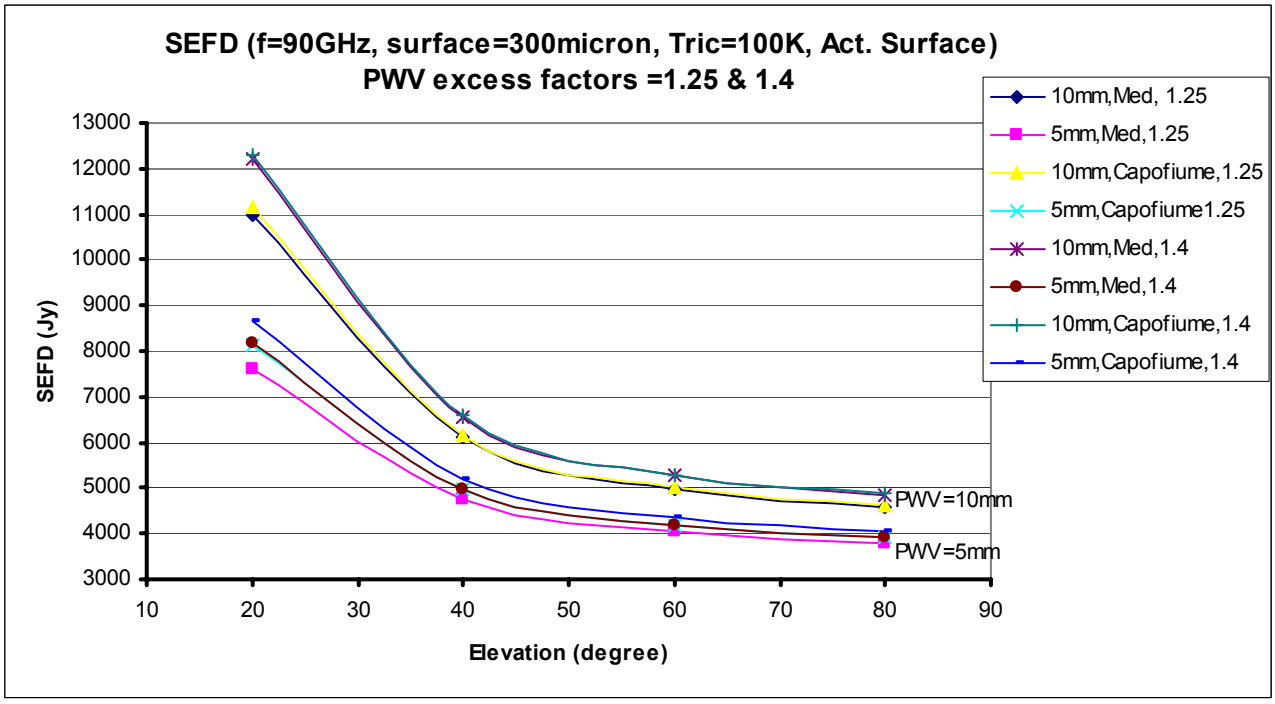
SEFD (f=90GHz, surface=300micron, Tric=100K, Act. Surface)
PWV excess factors =1.25 & 1.4
SEFD (Jy)
Elevation (degree)
PWV=10mm
PWV=5mm
10mm,Med, 1.25
5mm,Med,1.25
10mm,Capofiume,1.25
5mm,Capofiume1.25
10mm,Med,1.4
5mm,Med,1.4
10mm,Capofiume,1.4
5mm,Capofiume,1.4

Fig. 4.2

ACKNOWLEDGEMENTS

The author thanks Vincenzo Natale for the fruitful exchange of ideas on this subject, Franco Mantovani and Karl-Heinz Mack for the revision of the first draft of this document, and particularly Giuseppe Maccaferri for collecting opacity and meteorological data at Medicina site.

5. REFERENCES

1. A. Orfei
"Indagine sui siti di Medicina e Noto per un loro utilizzo nella banda 90 GHz (3 mm)"
IRA 393/06

2. A. Orfei
“Parabolic Antennas”
contribution to “Encyclopedia of Telecommunications” Wiley & Sons, 2002

3. W.M. Irvine, E. Carrasco, I. Aretxaga editors
“The Large Millimeter Telescope. Neighbors explore the Cosmos”, pag. 94
FCRAO and INAOE USA/Mexico

4. A. Cremonini
“On wafer Measurements performed on 4245-013/016/018/019 NGC InP Wafers "
IRA 404/07

5. P. Bolli
“Stima della Temperatura di Spillover per un Sistema d’Antenna a Doppio Specchio”
private communication, April 2007

6. G. Cortès
“Antenna Noise Temperature Calculations”, SKA Technical Memo Series 20/10/2004

7. G. Maccaferri, A. Orfei, A. Orlati
“Calibrazione in antenna del nuovo ricevitore 4.3-5.8 GHz per l’antenna parabolica di Medicina”
IRA 392/06, Appendice

8. Zacchiroli G., Fiocchi F., Maccaferri G., Morsiani M., Orfei A., Pernechele C., Pisanu T., Roda J., Vargiu G.
“I Pannelli per lo Specchio Primario e Secondario e il Sistema Superficie Attiva per il Nuovo Radio Telescopio SRT”
Proceedings del Workshop: Scienza con il Sardinia Radio Telescope, 10-11 maggio 2005 Bologna